國立臺灣大學生物資源暨農學院生物科技研究所

博士論文

Institute of Biotechnology

College of Bioresources and Agriculture

National Taiwan University

Doctoral Dissertation

具去除黃麴毒素 B1 能力之 *Chryseobacterium timonianum* 菌株的篩選與特性分析

Screening and Characterization of a *Chryseobacterium timonianum* Strain with Aflatoxin B1 Removal Ability

林亞理

Aniket Limaye

指導教授：劉嘉睿 博士

Advisor: Je-Ruei Liu, Ph.D.

中華民國 115 年 1 月

January 2026

doi:10.6342/NTU202600056

ACKNOWLEDGEMENTS

As I finish my doctoral studies, I need to thank the many people who made this journey possible. First and foremost, I am deeply grateful to my advisor, Professor Dr. Je-Ruei Liu. His constant support, encouragement, and guidance turned this long and challenging project into something achievable. He was always there to discuss ideas for future experiments, and he generously provided everything I needed—reagents, equipment, software, and funding—to keep the work moving forward without interruption. He also supported my publications every step of the way. I truly couldn't have done this without him.

I'm equally thankful to my committee members for accepting my oral exam application and allowing me to defend my thesis.

All the professors at the Institute of Biotechnology have been incredibly supportive. They freely shared their expertise in molecular biology, protein expression, and bioinformatics whenever I needed it. In particular, Dr. Lee Hsuan-Shu kindly provided the cell lines for my experiments without hesitation. Dr. Shih-Shun Lin offered invaluable advice on protein purification strategies. Dr. Kuan-Chen Cheng was always ready to help with urgent reagent requests. Dr. Shau-Ping Lin lifted my spirits with every conversation. Dr. Mong-Hsun Tsai guided me through the whole-genome sequencing aspects of my project. Dr. Chi-Te Liu provided crucial insights into phylogenetic analysis, and Dr. Jen-Chih Chen was a lifesaver for troubleshooting PCR optimization and other molecular biology challenges.

I also want to thank Dr. Vincent Cheng from National Yilan University for regularly checking in on my well-being and sharing his deep knowledge of AFB1 toxin production.

Dr. Yu-Liang Yang provided tremendous help with LC/MS and NMR analysis at the Agricultural Biotechnology Research Center, Academia Sinica.

doi:10.6342/NTU202600056

From India, my mentor, Dr. Milind Patole, gave me wonderful advice on writing the discussion sections of my papers and taught me how to respond thoughtfully to reviewers' comments.

On the administrative side, Ms. Hua-Yu was always quick to help with paperwork and formalities—thank you for making everything run more smoothly.

My labmates—Jerry Liao, Sunny, Sara, Yojia and John—made daily life in the lab enjoyable and productive. I'm lucky to have shared the bench with such great people.

My batchmates—Dr. Ji Rong Yang, Dr. Bolun Lee, Dr. Kai-Jiun Lo, Dr. Hsiao-Han, Dr. Wen-Jen Chen, and Dr. Yoyo were not only excellent colleagues but also true friends who enriched my time here.

None of this would have been possible without my family. I'm forever grateful to my father for his unwavering emotional and financial support through every difficulty. My mother, wife, and son stood by me with endless patience and love. A special thank you to Mr. Milind and Ms. Sharayu Bhagwat for taking care of so many household tasks and sending delicious home-cooked meals. Even music played a big role in keeping me going. I'm deeply thankful to my teacher, Maestro Faiyaaz Khan, for his beautiful lessons, which gave me strength during the toughest moments of my research. I want to express my gratitude to Mr. Nitin Sahasrabudhe for consistently offering entrepreneurial insights and wisdom to apply to my work.

Finally, I offer my heartfelt gratitude to my spiritual guides—Saint Dnyaneshwar Maharaj, Swami Madhavnath, and Swami Makarandnath—for inspiring me to stay true to my path with hope, passion, and perseverance.

Thank you all from the bottom of my heart. This thesis belongs to you as much as it does to me.

doi:10.6342/NTU202600056

中文摘要

黃麴毒素 B1（aflatoxin B1, AFB1）因其在呋喃環雙鍵形成環氧化物而具有強烈肝致癌性，是食品與飼料中危害性最高的黴菌毒素之一。相較於物理或化學解毒方法，微生物細胞外且有耐熱成分的生物解毒方式更具有應用潛力。本研究首先分離並鑑定具有 AFB1 去除能力的菌株，並進一步篩選出其中一株菌株 *Chryseobacterium timonianum* c4a，其胞外產物具有耐熱性且有 AFB1 降解活性。

本研究利用香豆素選擇性培養基，從雞盲腸內容物與富含羽毛之土壤樣本篩選具 AFB1 降解能力菌株。在篩選出的菌株中，c4a 具有最佳 AFB1 活性降解效果。c4a 在營養瓊脂上的菌落呈亮黃色、flexirubin 反應陽性、表面光滑且常帶有淡淡果香、為革蘭氏陰性、不產孢子的短桿菌，且不具運動性。API 生化試驗顯示其吲哚酶、尿素酶、氧化酶、esculin 與明膠水解均為陽性，並能同化葡萄糖、甘露糖、麥芽糖、檸檬酸、苦杏仁苷、海藻糖、澱粉、肝醣及 gentiobiose 等多種碳源。16S rRNA 之初步親緣分析及利用 rpoB、gyrB、rpoD 家族基因進行的串聯 MLSA 分析皆顯示 c4a 歸屬於 *Chryseobacterium timonianum* 之近緣支系。

c4a 之 AFB1 降解活性在其胞外培養上清液中，胞內與細胞壁幾乎不具活性。在明膠蛋白胨與牛肉萃取物比例為 4:1 的營養培養基中，添加 1 ppm AFB1，於 60°C、pH 8 並補充 Mn^{2+} 或 Mg^{2+} 的條件下，c4a 上清液於 72 小時內可降低約 93%的 AFB1 活性。c4a 上清液降解 AFB1 活性能力可耐受高壓滅菌，但在加入蛋白酶混合物或 SDS 後即完全喪失，顯示其為蛋白質。UPLCESI MS/MS 解析含 c4a 上清液與 AFB1 的反應混合物，偵測到一種水加成於呋喃環雙鍵之水合代謝物（m/z 331.08），其細胞毒性遠低於 AFB1。

利用 c4a 全基因體定序資料進行分析，並根據抗 AFB1 活性基因篩選，其中一個漆酶（laccase）與三個醛酮還原酶（aldoketo reductase, AKR）為目標基因。c4a 細胞亦可脫色 Remazol brilliant blue，顯示其可能具有氧化還原相關酶。所有目標基因皆成功以 pET32 Xa/LIC 進行克隆，但於 Rosettagami 2(DE3)pLysS 的表現中，即使補充銅離子，漆酶仍無法完整表現。其中 AKR 15_78 能順利表現與純化，偏好 NADPH 作為輔酶，其最適活性條件為 30°C、pH 7。然而，AKR 15_78 對 AFB1、玉米赤黴

doi:10.6342/NTU202600056

烯酮（zearalenone）及去氧雪腐鐮菌烯醇（deoxynivalenol）皆無活性，但可還原體積較大的酮類化合物。由 AKR 15_78 催化反應所得的手性產物，多數不適合作為藥物前驅物，惟乙基苯甲醯乙酸為例外。

總而言之，*C. timonianum* c4a 具構成性、胞外且耐熱的 AFB1 生物轉化能力，但其中包含的基因與酵素之分析，需利用如 *Pichia pastoris* 或 *Kluyveromyces marxianus* 等真核表現系統進一步研究。同時，AKR 15_78 催化形成的手性醇，仍需藉由不同手性色譜管柱與標準品進一步分析其立體選擇性與應用潛力。

關鍵詞：黃麴毒素 B1（AFB1）、*Chryseobacterium timonianum* c4a、胞外耐熱性生物轉化、代謝產物分析、基因體探勘

doi:10.6342/NTU202600056

ABSTRACT

Aflatoxin B1 (AFB1) ranks among the most hazardous mycotoxins in food and feed chains, owing to its potent hepatocarcinogenicity arising from epoxide formation at the furan ring double bond. Microbial detoxification strategies, especially those involving extracellular and thermostable components, provide practical benefits over physical or chemical alternatives. This thesis detailed the isolation and characterization of bacterial strains for AFB1 removal, with further characterization of the AFB1-degrading activity of the *Chryseobacterium timonianum* strain c4a, which was found to be thermostable.

A coumarin-selective medium was used to screen AFB1-degrading strains from chicken cecal digesta and feather-enriched soil samples. Out of the selected AFB1-degrading strains, c4a degraded AFB1 most effectively. Colonies of the c4a strain on nutrient agar were bright yellow, flexirubin-positive, smooth, and often had a faint fruity odor. Cells stained Gram-negative, appeared as non-motile rods lacking endospores. Biochemical tests via API systems were positive for indole, urease, oxidase, esculin, and gelatin hydrolysis, with assimilation of glucose, mannose, maltose, citrate, amygdalin, trehalose, starch, glycogen, and gentiobiose, among others. Initial 16S rRNA phylogenetic analysis, as well as concatenated MLSA analysis of housekeeping genes (*rpoB, gyrB, rpoD*), revealed that the c4a strain is closely related to *Chryseobacterium timonianum.*

AFB1 activity was localized to the extracellular supernatant, while the intracellular and cell wall fractions showed negligible activity. With nutrient broth at a 4:1 gelatin peptone: beef extract ratio, 1 ppm AFB1 at 60°C, pH 8, plus Mn^{2+} or Mg^{2+}, the c4a supernatant showed ~93% loss in 72 h. This activity survived autoclaving yet was abolished by protease cocktails or SDS, implying its proteinic nature. UPLC-ESI MS/MS analysis of the reaction mixture

doi:10.6342/NTU202600056

containing c4a supernatant and AFB1 showed a hydrated metabolite (m/z 331.08) from water addition across the furan double bond, which is reported to be significantly low in cytotoxicity compared to the original AFB1. Gene mining using whole genome sequencing data of the c4a strain revealed one laccase and three aldo-keto reductase (AKR) target genes, which are reported to be active against AFB1. Strain c4a cells also decolorized Remazol brilliant blue. pET-32 Xa/LIC cloning of all target genes succeeded, but Rosetta-gami 2(DE3)pLysS expression was incomplete in the case of laccase, despite copper supplementation. AKR 15_78, which was expressed and purified, preferred NADPH, with optimal activity at 30°C and pH 7, and was inactive against mycotoxins AFB1, zearalenone, and deoxynivalenol. However, it reduced bulky ketones. Chiral products formed after enzymatic reactions with AKR 15_78 were undesirable as pharmaceutical precursors, except for the case of the substrate ethyl benzoyl acetate.

Overall, *C. timonianum* strain c4a exhibited constitutive, extracellular, and thermostable AFB1 biotransformation, yet pinpointing the underlying genes and enzymes will likely require eukaryotic expression (e.g., *Pichia pastoris* / *Kluyveromyces marxianus*); in parallel, the putative AKR 15_78 mediated chiral alcohol transformation requires further investigation using alternative chiral HPLC columns and authentic reference standards.

Keywords： Aflatoxin B1 (AFB1), *Chryseobacterium timonianum* c4a, extracellular thermostable biotransformation, metabolite analysis, genome mining

doi:10.6342/NTU202600056

CONTENTS

ACKNOWLEDGEMENTS……..…….. i

ABSTRACT (Chinese version)……..…… iii

ABSTRACT (English version)…….…… v

CONTENTS…… vii

LIST OF FIGURES……..xi

LIST OF TABLES……...……...xiv

CHAPTER I……...1

Introduction……..……. 1

Mycotoxins…….…….. 1

Aflatoxins …….……... 4

Permissible Limits ……..……..……..……..8

Environmental and Geographical Distribution of Aflatoxins……...9

Aflatoxin B1…….……...…….…….. 10

Mechanism of DNA Damage and Immunogenicity……...……11

Species Specific Toxicity of AFB1 ……..……..12

Review of Aflatoxin B1 Degradation Strategies……13

Chemical Methods……..……13

Physical methods……..…….…..14

Biological methods……...…..15

CHAPTER II…….....20

doi:10.6342/NTU202600056

Screening and Characterization of *Chryseobacterium timonianum* Strain with Aflatoxin B1 Removal Ability…….....20

Abstract……...…….....……..…… 21

Introduction……...…….....……..…… 22

Materials and methods ……...…….....……..…… 24

Chemicals and Media ……...…….....……..…… 24

Experimental Samples ……...…….....……..……24

Bacterial Screening and Isolation ……..……..……..…. 24

AFB1 Removal Activities of the Isolated Bacterial Strains...……..…… 25

AFB1 Removal Activities of the Extracellular Supernatant, Intracellular Extract, and Cell Wall Fraction of the c4a Strain…….…....…..…… 25

HPLC Analysis of AFB1 Concentrations…….....……..…… 26

Phenotypic and Biochemical Characterization of the c4a Strain…..…… 27

Phylogenetic Characterization of the c4a Strain……27

Effect of Growth Medium Composition on AFB1 Removal Activity of the c4a Strain…….....…….....……..……..… 28

Effects of Reaction Temperature and pH, Mineral Ions, Heat Treatment, Protease Inhibitors, and SDS on AFB1 Removal Activity of the Extracellular Supernatant of the c4a Strain……. 29

Analysis of AFB1 Degradation Metabolites…….....……..…..…… 30

Statistical Analyses..…….....…….....……..….30

Results……..31

Isolation of Bacterial Strains with Potential for Removal of AFB1…….31

doi:10.6342/NTU202600056

Phenotypic, Biochemical, and Genomic Characteristics of the c4a Strain..31

Effect of Growth Medium Composition on AFB1 Removal Activity of the c4a Strain.....32

Effect of Reaction Temperature on AFB1 Removal Activity of the Extracellular Supernatant of the c4a Strain…….....33

Effect of Reaction pH on AFB1 Removal Activity of the Extracellular Supernatant of the c4a Strain…….....33

Effect of Mineral Ions on AFB1 Removal Activity of the Extracellular Supernatant of the c4a Strain.....33

Effect of Protease Inhibitors, SDS, and Autoclaved Treatments on AFB1 Removal Activity of the Extracellular Supernatant of the c4a Strain…….34

Analysis of AFB1 Degradation Metabolites…….34

Discussion…….34

CHAPTER III…….. 50

Unpublished Data……..…….…… 50

Materials and Methods ……..……..…....……..…..…50

Genome Sequencing and Assembly……..……..…50

Native Activity Assay of Strain c4a……..…….……. 51

Identification of Anti-Mycotoxin Genes…….……..… 51

Cloning of Target Genes……..……...……..... 52

Recombinant Protein Expression and Purification…….. 53

Enzyme Assays and Functional Characterization……..…….. 54

Results ……..….. 55

Genome Assembly and Annotation…….……. 55

doi:10.6342/NTU202600056

Native activity assay outcomes……..…….. 56

Identification and in silico Characterization Of Anti-Mycotoxin Candidates……..……. 56

Cloning Verification…….....56

Recombinant Protein Expression…….……..57

Biochemical Characterization of AKR 15_78…….....58

Functional Assays…….……... 59

Protein Sequences of c4a Strain Used In This Study In FASTA Format ….....
.....87

CHAPTER IV……..88

Concluding remarks…….88

References……91

Appendix…….…….……98

doi:10.6342/NTU202600056

LIST OF FIGURES

Figure 1-1. Chemical structures of important aflatoxins …….. 18

Figure 1-2. Enzymatic activation of AFB1 to highly toxic AFB1-8,9-epoxide……....19

Figure 2-1. AFB1 removal activity of the isolated bacterial strains……..… 39

Figure 2-2. High-performance liquid chromatography (HPLC) profile of AFB1 removal by the c4a strain……..……40

Figure 2-3. Removal of AFB1 by intracellular extract, cell wall fraction, and extracellular supernatant of the c4a strain……...…41

Figure 2-4. Macroscopic and microscopic examinations of the c4a strain……42

Figure 2-5. Neighbor-joining phylogenetic tree-based analyses of the 16S rRNA and DNA gyrase B (*gyrB)* genes of *Chryseobacterium* species.……..43

Figure 2-6. Neighbor-joining phylogenetic tree-based analyses of the RNA polymerase β subunit (rpoB), DNA gyrase B (*gyrB)*, and σ factor of RNA polymerase (rpoD) of *Chryseobacterium* species. ……..44

Figure 2-7. Effects of reaction temperature (a), reaction pH (b), supplementation of mineral Ions (c), and protease inhibitors, SDS, and autoclave treatment (d)…… ……. ……..…45

Figure 2-8. Effect of growth medium composition on the AFB1 removal activity of the c4a strain……..……46

Figure 2-9. a. MS-1 profile of strain c4a-mediated AFB1 degradation……47

Figure 2-9. b. MS-2 profile of ion fragment with m/z 331.08……..47

doi:10.6342/NTU202600056

Figure 2-9. c MS-2 profile of ion fragment with m/z 313.07……..48

Figure 3-1. Workflow for whole-genome sequencing and assembly of *C. timonianum* c4a ……..66

Figure 3-2. Decolorization of Remazol brilliant blue and growth in Congo red dye. ……..... 67

Figure 3-3. Customized workflow for genome-wide mining of anti-mycotoxin genes in *C. timonianum* c4a…….68

Figure 3-4. InterPro predicted domain organization of the protein sequence for scaffold 21_56 (Laccase)…….. .. 69

Figure 3-5. Conserved catalytic tetrad (Tyr-Lys-His-Asp) in aldo-keto reductases of c4a……...…70

Figure 3-6. Plasmid pET32 Xa/LIC gene map ……...……. 71

Figure 3-7. pET 32 Xa/LIC mediated gene cloning and transformation into an expression host ……72

Figure 3-8. Agarose gel electrophoresis of purified pET 32 Xa-LIC with Laccase gene inserts……..……..73

Figure 3-9. Agarose gel electrophoresis of purified pET 32 Xa-LIC with AKR gene inserts ……..74

Figure 3-10. SDS PAGE showing protein expressions of AKR 1_282, 4_167, 15_78 genes ……..…75

Figure 3-11. Protein expression in the soluble and insoluble fractions at 17°C after IPTG induction…….76

Figure 3-12. Laccase expression with CuSO4 supplementation ……..…77

Figure 3-13. General scheme for the recombinant expression of AKR 15_78 ……..…… ……78

doi:10.6342/NTU202600056

Figure 3-14. FPLC chromatogram of purified AKR 15_78 eluted in fraction number 5……..79

Figure 3-15. SDS PAGE showing AKR 15_78 expression in stages of purification……...80

Figure 3-16. Cofactor suitability test for AKR 15_78. NADH, NADP, and NADPH ……..…. 81

Figure 3-17. Optimum temperature assay for AKR 15_78 ……82

Figure 3-18. Optimum pH assay for AKR 15_78 ……..….83

Figure 3-19. Schematic diagram showing the overall strategy for the conversion of bulky ketones using chiral HPLC .. ……..……..……84

Figure 3-20. HPLC chromatograms of chiral products for the substrates a. Ethyl-2-oxo-4-phenylbutyrate and b. Ethyl benzoyl acetate ……..…….85

Figure 3-21. HPLC chromatograms of chiral products by AKR 15_78 enzyme against ethyl-4-chloroacetate as a substrate ……..……..... 86

doi:10.6342/NTU202600056

LIST OF TABLES

Table 2-1 Biochemical characteristics of c4a strain ……..…49

Table 3-1. *De novo* assembly results compared with other BioProject.....60

Table 3-2. Predictive genes mapping rate against the bacterial nr database….61

Table 3-3. BUSCO benchmark assessment for predictive genes ……..... 62

Table 3-4. Anti-mycotoxin genes identified in the *C. timonianum* c4a genome……..……..63

Table 3-5. Primers used in the study……64

Table 3-6. AKR 15_78 action on selected chirally important substrates……65

doi:10.6342/NTU202600056

CHAPTER I

Introduction

Mycotoxins

The metabolic interaction of xenobiotics with biological activities at both the molecular and organ levels in host animals causes harmful physiological and biochemical changes. Naturally occurring xenobiotics can be divided into two main classes: one comprising molecules inherently present in food, including bioactive polyphenols and plant toxins, such as solanine. Another toxic compound is an endogenous metabolite, either stored in food or synthesized by microorganisms during spoilage: mycotoxins, which are mainly produced by toxin-forming bacteria and fungi. Toxins of natural origin are produced chiefly by filamentous fungal genera, such as *Aspergillus*, *Penicillium*, and *Fusarium*; however, filamentous fungal genera such as *Alternaria* and *Stachybotrys* also produce significant quantities of toxins (Khan R., 2024; Bennett and Klich, 2003). Compounds classified as mycotoxins exhibit a range of structures and have varying biological effects. More than 300 to 400 mycotoxins have been classified, although approximately 20 mycotoxins are found in food and feed at levels that pose serious food safety issues (Haque et al., 2020; Latham et al., 2023). Mycotoxins are toxic secondary metabolites naturally produced by filamentous fungi during the invasion and colonization of agricultural produce. These secondary metabolites not only compromise food quality and safety but also cause significant economic losses, making mycotoxins globally one of the most significant and damaging categories of pollutants (Hussein et al., 2001; Khan, 2024). The Food and Agriculture Organization (FAO)

doi:10.6342/NTU202600056

estimates that mycotoxins are present in approximately 25% of all food crops in a given year, resulting in a loss of approximately 1 billion metric tons of food and food products (Eskola et al. 2020). Furthermore, contemporary assessments indicate that contamination rates could be as high as 60-80% across all food products, given that detectable contamination exceeds acceptable regulatory limits (Eskola et al. 2020). Contamination results in significant monetary losses due to reduced crop value, animal productivity, human health costs, and trade revenue, all estimated in the tens of billions of dollars globally (Zhang et al. 2024). In three Asian countries (Indonesia, the Philippines, and Thailand), losses of $900 million were reported due to aflatoxins, with the bulk of that cost attributed to human health effects (Pitt et al. 2012). Reports indicate that economic losses associated with mycotoxins in the U.S. and Canada range from $0.5 billion to more than $5 billion per year, even when human health costs or all crop yield losses are not considered (Mitchell et al., 2016). The threat posed by mycotoxins is not limited to local agricultural systems since these toxins often penetrate the food chain and animal feed globally, thus threatening human and animal health. Contamination is especially widespread in staple crops such as cereals, nuts, and dried fruits, which form the basic elements of nutrition in people's diets worldwide. Moreover, such contaminated feed is used in animal husbandry, which implies yet another channel of mycotoxin exposure via the products obtained from animals: milk, meat, and eggs. Eskola et al. (2020) reported a mycotoxin contamination rate of 60-80% across all analyzed samples. Therefore, such findings raise awareness about the omnipresence of mycotoxins and underpin the dire need to develop better means of their detection, imposing stricter laws and regulations for their inhibition at appropriate levels, along with the adoption of preventive measures against such contamination to ensure food and health safety of the humans on a global basis.

doi:10.6342/NTU202600056

The threat posed by mycotoxins is not limited to local agricultural systems, as these toxins often penetrate the food chain and animal feed globally, thereby threatening human and animal health. Contamination is especially widespread in staple crops such as cereals, nuts, and dried fruits, which form the basic elements of nutrition in people's diets worldwide. Moreover, since such contaminated feed is used in animal husbandry, this implies yet another channel of mycotoxin exposure via the products obtained from animals: milk, meat, and eggs (Alshannaq and Yu, 2017). Therefore, such findings raise awareness of the omnipresence of mycotoxins and underscore the need to develop more effective detection methods, to impose stricter laws and regulations to inhibit them at appropriate levels, and to adopt preventive measures against such contamination to ensure the food and health safety of humans on a global basis. Humans are primarily exposed to mycotoxins through contaminated plant-based foods. Still, they can also be indirectly exposed by consuming animal products (i.e., meat, milk, and eggs) from animals that have consumed contaminated feed (Haque et al. 2020). Mycotoxicosis refers to adverse health effects observed in humans and animals and can be acute (poisoning following high-level exposure) and chronic (effects following long-term, low-level ingestion) (Omotayo et al., 2019). The chronic effects may include carcinogenicity, mutagenicity, teratogenicity, immunotoxicity, hepatotoxicity, nephrotoxicity, neurotoxicity, and estrogenic effects (Liew and Mohd-Redzwan 2018). The severity of mycotoxicosis may be influenced by several factors, including the specific mycotoxin, level and duration of exposure, and individual characteristics such as age, sex, nutritional status, and health (Omotayo et al., 2019). In addition, multiple mycotoxins present in a food or feed product can exhibit additive or synergistic toxic effects, complicating risk analysis and management (Alassane-Kpembi et al., 2017).

doi:10.6342/NTU202600056

In terms of global management of mycotoxin contamination, several challenges exist. First, the complex and heterogeneous distribution or concentration of mycotoxins within a food lot can make representative sampling difficult (Koppen et al., 2010). Additionally, there are hurdles with analytical detection, for instance needing methods sensitive enough to detect very low regulatory limits (which often occur in parts per billion), or complex food matrices that hinder analysis, or presence of "masked", or modified, mycotoxins, which are toxic derivatives from the parent toxin and may not be detected by standard analytical methods (Berthiller et al., 2013). There are very few globally regularized regulations for many mycotoxins. The infrastructure and resources for effective monitoring and control programs may be lacking, particularly in developing countries where exposure risk is often the greatest (van Egmond et al., 2007). Climate change is also expected to intensify mycotoxin issues, including changes in fungal growth patterns and proximity to regions vulnerable to contamination (Medina et al., 2017).

Aflatoxins

Aflatoxins are a category of mycotoxins characterized by structural similarities and produced by fungi in the *genus Aspergill*us, specifically *Aspergillus flavus* and *Aspergillus parasiticus* (Varga et al., 2011). Aflatoxins were identified in the early 1960s, as a result of an outbreak of "Turkey X disease" in the UK, where thousands of turkey poults died after being fed a contaminated peanut meal (Groopman et al., 2008). The toxic agents were found to be metabolites produced by *Aspergillus flavus*, hence the name "aflatoxin" or *A. flavus* toxin (Sargeant et al., 1961). Although *A. flavus* and *A. parasiticus* are the best known, other species in the *Aspergillus* genus, such as *A. nomius*, *A. pseudotamarii*, *A. bombycis*, *A. minisclerotigenes*, *A. pseudocaelatus*, and *A. pseudonomius* (newly identified), can produce

doi:10.6342/NTU202600056

various aflatoxins (Varga et al., 2011; Frisvad et al., 2005; Probst et al., 2012). These fungi are ubiquitous soil-borne molds that can colonize a wide array of crops both before harvest and during storage (Cotty 2006; Kumar et al., 2017). Aflatoxins are categorized as B1, B2, G1, G2, M1, and M2. In fact, more than 20 aflatoxins have been identified, but the B and G series, along with their metabolites M1 and M2, are the most significant in terms of toxicity and prevalence in foods and feeds (Kumar et al., 2017). Aflatoxins are generally soluble in moderately polar organic solvents like methanol, acetone, and chloroform, but are only slightly soluble in water. They are relatively unstable to UV light and air, especially when in solution in highly polar solvents, though chloroform solutions can be stable for years if stored in the dark and cold. The four principal varieties of aflatoxins include AFB1, AFB2, AFG1, and AFG2, with AFB1 recognized as both the most prevalent and the most toxic variant. The order of acute toxicity is generally considered to be AFB1 > AFG1 > AFB2 > AFG2 (Kumar et al., 2017). The classification of these compounds is fundamentally based on their fluorescence characteristics; specifically, "B" denotes blue fluorescence, while "G" signifies green fluorescence. Additionally, a numerical identifier is used to represent the mobility of the compounds as observed in thin-layer chromatography. The B-series aflatoxins (AFB1, AFB2) are characterized by the fusion of a cyclopentenone ring to the coumarin moiety, while the G-series (AFG1, AFG2) possess a six-membered lactone ring instead of the cyclopentenone ring (Groopman et al., 2011; Iram et al., 2016). The numerical subscript indicates the relative chromatographic mobility; for example, AFB1 and AFG1 have an unsaturated bond at the 8,9 positions of the terminal furan ring, whereas in AFB2 and AFG2 this bond is saturated (Iram et al., 2016). This terminal furan ring is crucial for their toxicity. Structurally, aflatoxins are derivatives of difuranocoumarin synthesized through a polyketide pathway, utilizing a cluster of 17 genes responsible for 12 enzymatic transformations.

doi:10.6342/NTU202600056

Various species of fungi exhibit differences in their synthesis of specific aflatoxins. For example, AFB1 and AFB2 are predominantly produced by *A. flavus*, whereas AFB1, AFG1, and AFG2 are generated by *A. parasiticus*. Aflatoxin M1 represents a prevalent hydroxylated derivative of AFB1 found in both human and bovine milk, resulting from the metabolism of ingested AFB1. Aflatoxin M2 (AFM2) is also a hydroxylated metabolite of AFB2 (Kumar et al., 2017). Both AFM1 and AFM2 can be excreted in the milk of lactating animals, including dairy cows, that have consumed animal feed contaminated with AFB1 and AFB2, respectively, posing a risk to milk consumers (Hussain and Anwar 2008). Figure 1-1 represents chemical structures of important aflatoxins. The species of *Aspergillus* that produce aflatoxins thrive under warm and humid conditions, making improperly stored food products particularly vulnerable to contamination, especially during the critical post-harvest phase. *Aspergillus flavus* can grow at a broad temperature range. The optimal aflatoxin production occurs at 25-37°C with water activity (aw) above 0.85 (Klich 2007; Kumar et al., 2017). Drought stress, heat during crop maturation, insect damage to crops, inadequate harvesting and drying procedures are some of the many factors contributing to the risk of pre-harvest and post-harvest contamination (Payne 1998; Fountain et al., 2014). These fungi exhibit good growth and subsequent toxin production when carbohydrates are abundant (Klich 2007). The impact of aflatoxins is especially severe in developing countries located between the latitudinal lines of 35° N and 35° S, where the environmental conditions are most conducive to their production, and storage practices may be less regulated or monitored. Aflatoxin contamination is prevalent in maize, peanuts (also known as groundnuts), cottonseed, tree nuts (such as almonds and pistachios), rice, figs, and spices worldwide. Some studies have reported that a significant proportion of cereals tested contained at least one form of aflatoxin (Andrade and Caldas 2015). AFB1 contamination poses significant

doi:10.6342/NTU202600056

economic consequences for agricultural production, international trade, and human and animal health. The strict AFB1 regulations in food and feed, especially by EU, result in import rejections, which adversely affect exporting developing nations. The EU generally applies limits of 2 μg/kg (ppb) for AFB1 and 4 μg/kg for total aflatoxins (B1, B2, G1, G2) in food for human consumption (Iqbal et al., 2019). The FDA has an action level of 20 μg/kg for total aflatoxins in many food and feed commodities (Iqbal et al., 2019). The EU also has a standard of 0.05 μg/kg for aflatoxin M1 in milk, and the US has a standard of 0.5 μg/kg (Iqbal et al., 2019).

The global health and trade implications of aflatoxins require global cooperation and guidance (van Egmond et al., 2007). The FAO and WHO created the Codex Alimentarius Commission to develop international food standards, guidelines, and codes of practice to protect consumer health and promote fair trade practices in the food trade (van Egmond et al., 2007). Codex has established codes of practice to reduce contamination in peanuts and cereals collectively, as well as maximum levels (MLs) of aflatoxins in food (Codex Alimentarius Commission, 1997). The Code of Practice for the Reduction of Aflatoxin B1 in Raw Materials and Supplementary Feeding Stuffs for Milk-Producing Animals (CXC 45-1997) aims to reduce AFB1 in dairy feedstuffs and AFM1 in milk (Codex Alimentarius Commission 1997). The global health and trade implications of aflatoxins require global cooperation and guidance (van Egmond et al., 2007). The FAO and WHO created the Codex Alimentarius Commission to develop international food standards, guidelines, and codes of practice to protect consumer health and promote fair trade practices in the food trade (van Egmond et al., 2007). Codex has established codes of practice to reduce contamination in peanuts and cereals collectively as well as maximum levels (MLs) of aflatoxins in food

doi:10.6342/NTU202600056

(Codex Alimentarius Commission, 1997). The Code of Practice for the Reduction of Aflatoxin B1 in Raw Materials and Supplementary Feeding Stuffs for Milk-Producing Animals (CXC 45-1997) aims to reduce AFB1 in dairy feedstuffs and AFM1 in milk (Codex Alimentarius Commission, 1997).

Developing countries often cite the Codex Standards and Guidelines as a reference for developing their national food standards or regulations; however, the specific aflatoxin limits subsequently included in legislation can vary significantly based on economic factors, dietary exposure habits, and risk assessment policies applied by different countries.

Permissible Limits

Permissible limits for AFB1 in animal feed (often expressed in μg/kg, equivalent to ppb) are critical for protecting animal health and productivity and preventing toxin carry-over into human food products like milk, meat, and eggs. Regulations vary by region and animal type, reflecting different sensitivities and production goals.

- The European Union (EU) imposes strict restrictions. The maximum level for AFB1 is generally 20 μg/kg (European Commission Directive 2002/32/EC) for most feed materials and complementary/complete feedstuffs intended for animals like cattle, sheep, goats, pigs, and poultry. Aiming to minimize AFM1 carry-over into milk, the limit for AFB1 is much lower at 5 μg/kg for complete feedstuffs for dairy animals (e.g., dairy cows) (European Commission Directive 2003/100/EC). Because of their greater sensitivity, young animals often have even more strict limits.
- United States (US): The US Food and Drug Administration (FDA) establishes action levels for total aflatoxins (B1, B2, G1, G2). For the majority of animal feeds, the

doi:10.6342/NTU202600056

broad action level is set at 20 µg/kg. Different action levels are specified for several classes of animals: notably, 20 µg/kg for finishing swine weighing over 100 lbs and beef cattle; a much less stringent level of 100 µg/kg for breeding swine, breeding beef cattle, and poultry; and, under certain conditions, up to 300 µg/kg for beef cattle in feedlots. For the milk of dairy animals to have an AFM1 level no higher than the action level of 0.5 µg/kg, the feed must contain less than 20 µg/kg of total aflatoxins (FDA CPG Sec. 683.100, 2024)

- Other Regions: Many other countries have established their own regulations. For example, the Bureau of Indian Standards (BIS) has set a maximum permissible level of 20 µg/kg for AFB1 in most animal feeds in India (Thakur et al., 2022). Particularly in regions with limited resources, the effective monitoring, implementation, and enforcement of the regulatory limits remain a critical global challenge (van Egmond et al., 2007).

Environmental and Geographical Distribution of Aflatoxin Contamination

Climate change, driven by steadily rising global temperatures, has expanded the range of aflatoxin contamination in agricultural commodities (Battilani et al., 2016). Higher mean temperatures combined with shifts in precipitation regimes created conditions more conducive to the growth of *Aspergillus* species and subsequent toxin production. Regions once considered at low risk now face elevated contamination pressure. Southeastern Europe, in particular, registered a clear upward trend in aflatoxin occurrence over recent decades. Predictive models suggested that an additional 2°C warming would elevate aflatoxin risk in maize to levels requiring regulatory attention across much of continental Europe, notably including Eastern Europe and the Balkans, where such problems had previously been rare

doi:10.6342/NTU202600056

(Battilani et al., 2016). Beyond direct effects on temperature and water availability—parameters that control both fungal colonisation and aflatoxin biosynthesis—climate change increased plant stress and expanded the distribution of insect pests whose feeding damage provided entry points for fungal infection (Medina et al., 2017). Current efforts, therefore, focused on mechanistic forecasting tools that integrate temperature, relative humidity, and rainfall patterns to anticipate regional risk and guide pre-emptive intervention (Leggieri et al., 2021)

Aflatoxin B1

Chemical Structure and Toxic Moiety

AFB1 contains a core structure comprising dihydrofuro [2,3-b] furan and a coumarin ring, where the double bond within the furan ring serves as the critical toxic moiety. This terminal furan ring, specifically the 8,9-double bond, is responsible for the AFB1 mutagenicity and carcinogenicity (Eaton and Gallagher 1994).

Metabolic Activation

The molecule itself is relatively inert until it undergoes metabolic activation by hepatocytes. This double bond (C-8/C-9) is transformed in the liver into AFB1-8,9-epoxide, which forms highly toxic adducts with DNA, glutathione S-transferase, or N7-guanine. Metabolic activation of AFB1 to its reactive AFB1-8,9-exo-epoxide is primarily catalyzed by hepatic cytochrome P450 (CYP450) enzymes (Figure 1-2), though other tissues can also be involved (Guengerich et al., 1998). CYP3A4 and CYP1A2 are the main CYP450s responsible, with

doi:10.6342/NTU202600056

lesser contributions from CYP3A5 and CYP2A13 (prominent in the respiratory tract) in humans (Guengerich et al., 1998).

Mechanism of DNA Damage, Immunogenicity

The International Agency for Research on Cancer (IARC) has classified aflatoxins as Class 1 carcinogens, considering their high toxicity and significant health risks (IARC, 2012). The fundamental mechanism of AFB1-induced DNA damage via hepatic epoxidation and subsequent adduct formation is recognized across susceptible species, though the extent and specific consequences can vary. The resultant AFB1-8,9-exo-epoxide, an electrophilic intermediate, readily targets nucleophilic sites on cellular macromolecules. Its critical carcinogenic reaction is with DNA, predominantly forming covalent adducts with guanine's N7 atom, yielding 8,9-dihydro-8-(N7-guanyl)-9-hydroxy-AFB1 (AFB1-N7-Gua) adducts. These unstable adducts, if unrepaired, can cause depurination (forming apurinic sites) or undergo ring-opening to the more stable AFB1-formamidopyrimidine (AFB1-FAPY) adduct. Unrepaired AFB1-N7-Gua adducts can lead to G-to-T transversion mutations during DNA replication, particularly if not removed by nucleotide excision repair (NER), which is strongly linked to AFB1-induced hepatocellular carcinoma (Smela et al., 2001).

Additionally, AFB1 is a significant immunotoxicant. It can impair both cell-mediated and humoral immunity by affecting the function and proliferation of T-lymphocytes, B-lymphocytes, macrophages, and natural killer (NK) cells (Meissonnier et al., 2008). AFB1 exposure has been shown to decrease antibody responses to vaccines, reduce cytokine production (such as IFN-γ and IL-2), and alter lymphocyte subset populations, thereby increasing susceptibility to infectious diseases (Meissonnier et al., 2008).

doi:10.6342/NTU202600056

Species-Specific Toxicity of AFB1

The toxicity of AFB1 in livestock and humans has real economic and health implications. Approximately 500 million people, mostly from economically disadvantaged areas in sub-Saharan Africa, Latin America, and some parts of Asia, are currently exposed to aflatoxin levels higher than internationally established safety limits (Williams et al., 2004). The ingestion of food components contaminated with AFB1 has severe dose-dependent effects on both livestock and humans. The balance between the efficiency of metabolic activation and detoxification pathways exhibits significant differences among species, largely accounting for differences in susceptibility (Eaton and Gallagher 1994).

In humans, considerable variability in enzyme expression (CYP450s and GSTs) is influenced by genetic polymorphisms, age, sex, nutritional status, and co-exposures. Upon metabolic activation of AFB1 in hepatocytes through CYP450 enzymes, the toxic metabolite AFB1-8,9-epoxide is produced, forming covalent bonds with nucleic acids and proteins.

Aflatoxicosis is caused by aflatoxin consumption, leading to acute liver cirrhosis, death, and chronic nutritional/immunological effects depending on dose (Omotayo et al., 2019). Toxicity varies by age, gender, species, dosage, and exposure time. Young poultry show extreme sensitivity: chick embryos (oral LD50 0.025 mg/kg bw), ducklings (0.3 mg/kg bw), turkey poults (0.5 mg/kg bw), compared to some chicken breeds (2.0–6.3 mg/kg bw) (Kavitha et al., 2015). Aflatoxicosis in chickens is characterized by weakness, low weight gain, poor feed efficiency, reduced egg production, liver hemorrhage, and lipid accumulation. Biochemical indicators include elevated AST/ALT and reduced total protein/albumin; histopathological changes involve fatty degeneration, necrosis, bile duct hyperplasia, fibrosis, and nephrotoxicity (Tessari et al., 2006; Mughal et al., 2017). AFB1 impairs avian immunity

doi:10.6342/NTU202600056

by reducing T-lymphocyte numbers and disrupting cytokine production, and accumulates in eggs (Ogwuegbu et al., 2024).

Swine have higher susceptibility than cattle but less than young poultry (oral LD50 ~0.6 mg/kg bw) (Popescu et al., 2022). Their detoxification is less effective, increasing the risk of toxicosis. Exposure causes liver damage, lesions in spleen, lymph nodes, kidneys, reproductive organs, intestinal microbiota disruption, oxidative stress, impaired barrier/nutrient absorption, organ weight increases (kidneys, liver, spleen, pancreas), impaired lymphocyte activation, reduced vaccination efficacy, and pro-inflammatory cytokines (IL-6, IFN-γ, IL-10), with growing pigs and pregnant sows particularly vulnerable (Popescu et al., 2022; Meissonnier et al., 2008)

Review of Aflatoxin B1 Degradation Strategies: Chemical, Physical, and Biological Methods

Chemical Methods

Effective strategies to mitigate AFB1 contamination fall into three categories: chemical, physical, and biological methods. This review summarizes significant reports on these strategies, with particular emphasis on biological approaches. Ozonation attacks the 8,9-double bond in AFB1's furan ring, yielding lower-toxicity products through primary ozonide formation and rearrangement (Kutasi et al., 2021). Efficacy depends on contact time, ozone concentration, moisture, and matrix; optimization is required to avoid quality loss (Sipos et al., 2021). Acid treatments (e.g., citric or lactic acid) degrade AFB1 via lactone ring hydrolysis, enhanced by heat, though efficiency varies and food properties may be affected (Sipos et al., 2021). Sodium hypochlorite has been investigated, but is limited by residue concerns. Ammoniation achieves >95% detoxification in feedstocks (Samarajeewa et al.,

doi:10.6342/NTU202600056

1990). Adsorption using activated carbon or montmorillonite clays reduces bioavailability via hydrophobic interactions, van der Waals forces, or chelation of the β-dicarbonyl moiety with metal ions (Phillips et al., 2008; Sipos et al., 2021). Recent advances include functionalized nanoparticles for enhanced binding and green-synthesized nanomaterials for dual adsorption and fungal inhibition (Gelaye and Luo, 2025). While chemical methods are efficient, challenges include scalability, cost, safety, potential toxic byproducts, and preservation of nutritional/sensory quality, which limit their practical application.

Physical Methods

Researchers have examined a range of physical methods for reducing AFB1 levels in contaminated commodities, principally thermal treatments, irradiation, and adsorption (Sipos et al., 2021). Dry heat processes such as roasting or autoclaving lowered toxin concentrations only modestly and usually compromised organoleptic and nutritional properties; peanuts roasted at 150 °C for 30 min, for example, still contained about 70 % of the original AFB1 (Rustom, 1997). Everyday thermal treatments such as boiling or pasteurization had little effect on this remarkably stable molecule, whereas extrusion under high-moisture conditions combined heat and shear forces to achieve substantially greater degradation (Sipos et al., 2021). Both gamma and electron-beam irradiation cleaved bonds through free-radical intermediates (Sipos et al., 2021). AFB1 is more sensitive to UV radiation at a wavelength of 362 nm due to chemical structural modifications in the terminal furan ring (Sanchez et al., 2022). More recent non-thermal approaches, notably pulsed light and cold atmospheric plasma, rely on reactive oxygen and nitrogen species to rapidly oxidise the critical furan moiety without heating the substrate (Sanchez et al., 2022). Clay minerals sequestered the toxin tightly in the gastrointestinal tract and thereby reduced systemic uptake (Phillips et al., 2002). Simple mechanical procedures—sorting by color, density, or UV fluorescence, or

doi:10.6342/NTU202600056

thorough washing—discarded heavily contaminated kernels while leaving the toxin itself untouched (Sipos et al., 2021). In practice, the methods need careful calibration to strike an acceptable balance between detoxification efficiency and preservation of product quality.

Biological Methods

Compared with physical or chemical treatments, biological approaches often prove preferable for their milder operating conditions, which limit loss of nutritional and sensory attributes. Microorganisms transform AFB1 into metabolites of lower toxicity under milder reaction conditions, causing less disruption to food or feed matrices than most physical or chemical approaches. Specificity provides the chief advantage: extracellular activities from several isolates target structural elements—the terminal furan ring in particular—directly implicated in genotoxicity, rendering these systems well-suited to matrix-preserving applications (Alberts et al., 2006).

AFB1 degradation occurs across a wide range of bacteria and fungi, yet systems that provide defined extracellular fractions or purified enzymes hold greater promise for practical use. *Rhodococcus erythropolis* cultures substantially reduced AFB1 concentrations, suggesting enzymatic modification rather than adsorption alone (Alberts et al., 2006). A thermostable lipase accounted for most activity in *Pseudomonas putida* (Singh and Mehta, 2022). In practice, enzyme-based approaches allow tighter standardization—supernatants, crude extracts, immobilised preparations, or purified catalysts lend themselves to consistent quality control in ways that whole-cell mixtures do not.

Laccases represent the class of oxidoreductases active in aflatoxin B1 (AFB1) detoxification. Several studies have tested fungal laccases directly against AFB1; treatment typically yielded substantial degradation and markedly lower mutagenicity (Alberts et al., 2009). Bacterial

doi:10.6342/NTU202600056

multicopper oxidases, however, attract increasing interest owing to their greater robustness and simpler large-scale production. CotA laccase from Bacillus subtilis, for instance, degraded AFB1 almost completely in mediator-supplemented reactions when pH, temperature, and residence time were optimized—a clear demonstration that careful reaction engineering can translate intrinsic activity into consistent, high-level performance (Wang et al., 2019). Cost remains a central barrier for widespread enzyme use, which is why low-cost enzyme sources are being explored. An enzymatic extract from spent mushroom substrate of *Pleurotus eryngii* efficiently degraded AFB1. It is positioned as a circular, waste-to-value route for sourcing ligninolytic activities (Branà et al., 2020). Apart from white-rot fungi, filamentous fungi are also shown to be active against AFB1. *Trichoderma reesei* has been characterized for its strong AFB1-degrading activity, extending beyond buffered model systems and into contaminated matrices (Yue et al., 2022).

A complementary approach relies on reducing AFB1 bioavailability through probiotics and food-grade bacteria, notably lactic acid bacteria (LAB). Initial studies showed that certain LAB strains bind AFB1 at the cell surface; binding efficiency differed markedly between strains and depended on conditions such as pH and prior heat treatment (Haskard et al., 2001). It was found that specific peptidoglycan and carbohydrate components in the cell envelope were primary binding sites for Lactobacillus *rhamnosus* GG (Lahtinen et al., 2004). This mechanistic insight shifts strain selection from empirical screening toward targeted choice based on envelope composition. *In vitro* evidence of functional impact was obtained from co-incubation experiments in Caco-2 monolayers, where *L. rhamnosus* GG significantly reduced AFB1 transepithelial transport, intracellular accumulation, and cytotoxicity (Gratz et al., 2007). These findings support a sequestration-based mechanism limiting epithelial

doi:10.6342/NTU202600056

exposure without direct AFB1 degradation. *In vivo* efficacy varies with dose, matrix effects, and transit time.

Biological control is not limited to post-harvest detoxification. Pre-harvest biocontrol using atoxigenic (non-aflatoxigenic) *Aspergillus flavus* strains aims to displace toxigenic populations and reduce aflatoxin accumulation in crops competitively. Field-oriented evaluations in maize support measurable reductions in contamination when appropriate atoxigenic isolates are selected and deployed effectively (Atehnkeng et al., 2008). Molecular tools add a more targeted layer. Host-induced gene silencing (HIGS) involves the transgenic expression of dsRNA constructs targeting essential genes in the aflatoxin biosynthesis pathway of *Aspergillus flavus*. This strategy has yielded maize lines with substantially lower aflatoxin contamination (Thakare et al., 2017). Its field trials demonstrated that silencing targeted to the aflM gene, which encodes versicolorin A dehydrogenase, remained effective under standard agronomic conditions. This led to meaningful reductions in aflatoxin levels (Raruang et al., 2020). From the pathogen's perspective, CRISPR/Cas9 editing has enabled precise deletion of large chromosomal regions encompassing the complete aflatoxin cluster. The resulting strains are stably atoxigenic and prove valuable for functional studies; with additional characterization, they could refine existing biocontrol products (Chang, 2024).

doi:10.6342/NTU202600056

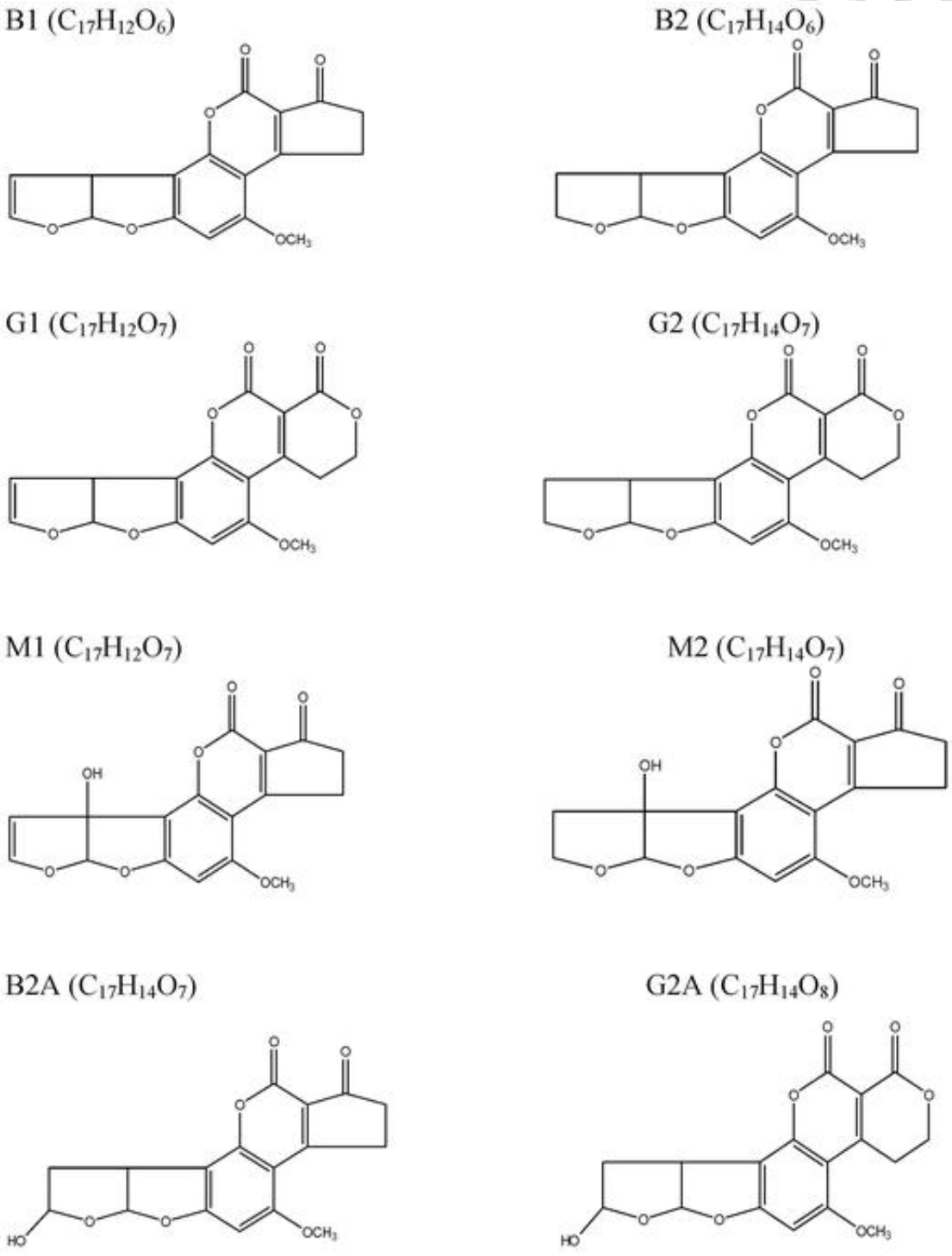


Figure 1-1. Chemical structures of important aflatoxins (adopted from Owuor et al., 2020)

doi:10.6342/NTU202600056

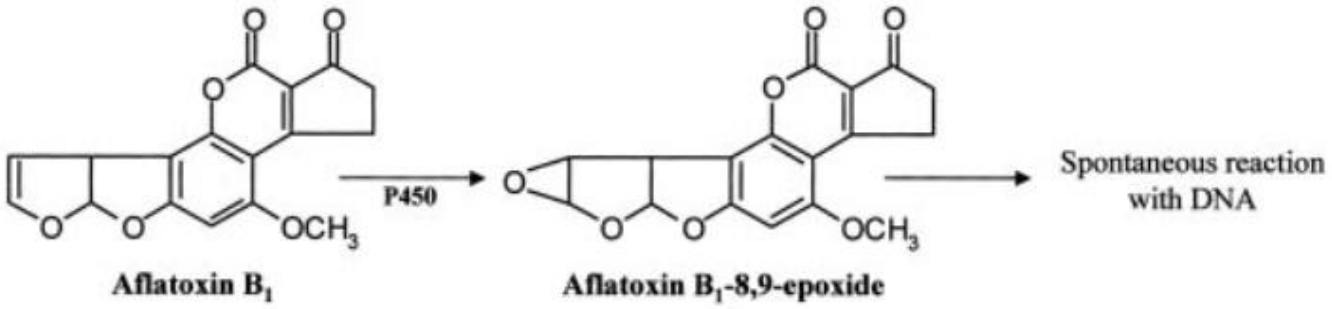


Figure 1-2. Enzymatic activation of AFB1 to highly toxic AFB1-8,9-epoxide. (adopted from Jowsey et al., 2003)

doi:10.6342/NTU202600056

CHAPTER II

Screening and Characterization of *Chryseobacterium timonianum* Strain with Aflatoxin B1 Removal Ability

The content in Chapter II has been published in the journal Microbial Physiology as shown below. This publication is the first author's work, and its quality fulfills the PhD thesis examination application requirement of the Institute of Biotechnology, National Taiwan University. The dissertation, or any part thereof, has not been submitted for any degree, diploma, or other qualification at any other university. It is the result of my own work, except where otherwise stated in the text.

Limaye A, Liu JR. Screening and Characterization of a Chryseobacterium timonianum Strain with Aflatoxin B1 Removal Ability. Microb Physiol. 2024;34(1):182–196. doi:10.1159/000540803.

Aniket Limaye performed material preparation, data collection, and analysis. Aniket Limaye and Dr. Je Ruei Liu wrote the first draft of the manuscript. Dr. Je Ruei Liu is the corresponding author.

doi:10.6342/NTU202600056

Abstract:

Introduction: Aflatoxin B1 (AFB1) is a potent hepatocarcinogenic mycotoxin found in animal feed and human food components. AFB1 contamination poses severe food safety and economic consequences. **Methods**: In this study, we used a coumarin-selective medium to isolate bacterial strains that can remove AFB1. Among the isolated bacterial strains, strain c4a exhibited the highest AFB1 removal activity. This strain was subjected to biochemical and phylogenetic characterization. The AFB1 removal activity of the extracellular supernatant of this strain was optimized for growth medium, reaction temperature, pH, and metal ions. The degradation products were analyzed using UPLC-ESI MS/MS. **Results**: Strain c4a was found to be most closely related to *Chryseobacterium* timonianum. The extracellular supernatant of *C. timonianum* c4a grown in a modified nutrient broth (with gelatin peptone and beef extract in a 4:1 ratio) demonstrated the highest AFB1 removal activity when incubated with 1 ppm AFB1 at 60°C, pH 8, and Mn2+ or Mg2+ supplementation for 72 h. Surprisingly, the autoclaved extracellular supernatant also retained AFB1 removal activity. UPLC-ESI MS/MS analysis suggested that AFB1 was transformed into a metabolite (m/z value 285.08) by water molecule addition on furan ring double bond. **Conclusion**: The AFB1 removal activity of *C. timonianum* c4a was extracellular, constitutive, and highly thermostable, structurally transforming AFB1 into a much less toxic product. Herein, we present the first evidence of thermostable AFB1 removal activity of a strain belonging to *C. timonianum.*

doi:10.6342/NTU202600056

Introduction

Aflatoxins belong to the family of structurally related mycotoxins secreted by *Aspergillus flavus* and *A. Parasiticus.* The four main aflatoxins are B1, B2, G1, and G2. The letters represent blue or green ultraviolet (UV) fluorescence, while the numbers represent their migration distance across a thin-layer chromatographic plate (Klich et al., 2007). These secondary metabolites are difuranocoumarin derivatives produced by a common polyketide pathway involving seventeen genes encoding twelve enzymatic conversions (Bhatnagar et al., 2003; Abrar et al., 2013).

AFB1 has a core structure comprising dihydrofuro (Bhatnagar et al., 2003, Abrar et al., 2013) furan and a coumarin ring, with the key toxic component being the furan ring's double bond. In the liver, this double bond (C-8/C-9) gets converted to AFB1-8,9-epoxide, forming highly toxic adducts with DNA, glutathione S-transferase, or N7 guanine (Wang et al., 2021). The International Agency for Research on Cancer (IARC) has announced aflatoxins as Class 1 carcinogens, which are highly poisonous toxic substances. Among the aflatoxins, aflatoxin B1 (AFB1) is the most potent. The Food and Agriculture Organization (FAO) of the United Nations has estimated that about 25% or more of the world's food crops are affected and destroyed by AFB1 contamination each year.

Aspergillus species thrive in humid, warm tropical and subtropical areas where aflatoxin destroys crops. During preharvest to storage, aflatoxin can contaminate peanuts, corn, wheat, and soybeans (Abrar et al., 2013). AFB1 metabolism and toxicity in livestock depend on species, age, sex, feed mix, dosage, and exposure time. Resulting conditions include induced immunosuppression with poor cellular and humoral immunity, liver bleeding, renal necrosis, pancreatic cancer, and decreased body weight gain, milk, and egg production (Peles et al.,

doi:10.6342/NTU202600056

2019). Thus, AFB1-mediated livestock toxicity and further AFB1 carryover can be restricted by physical, chemical, or biological means. AFB1 can be physically adsorbed by bentonite or yeast cell walls (Vekiru et al., 2015) or chemically degraded by ozone, hydrogen peroxide, acidic electrolyzed water solution, and gamma and UV radiation (Adegoke et al., 1991; McKenzie et al., 1998; Diao et al., 2015; Sen et al., 2019). Existing physical and chemical methods do not fully meet commercial productivity, safety, and cost standards (Verheecke et al., 2016). Research indicates that AFB1-metabolizing bacteria or their derived metabolites effectively eliminate AFB1 (Peng et al., 2018; Shu et al., 2018; Mwakinyali et al., 2019; Wang et al., 2018; Cai et al., 2020; Zhang et al., 2021). However, this approach, while relatively safe, may yield toxic bio-transformed metabolites, necessitating assessment of AFB1 biodegradation and metabolite profiles.

Coumarin has been used as a carbon source in selective media for screening AFB1-removing bacteria [Guan et al., 2008]. In this study, we employed a coumarin-selective medium to isolate AFB1-removing bacteria. Bacterial strains capable of growing in a coumarin-selective medium were selected for further analysis. Our laboratory-isolated bacterium, the c4a strain, was included in the screening because its genome contains important AFB1-degrading enzyme genes, including multicopper oxidase (NCBI accession number: WP_228452318) and DyP-peroxidase (NCBI accession number: WP_160139647). Given its high growth rate in the coumarin medium, we investigated whether the c4a strain can metabolize AFB1. The c4a strain demonstrated the highest AFB1 degradation among the selected coumarin-degrading strains. The c4a strain was identified as *C. timonianum* through physiologically, biochemically, and phylogenetically. The AFB1 removal activity of the c4a strain was optimized by adjusting the medium composition, reaction temperature, pH, and metal ion supplementation. The final transformed metabolites were subjected to LC-MS/MS analysis

doi:10.6342/NTU202600056

to determine possible structural changes in the AFB1 molecule, followed by a comparative toxicity study. Here, we report a novel, highly thermostable, extracellular AFB1 removal phenomenon by the *C. timonianum*c4a strain, resulting in structural modification of the furan ring of AFB1, which is linked to its toxicity.

Materials and Methods

Chemicals and Media

Luria-Bertani (LB) broth, nutrient broth, tryptone-yeast extract (TYE) broth, and M9 medium were purchased from Acumedia (Lansing, MI, USA), while coumarin and AFB1 were purchased from Sigma-Aldrich, Inc. (St. Louis, MO, USA). A coumarin medium, which contained coumarin as the sole carbon source, was prepared according to the method described by Guan et al.,2008. Each liter of coumarin medium contained 10.0 g coumarin, 0.25 g KH_2PO_4, 1.0 g NH_4NO_3, 1.0 g $CaCl_2$, 0.25 g $MgSO_4$, 1.0 mg $FeSO_4$, and 15.0 g agar, while the pH was adjusted to 7.0.

Experimental Samples

Forty Arbor Acres broilers (1 day old) were randomly divided into two groups: group A birds were not fed mycotoxin, and group B birds were given feed containing 200 ppb of AFB1. On day 35, the cecal digesta samples of one bird from group A and two from group B were subjected to bacterial screening. A soil sample enriched with chicken feathers obtained from the experimental farm of National Taiwan University (Taipei, Taiwan) was also used for bacterial screening.

Bacterial Screening and Isolation

The cecal digesta and soil samples (1 g each) were homogenized with 9 mL of sterile phosphate-buffered saline (PBS buffer, 0.1 m, pH 7.0) and serially diluted from 10^{-1}–10^{-4} fold

doi:10.6342/NTU202600056

before plating onto coumarin agar. The plates were incubated at 37°C aerobically and anaerobically for 4–7 days until colonies appeared. The colonies were transferred to new coumarin plates three consecutive times, following which single colonies were inoculated in coumarin broth and cultured at 37°C and 220 rpm, with bacterial growth monitored using a spectrophotometer at 600 nm. All isolated bacterial strains were further determined for their AFB1 removal activity.

AFB1 Removal Activities of the Isolated Bacterial Strains

Overnight cultures of the isolated bacterial strains were inoculated into 10 mL sterile LB broth containing 1 ppm of AFB1 and incubated at 37°C at 220 rpm agitation for 72 h. A 450 μL aliquot of culture media was centrifuged at 10,000 *g*for 10 min at 4°C, and the amount of residual AFB1 in the LB broth was analyzed by high-performance liquid chromatography (HPLC). The bacterial strain, c4a, showing the maximum AFB1 biodegradation, was subjected to further characterization studies.

AFB1 Removal Activities of the Extracellular Supernatant, Intracellular Extract, and Cell Wall Fraction of the c4a Strain

A single colony of the c4a strain was inoculated into 3 mL LB broth and incubated at 30°C with 220 rpm agitation. After 7.5 h, the exponentially growing culture was added to 10 mL of sterile LB broth to obtain a final bacterial concentration of 1×10^9 CFU/mL. After 24 h under the same incubation regime, extracellular supernatant and cell pellets were separately obtained by centrifugation at 13,000 *g* for 10 min at 4°C. The cell pellet was washed twice with sterile PBS (0.1 m, pH 7.0), resuspended in 5 mL of sterile PBS, and sonicated on ice for 10 min with an ultrasonicator (Model XL, Misonix, Farmingdale, NY, USA). The intracellular extracts and cell wall fractions were obtained by centrifuging the sonicated cells

doi:10.6342/NTU202600056

at 13,000 *g* for 10 min at 4°C. The cell wall fraction was redissolved in sterile PBS with 1 ppm AFB1, while the extracellular supernatant and intracellular extract were mixed with 1 ppm AFB1, and all mixtures were incubated at 30°C and 220 rpm agitation for 96 h. During the incubation, 450 μL of aliquots were collected every 24 h for HPLC analysis of AFB1 concentration.

HPLC Analysis of AFB1 Concentrations

After filtration through a 0.2 μm membrane syringe filter (Pall Corporation, New York, NY, USA), 15 μL of each sample was subjected to HPLC analysis using an LC-20 AT delivery system (Shimadzu, Kyoto, Japan) equipped with an RF-10AXL fluorescence detector (Shimadzu), a Cosmosil 5C18-ARII column (Nacalai Tesque Inc., Kyoto, Japan; 250 × 4.6 mm i.d., particle size 5 μm) with a guard column (4 × 4 mm, 5 μm particle size), and a SIL-10A autoinjector (Shimadzu). The binary gradient HPLC protocol was adopted (Petchkongkaew et al., 2008) with slight modifications. It involved a fluorescence (RF) detector (λ ex = 364 nm; λ em = 440 nm) and an UV detector (λ = 225 nm and 362 nm solvents, 0.1% phosphoric acid and acetonitrile: methanol, in a ratio of 1:1 [v/v]). The organic solvent concentration was increased from 0 to 100% over 35 min, with a flow rate of 1 mL/min and column temperature of 30°C. Commercial AFB1 standards were used to generate a standard curve to quantify the AFB1 concentration, and the AFB1-residual rate was obtained using the following formula:

$$\frac{\text{AFB1 peak area in treatment}}{\text{AFB1 peak area in control}} \times 100\%$$

doi:10.6342/NTU202600056

Phenotypic and Biochemical Characterization of the c4a Strain

The c4a strain showed the highest AFB1 removal activity among the isolated strains and thus was subjected to further morphological and biochemical characterization. The c4a strain was streaked onto a sterile LB agar plate and incubated overnight at 30°C to observe colony morphology. The c4a cells were Gram stained and then observed under a microscope. The biochemical characterization and carbohydrate metabolism profiling of the c4a strain was performed using API 20 NE and API 50 CH kits (bioMerieux Inc., Marcy l'Etoile, France) according to the manufacturer's instructions.

Phylogenetic Characterization of the c4a Strain

Phylogenetic trees were constructed using single genes (*16S rRNA* and *gyrB*) and concatenated gene sequences (*rpoB*, *gyrB*, and *rpoD*). The *16S rRNA*, *gyrB*, *rpoB*, and *rpoD* gene sequences of the c4a strain (GenBank assembly accession number GCA_009900745.1) and selected type strains, including *Chryseobacterium balustinum* DSM 16775, *C. culicis* DSM 23031, *C.glaciei* IHBB 10212, *C. gleum* ATCC 35910, *C. indologenes* NBRC 14944, *C.nakagawai* G0041 (GCF_900637665.1), *C. piscium* CCUG 51923 (GCA_003385415.1), *C. scophthalmum* DSM 16779 (GCA_900143185.1), *C.timonianum* G972 (GCA_900078205.2), and *Riemerella anatipestifer* ATCC 11845 (GCA_000252855.1), were obtained from the NCBI whole genome sequence data. For the type strain, *Chryseobacterium lecithinasegens* PAGU 2197, the NCBI database contained the housekeeping genes used in this study; but the whole genome sequence was unavailable. Upon sequence alignment with BioEdit, MEGA 10.0.4 software was used to construct phylogenetic trees with 1,000 bootstrap replications using neighbor-joining and maximum likelihood algorithms.

doi:10.6342/NTU202600056

Effect of Growth Medium Composition on AFB1 Removal Activity of the c4a Strain

The extracellular supernatant of the c4a strain grown in nutrient broth, LB broth, TYE broth, and M9 medium was tested for AFB1 removal. 1% overnight c4a culture was inoculated into 100 mL growth media and incubated for 72 h in an orbital shaker at 30°C and 220 rpm. The extracellular supernatant was collected by centrifuging the bacterial culture at 10,000 *g* for 10 min at 4°C. The extracellular supernatant was mixed with 1 ppm AFB1 stock solution and incubated at 30°C for 72 h. The extracellular supernatant of the c4a strain grown in nutrient broth with gelatin peptone and beef extract in a 5:3 ratio had maximum AFB1 removal activity, so the ratio was optimized. The modified nutrient broth contained gelatin peptone and beef extract in a ratio of 1:9, 3:7, 1:1, 5:3, 7:3, 4:1, or 9:1, and the final total concentration of gelatin peptone and beef extract in the modified nutrient broth was 8 g/L. Based on AFB1 removal activity, the modified nutrient broth (modified NB) with gelatin peptone and beef extract in a 4:1 ratio was chosen as the final growth medium. Figure 5 shows phylogenetic trees based on *16S rRNA* and *gyrB* gene sequences. In the 16S rRNA phylogenetic tree, the c4a strain is located on a distinct branch with closely related neighbors, *C. timonianum* and *C. lecithinasegens* (Fig. 5a). In the gyrB phylogenetic tree, the c4a strain shared a phylogenetic branch with *C. nakagawai* and *C. lecithinasegens* (Fig. 5b). These phylogenetic trees could not determine the phylogenetic placement of the c4a strain. To improve phylogenetic resolution, multilocal sequence alignment (MLSA) was performed with a concatenated sequence of three housekeeping genes (*rpoB-gyrB-rpoD*) (Fig. 6). The c4a strain formed a direct branch with its closest neighbor, *C. timonianum*, suggesting that it might belong to *C. timonianum*.

doi:10.6342/NTU202600056

Effects of Reaction Temperature and pH, Mineral Ions, Heat Treatment, Protease Inhibitors, and SDS on AFB1 Removal Activity of the Extracellular Supernatant of the c4a Strain

The extracellular supernatant of the c4a strain was prepared as described above. To study the effects of reaction temperature on AFB1 removal activity, the extracellular supernatant of the c4a strain was mixed with AFB1 stock solution to achieve a final concentration of 1 ppm AFB1 and then incubated at 15, 20, 30, 40, 50, or 60°C for 72 h on an orbital shaker at 220 rpm. To study the effects of reaction pH on AFB1 removal activity, the extracellular supernatant of the c4a strain was mixed with AFB1 stock solution to achieve a final concentration of 1 ppm AFB1, and then the pH values of the mixtures were adjusted to 6, 7, 8, or 9 using 1 N HCl or 1 N NaOH and then incubated at 30°C for 72 h on an orbital shaker at 220 rpm. To study the effects of mineral ions on AFB1 removal activity, the extracellular supernatant of the c4a strain was mixed with $MgCl_2$, $ZnSO_4$, $CuSO_4$, $MnCl_2$, LiCl, or $FeCl_3$ stock solutions to achieve a final concentration of 10 mm of each mineral ion. Then, the mixture was mixed with AFB1 stock solution to achieve a final concentration of 1 ppm AFB1 and incubated at 30°C for 72 h on an orbital shaker at 220 rpm. To study the effects of heat treatment on AFB1 removal activity, the extracellular supernatant of the c4a strain was autoclaved at 121°C for 15 min and then mixed with AFB1 stock solution to achieve a final concentration of 1 ppm AFB1 and incubated at 30°C for 72 h on an orbital shaker at 220 rpm. To study the effects of protease inhibitors and SDS on AFB1 removal activity, the extracellular supernatant of the c4a strain was mixed with an EDTA-free protease inhibitor (cOmplete ULTRA Tablets, Mini, Roche Diagnostics, Basel, Switzerland) or SDS (5%). Then, the mixture was mixed with AFB1 stock solution to achieve a final concentration of 1 ppm AFB1 and incubated at 30°C for 72 h on an orbital shaker at 220 rpm. At the end of the experiment, aliquots of 450 μL from each sample were taken to analyze AFB1 concentration.

doi:10.6342/NTU202600056

Analysis of AFB1 Degradation Metabolites

The high-resolution LC-MS and LC-MS/MS data were collected by a Thermo UPLC-ESI Orbitrap Elite mass spectrometer equipped with an ACQUITY UPLC system (0–6 min 5–99.5% ACN, 6–8 min 99.5% ACN, 8–8.2 min 99.5–5% ACN, 8.2–10 min 5% ACN, both ACN and H2O contain 0.1% formic acid; ACQUITY UPLC BEH C18, 1.7 μm, 2.1 × 100 mm; flow rate: 0.4 mL/min). The extracellular fraction of the c4a strain and sterile growth media were dosed with 2 ppm AFB1 under optimum reaction conditions. The sample injection volume was 10 μL. Positive ion mode mass data were acquired between m/z 100–1,500 at 15,000 resolution. The top four intense ions from each full mass scan were selected for collision-induced dissociation. The selected ions were fragmented with normalized collision energy 35.0, activation Q 0.250, activation time 10.0, and 15,000 resolution for collision-induced dissociation. The isolation width was 2.5 Da (Toopaang et al., 2023). MS/MS data were obtained in duplicates utilizing data-dependent acquisition. MS scan was performed using Thermo Xcalibur 2.2 SP 1.48 software over mass-to-charge (m/z) range 100–1,500.

Statistical Analyses

All AFB1 removal experiments were performed in triplicate, and the generated data were analyzed via one-way analysis of variance (ANOVA) using RStudio version 1.2.5. Duncan's multiple range test was performed to detect statistical differences, and a p value <0.05 was considered statistically significant.

doi:10.6342/NTU202600056

Results

Isolation of Bacterial Strains with Potential for Removal of AFB1

Bacterial strains with AFB1 removal potential were isolated from chicken digesta and soil samples using the coumarin-selective medium. Three bacterial strains, 3PB1, BN5, and 4CW, were isolated from mycotoxin-fed chicken digesta; one bacterial strain, IL1, was isolated from non-mycotoxin-fed chicken digesta; and one bacterial strain, c4a, was isolated from the soil. As shown in figure 2-1, the c4a strain was the most effective AFB1 remover of the five isolated strains, so it was chosen for further investigation. Figure 2-2 represents the HPLC profile of AFB1 removal by extracellular supernatant of strain c4a, demonstrating AFB1 removal activity. The AFB1 removal activities of the intracellular extract and cell wall fraction of the c4a strain were also tested. As shown in figure 2-3, the intracellular extract and cell wall fraction of the c4a strain had negligible AFB1 removal activity, implying that c4a-mediated AFB1 removal occurs exclusively extracellularly.

Phenotypic, Biochemical, and Genomic Characteristics of the c4a Strain

When grown on LB or nutrient agar, the c4a strain produced bright yellow colonies (1–3 mm). After 18–24 h of incubation at 30°C, the isolated colonies become elevated and smooth, with a buttery consistency (figure 2-4a). The yellow-orange convex colonies indicated the presence of flexirubin pigment, which turns red when 20% KOH is added. When grown on LB agar, these colonies also emit a fruity odor. Microscopic examination of the Gram-stained c4a cells revealed red-colored rods (figure 2-4b), which were Gram-negative and exhibited no motility or endospore formation. The biochemical properties of the c4a strain were investigated using the API 20 NE system. The substrate assimilation profile of strain c4a revealed that it produced indole (tryptophan positive), urease, oxidase, hydrolyzed esculin, gelatin, assimilated glucose,

doi:10.6342/NTU202600056

mannose, maltose, and citrate. The c4a strain could not reduce nitrate to nitrogen, ferment glucose, produce arginine dihydrolase, and assimilate arabinose, n-acetylglucosamine, potassium gluconate, capric acid, adipic acid, malic acid, and phenylacetic acid. Based on these findings, the c4a strain was 99.4% identical to *C. indologenes*. However, the API database listed *C. indologenes* as the only species of the *Chryseobacterium* genus. The API 50 CH system was used to investigate further carbohydrate substrate utilization in the c4a strain. The results revealed that the c4a strain metabolized glycerol, amygdalin, esculin, d-trehalose, amidon, glycogen, gentiobiose, and xylitol (Table 2-1). Figure 5 shows phylogenetic trees based on *16S rRNA* and *gyrB* gene sequences. In the 16S rRNA phylogenetic tree, the c4a strain is located on a distinct branch with closely related neighbors, *C. timonianum* and *C. lecithinasegens* (figure 2-5a). In the gyrB phylogenetic tree, the c4a strain shared a phylogenetic branch with *C. nakagawai* and *C. lecithinasegens* (figure 2-5b). These phylogenetic trees could not determine the phylogenetic placement of the c4a strain. To improve phylogenetic resolution, multilocal sequence alignment (MLSA) was performed with a concatenated sequence of three housekeeping genes (*rpoB-gyrB-rpoD*) (figure 6). The c4a strain formed a direct branch with its closest neighbor, *C. timonianum*, suggesting that it might belong to *C. timonianum*.

Effect of Growth Medium Composition on AFB1 Removal Activity of the c4a Strain

To improve the AFB1 removal activity, the c4a strain was cultured in different growth media, and the AFB1 removal activity of the extracellular supernatants of the c4a strain was compared. As shown in figure 2-7a, the extracellular supernatant of the c4a strain cultured in nutrient broth showed the highest AFB1 removal activity, followed by those cultured in LB broth and TYE broth. The extracellular supernatant of the c4a strain cultured in M9 minimal salt (M9) medium showed the lowest AFB1 removal activity. Figure 2-7b shows the effects of varied combinations of gelatin peptone and beef extract on the AFB1 removal activity of

doi:10.6342/NTU202600056

the extracellular supernatant of the c4a strain. The extracellular supernatant of the c4a strain cultured in the modified nutrient broth containing gelatin peptone and beef extract in a ratio 4:1 showed the highest AFB1 removal activity.

Effect of Reaction Temperature on AFB1 Removal Activity of the Extracellular Supernatant of the c4a Strain

The effect of reaction temperature on AFB1 removal activity of the extracellular supernatant of the c4a strain was determined after 72 h of incubation of the extracellular supernatant of c4a with 1 ppm of AFB1 at 15, 20, 30, 40, 50, or 60°C. As shown in figure 2-8a, the AFB1 removal activity of the extracellular supernatant of the c4a strain was favored at higher temperatures, reaching a maximum at 60°C.

Effect of Reaction pH on AFB1 Removal Activity of the Extracellular Supernatant of the c4a Strain

The effect of reaction pH on AFB1 removal activity of the extracellular supernatant of the c4a strain was determined after 72 h of incubation of the CFF of c4a with 1 ppm of AFB1 at pH 6, 7, 8, or 9. As shown in figure 2-8b, the AFB1 removal activity of the extracellular supernatant of the c4a strain was more effective in the alkaline range and maximal at pH 8.

Effect of Mineral Ions on AFB1 Removal Activity of the Extracellular Supernatant of the c4a Strain

The addition of metal ions in the extracellular supernatant of the c4a strain altered the AFB1 removal activity. As shown in figure 2-8c, the addition of $Mn^{2+}$and Mg^{2+} ions significantly increased the AFB1 removal activity of the extracellular supernatant of the c4a strain while adding Fe^{3+} ions in the extracellular supernatant of the c4a strain decreased the AFB1 removal activity.

doi:10.6342/NTU202600056

Effect of Protease Inhibitors, SDS, and Autoclaved Treatments on AFB1 Removal Activity of the Extracellular Supernatant of the c4a Strain

The addition of the protease inhibitor cocktails in the extracellular supernatant of the c4a strain significantly reduced the AFB1 removal activity, and the addition of SDS completely deactivated the AFB1 removal activity of the extracellular supernatant of the c4a strain, thus suggesting that the molecule(s) in the extracellular supernatant of the c4a strain-mediated the AFB1 removal is proteinic. The AFB1 removal activity of the autoclaved extracellular supernatant of the c4a strain was retained, indicating that heat treatment did not affect the AFB1 removal activity of the extracellular supernatant of the c4a strain (figure 2-8d).

Analysis of AFB1 Degradation Metabolites

The AFB1 degradation pattern (m/z values) by the c4a strain was found to be 417.21 → 412.25 → 331.08 → 313.07 → 285.08, with loss of H_2O in the second last step, followed by loss of CO in the final step. The final degradation product had the molecular formula $C_{17}H_{14}O_7$. Figure 2-9a shows the MS-1 profile of strain c4a-mediated AFB1 degradation. It showed the predominant presence of an ion fragment of m/z 313.07. Figure 2-9b shows the MS-2 profile at m/z 331. 08, which shows the dominant presence of ion fragment m/z 313.07. Figure 2-9c shows the MS-2 profile at m/z 313.07 having an ion fragment of m/z 285.08.

Discussion

Coumarin is a phenolic compound derived from cis-*O*-hydroxycinnamic acid with a structure similar to that of AFB1, and so has been used in the selection media to screen for AFB1-degrading microbial strains (Guan et al, 2008; Rao et al, 2017; Ming et al, 2019). Coumarin media was thus employed to selectively isolate bacterial strains with the potential to remove

doi:10.6342/NTU202600056

AFB1 in the present study. Five bacterial strains, 3PB1, BN5, 4CW, IL1, and c4a, were obtained following coumarin-selective screening. The c4a strain, isolated from the chicken feather enriched soil sample, showed the highest AFB1 removal activity among the isolated strains and thus was subjected to further study.

The primary morphological and biochemical characteristics of the c4a strain were similar to the other members of the genus *Chryseobacterium*. A comparative analysis of the biochemical profiles to understand the unique metabolic capabilities of the c4a strain and its close neighbors, *C. timonianum*G972 (Abou et al., 2017) and *C. lecithinasegens* CCUG 17150 (Kutsuna et al, 2021), was carried out. All three strains tested positive for acid production using d-glucose, d-mannose, esculin, d-maltose, d-trehalose, and gentibiose. *C. lecithinasegens* and the c4a strain utilized amygdalin and produced indole, whereas *C. timonianum* did not. These comparisons revealed that the c4a strain and *C. timonianum* have a more varied metabolic profile than *C. lecithinasegens*. Unlike *C. lecithinasegens* and *C. timonianum*, the c4a strain could not metabolize glycogen or glycerol.

The 16S rRNA-based phylogenetic tree showed that the c4a strain formed a monophyletic branch with *C. timonianum* (99.21%) and *C. lecithinasegens*(98.92%). To understand the differentiation of strain c4a within this genus, another phylogenetic tree was created using *gyrB* gene sequences. The most similar sequences to strain c4a were *C. lecithinasegens* (92.92%), followed by *C. nakagawai* (92.87%) and *C. timonianum* (91.58%). The c4a strain's gyrB sequence was less than 89% similar to other *Chryseobacterium* strains. We created an additional phylogenetic tree using a rpoB-gyrB-rpoD concatenated sequence of conserved housekeeping genes and found that the c4a

doi:10.6342/NTU202600056

strain and *C. timonianum*shared a close phylogenetic relationship, implying that it may belong to *C. timonianum*.

The *Chryseobacterium* genus is classified within the Flavobacteriaceae family, Flavobacteriales order, and in the *Flavobacteriia* class. The majority of *Chrsyeobacterium* species were found in soil, freshwater or saltwater, insects, biofilms, and industrial sources like beer bottling factories. Although some *Chryseobacterium species* have been isolated from human clinical samples, it is difficult to determine whether they are direct or opportunistic pathogens or merely contaminants (Hugo). Similarly, the c4a strain was isolated from farm soil that had not been fertilized or treated with chemicals, whereas *C. timonianum*was isolated from sputum.

Characterization studies showed that the c4a strain-mediated AFB1 removal was constitutive and extracellular. There is abundant evidence of microbial degradation across multiple genera, and physical AFB1 binding to bacterial and yeast cell walls has been widely reported (Peng et al., 2018). This surface binding may not be specific, leading to binding minerals and trace nutrients like vitamins (Chung et al., 1990; Tombaevi et al., 2000). Enzymatic degradation is a more effective and targeted biocontrol strategy for AFB1 contamination. After 72 h, the c4a strain's extracellular supernatant removed the highest AFB1 in this study. The growth media components affected the c4a strain's AFB1 removal activity, with gelatin peptone being a critical media component. AFB1 removal activity of strain c4a spanned a wide temperature range and was found to be highly thermotolerant. We observed that autoclaving did not affect this phenomenon. A microbial consortium with dominant *Geobacillus* and *Tepidimicrobium* species (Wang et al., 2017) and single bacterial strains like *Escherichia coli* CG1061 (Wang et al., 2018), *Bacillus velezensis* DY3108 (Shu

doi:10.6342/NTU202600056

et al., 2018), and *Stenostrophomonas* sp. CW117 (Cai et al., 2020) have shown thermostable AFB1 removal activity at 80°C–100°C.

The pH dependence and metal cofactor specificity for the AFB1 removal activity of the c4a strain were observed, with acidic pH significantly reducing the AFB1 removal activity of the c4a strain, similar to *B. velezensis* AD8 (Zhao et al., 2022). The highest AFB1 removal activity of the c4a strain was found at pH 8, similar to that observed for *E. coli* CG1061 (Wang et al., 2018). The addition of a protease inhibitor caused a reduction in AFB1 removal activity of the c4a strain, which implied that the presence of protease positively affected AFB1 removal activity. The proteinic AFB1 removal activity was completely inhibited after SDS addition, as SDS causes the structural disintegration of proteins in the extracellular cell-free fraction. The AFB1 removal activity of the c4a strain was dependent on metal ions supplementation, with Fe^{3+} ion addition reducing AFB1 removal activity, whereas Mn^{2+} and Mg^{2+} ions significantly improved AFB1 removal activity. Fe^{3+}induced inhibition of AFB1 removal activity was found to be similar to the case of the bacterium *Myroides odoratimimus* (Mwakinyali et al., 2019). AFB1 removal improvement effect in the case of Mn^{2+} and Mg^{2+} ion additions was found to be identical to that reported for *Stenotrophomonas* sp. CW117 (Cai et al., 2020). These characterization results indicate that the AFB1 removal activity of the c4a strain resulted from complex protein interactions with excellent thermotolerance and a specific preference for pH and metal ions.

UPLC-ESI MS/MS analysis gave insight into strain c4a-mediated AFB1 degradation. At 2.55 s, a metabolite peak of various ionic fragments emerged. The MS-1 and MS-2 analyses of this peak showed that ion 313.07 m/z disintegrated into a final transformed product of 285.08. Recently, an interesting work documented all AFB1 breakdown products after UV irradiation

doi:10.6342/NTU202600056

using UPLC-Q-TOF-MS/MS and NMR (Wang et al., 2021). This report revealed the same degradation product with chemical formula C17H14O7 as the c4a strain (285.08 m/z). The transformation pattern suggested water molecule addition on the double bond (C-8/C-9) of AFB1. The article assayed degradation product toxicity on LO-2, Hep-G2, and MCF-7 cell lines (Wang et al., 2021). The cytotoxic activity (μM) of the transformed product (m/z 285.08) was much lower (>100 μm) than pure AFB1(22.47, 29.08, 36.57 μm) against LO-2, HepG2, and MCF-7 cell lines. These findings showed that strain c4a extracellular supernatant may target the C8-C9 double bond of AFB1's furan ring, lowering its cytotoxicity.

Based on the relevant literature review, AFB1 removal activity of any *Chrsyeobacterium* species has not been reported yet. To the best of our knowledge, this is the first report of the AFB1 removal potential of a bacterial strain belonging to *C. timonianum*. This evidence makes the current study a promising reference for future studies concerning the environmental biocontrol of AFB1 by *C. timonianum*.

doi:10.6342/NTU202600056

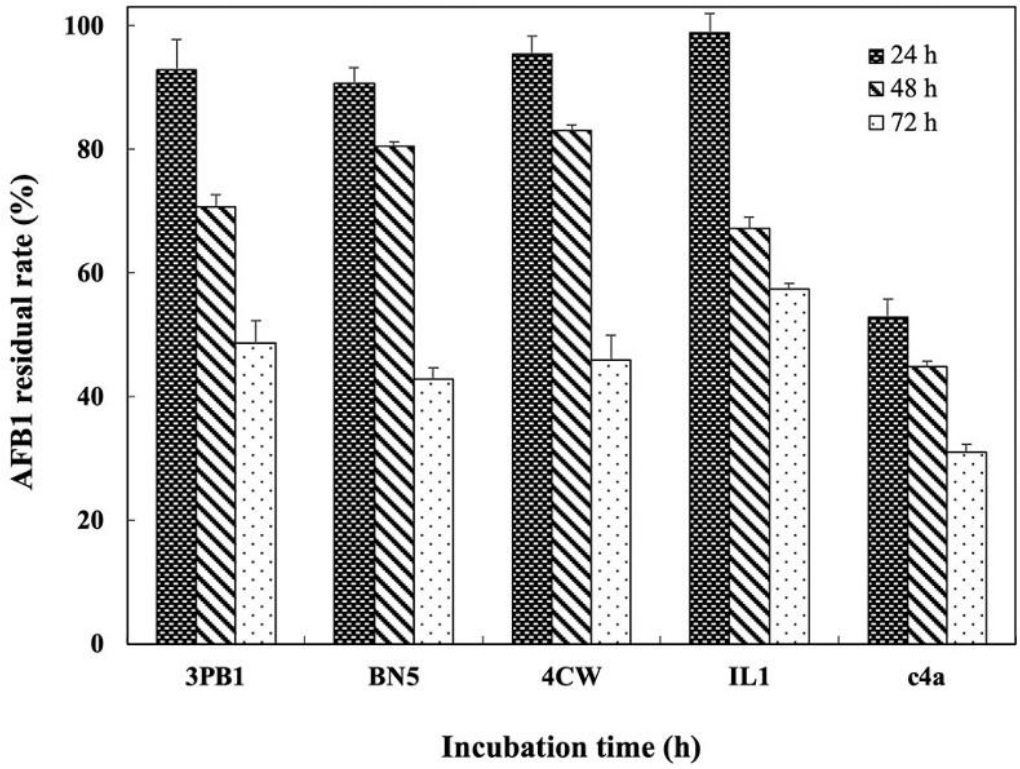


Figure 2-1. AFB1 removal activity of the isolated bacterial strains. All data are expressed as mean ± SD (n = 3).

doi:10.6342/NTU202600056

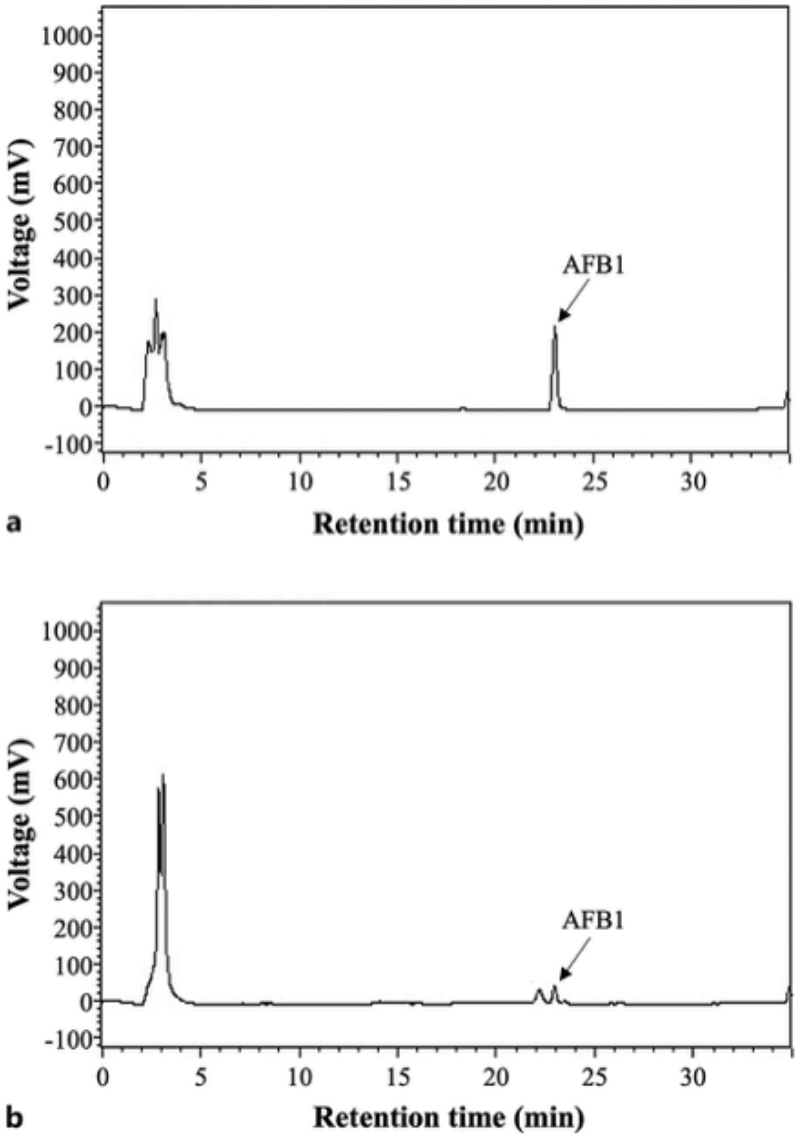


Figure 2-2. High-performance liquid chromatography (HPLC) profile of AFB1 removal by the c4a strain. **a.** HPLC profile of AFB1 in nutrient broth. **b.** HPLC profile of AFB1 removal by the extracellular supernatant of the c4a strain.

doi:10.6342/NTU202600056

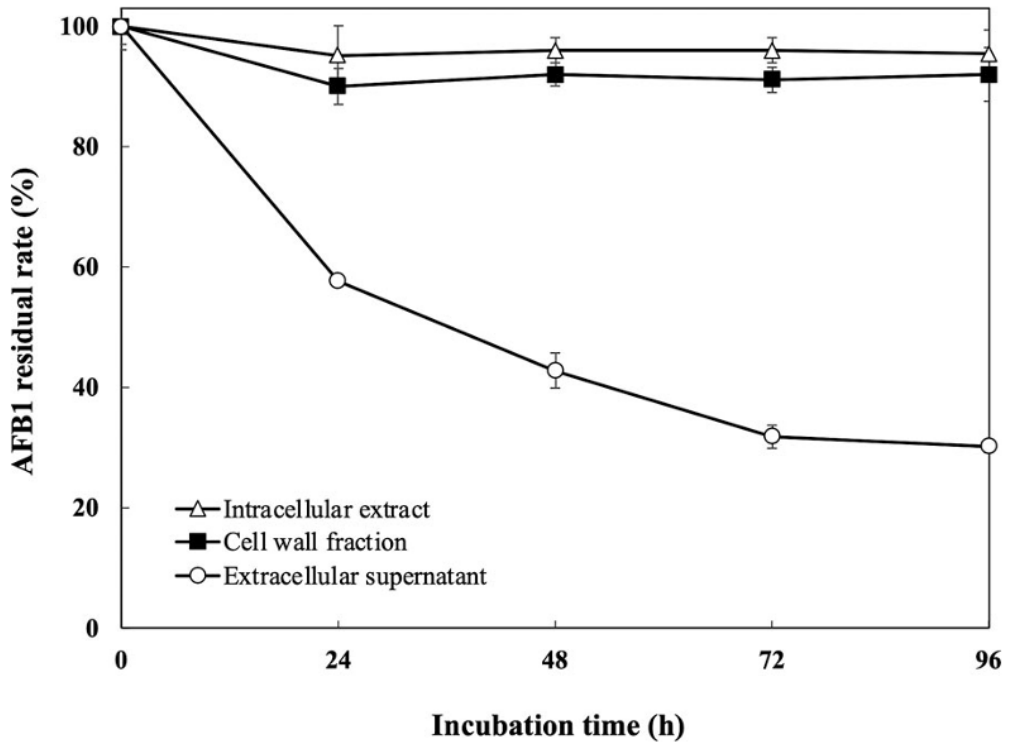


Figure 2-3. Removal of AFB1 by intracellular extract, cell wall fraction, and extracellular supernatant of the c4a strain. All data are expressed as mean ± SD (*n* = 3).

doi:10.6342/NTU202600056

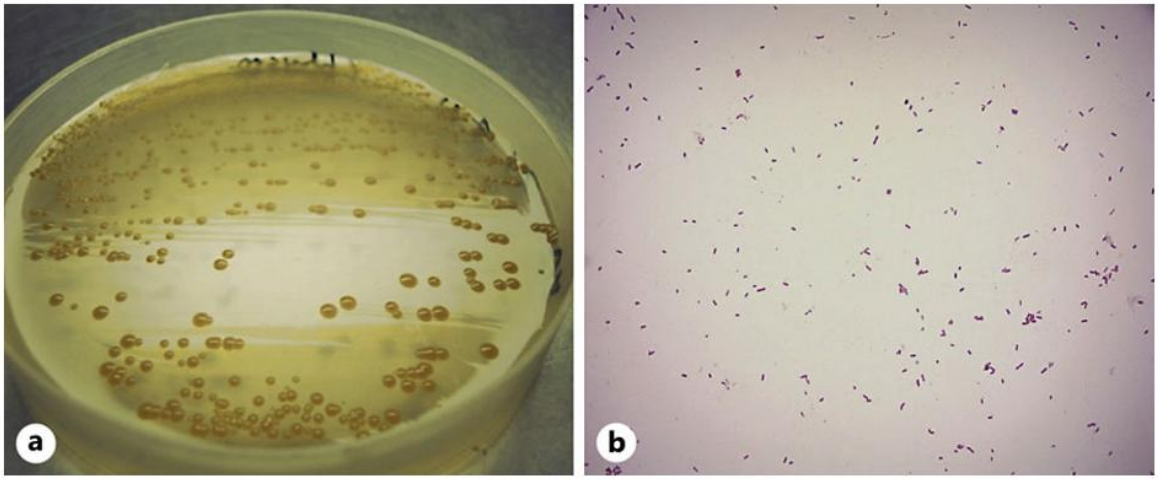


Figure 2-4. Macroscopic and microscopic examinations of the c4a strain. **a.** The colony morphologies of the c4a strain on LB agar plate. **b.** Gram-stained c4a cells observed under a phase-contrast microscope (×1,000).

doi:10.6342/NTU202600056

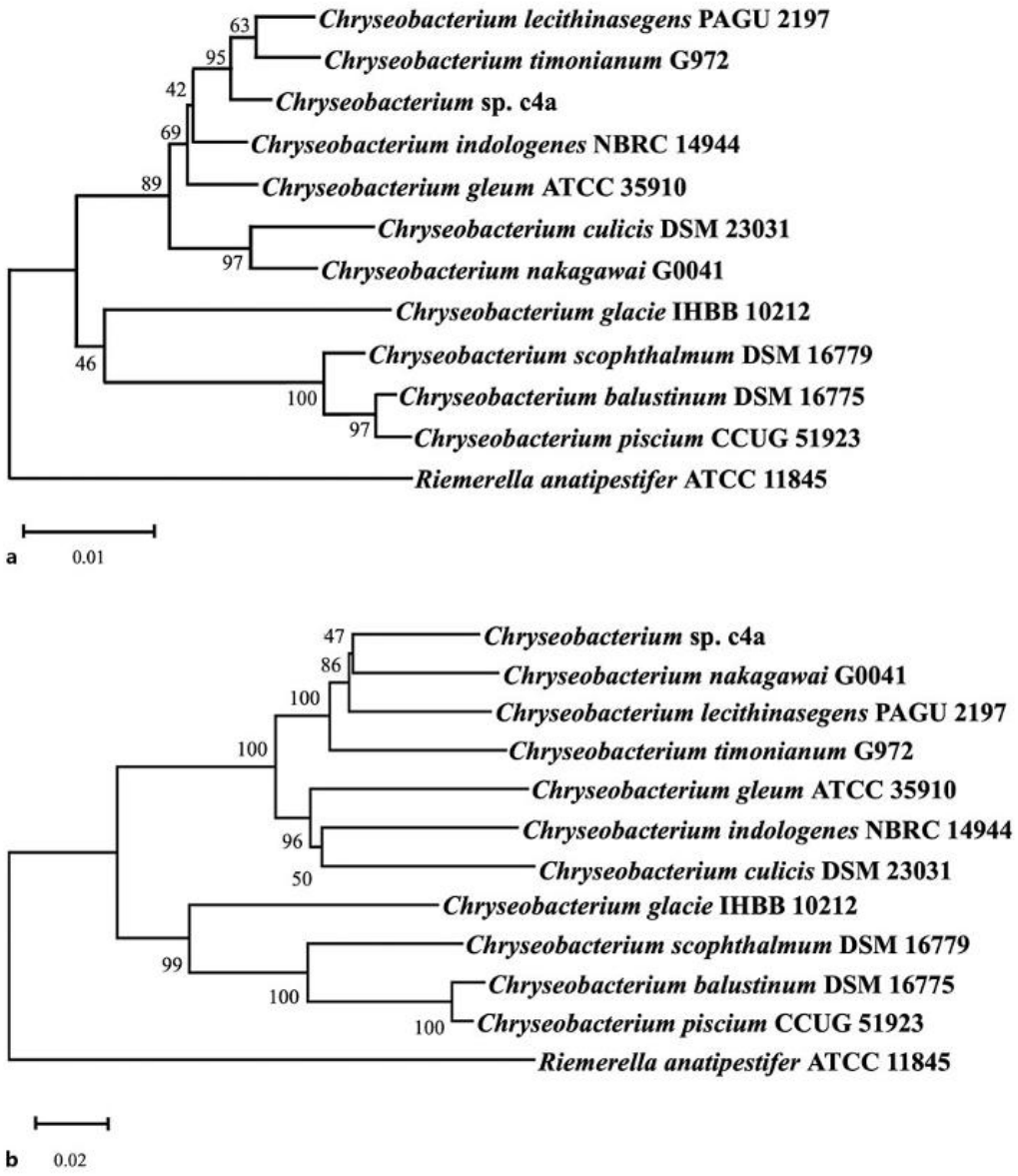


Figure 2-5. Neighbor-joining phylogenetic tree-based analyses of the 16S rRNA and DNA gyrase B (*gyrB)* genes of *Chryseobacterium* species. **a.** Neighbor-joining phylogenetic tree based on *16S rRNA* gene sequences. The scale bar represents 0.01 nucleotide substitution per nucleotide position. **b.** Neighbor-joining phylogenetic tree based on *gyrB* gene sequences. The scale bar represents 0.02 nucleotide substitution per nucleotide position. At major nodes, bootstrap percentages for 1,000 re-samplings are shown.

doi:10.6342/NTU202600056

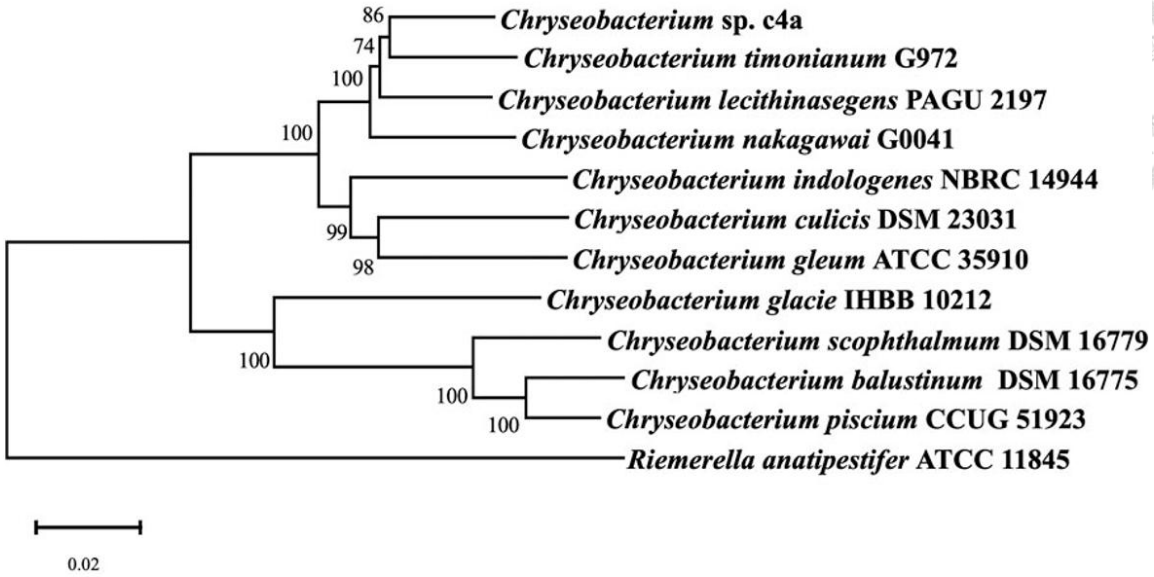


Figure 2-6. Neighbor-joining phylogenetic tree-based analyses of the RNA polymerase β subunit (rpoB), DNA gyrase B (*gyrB)*, and σ factor of RNA polymerase (rpoD) of *Chryseobacterium* species. The scale bar represents 0.02 nucleotide substitution per nucleotide position. At major nodes, bootstrap percentages for 1,000 re-samplings are shown.

doi:10.6342/NTU202600056

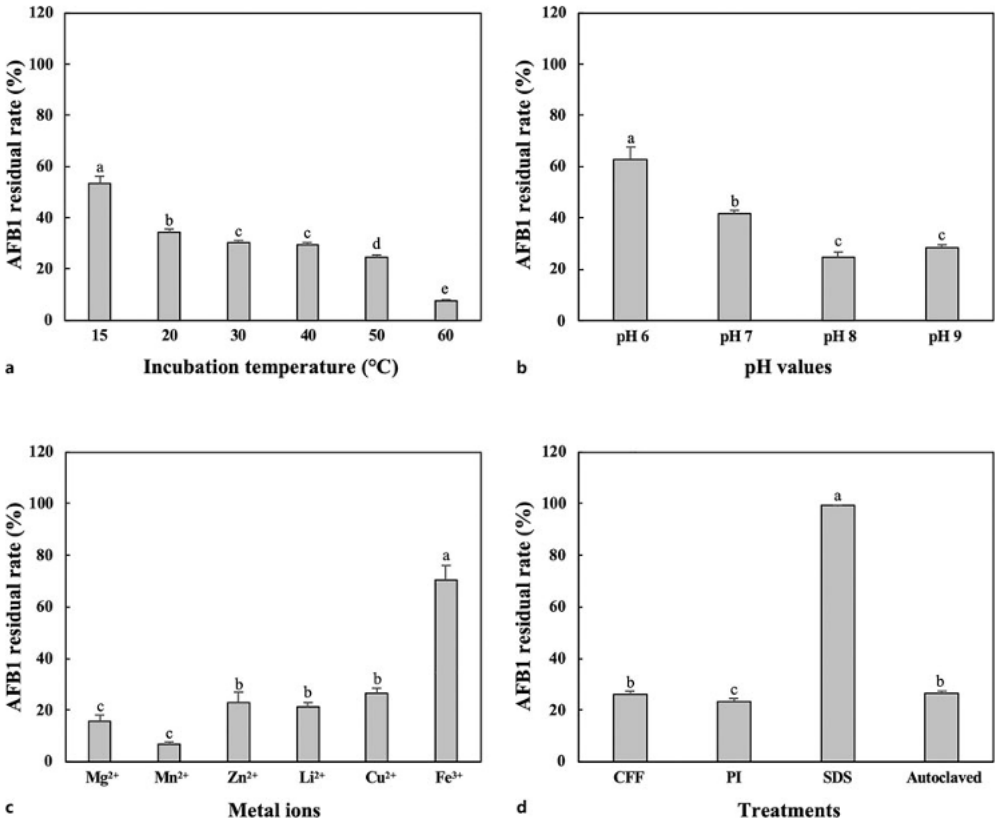


Figure 2-7. Effects of reaction temperature (**a**), reaction pH (**b**), supplementation of mineral Ions (**c**), and protease inhibitors, SDS, and autoclave treatment (**d**) on the AFB1 removal activity of the extracellular supernatant of c4a strain. Effects of incubation temperatures, pH values, mineral ions, heat, and proteinase inhibitor on AFB 1 biodegradation by the c4a strain. All data are expressed as mean ± SD (n = 3). Bars marked with the same letter are not significantly different ($p > 0.05$).

doi:10.6342/NTU202600056

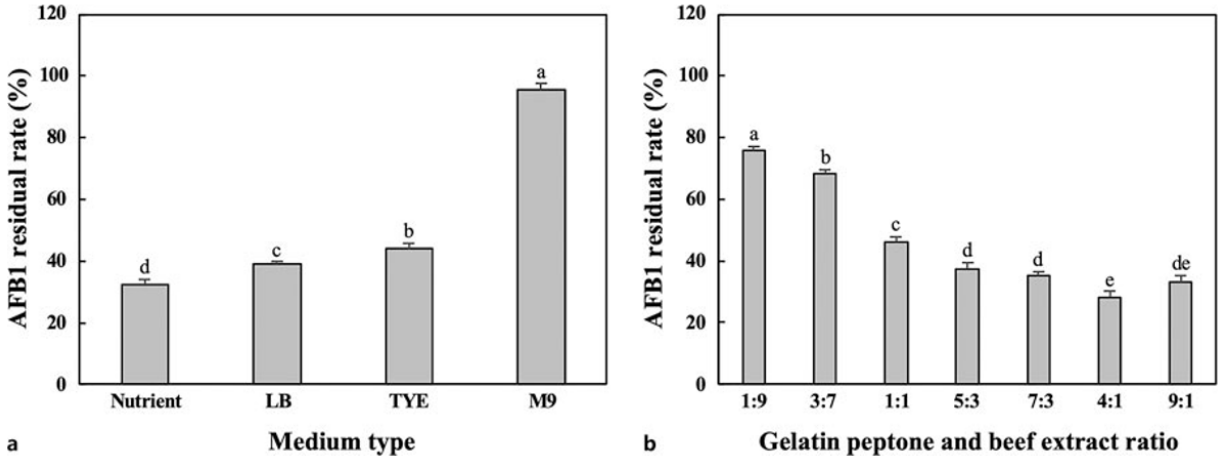


Figure 2-8. Effect of growth medium composition on the AFB1 removal activity of the c4a strain. **a** Effect of nutrient broth, LB broth, TYE broth, and M9 medium on the AFB1 removal activity of the c4a strain. **b** Effect of the ratio of gelatin peptone and beef extract in the nutrient broth on the AFB1 removal activity of the c4a strain. All data are expressed as mean ± SD (n = 3). Bars marked with the same letter are not significantly different (p > 0.05).

doi:10.6342/NTU202600056

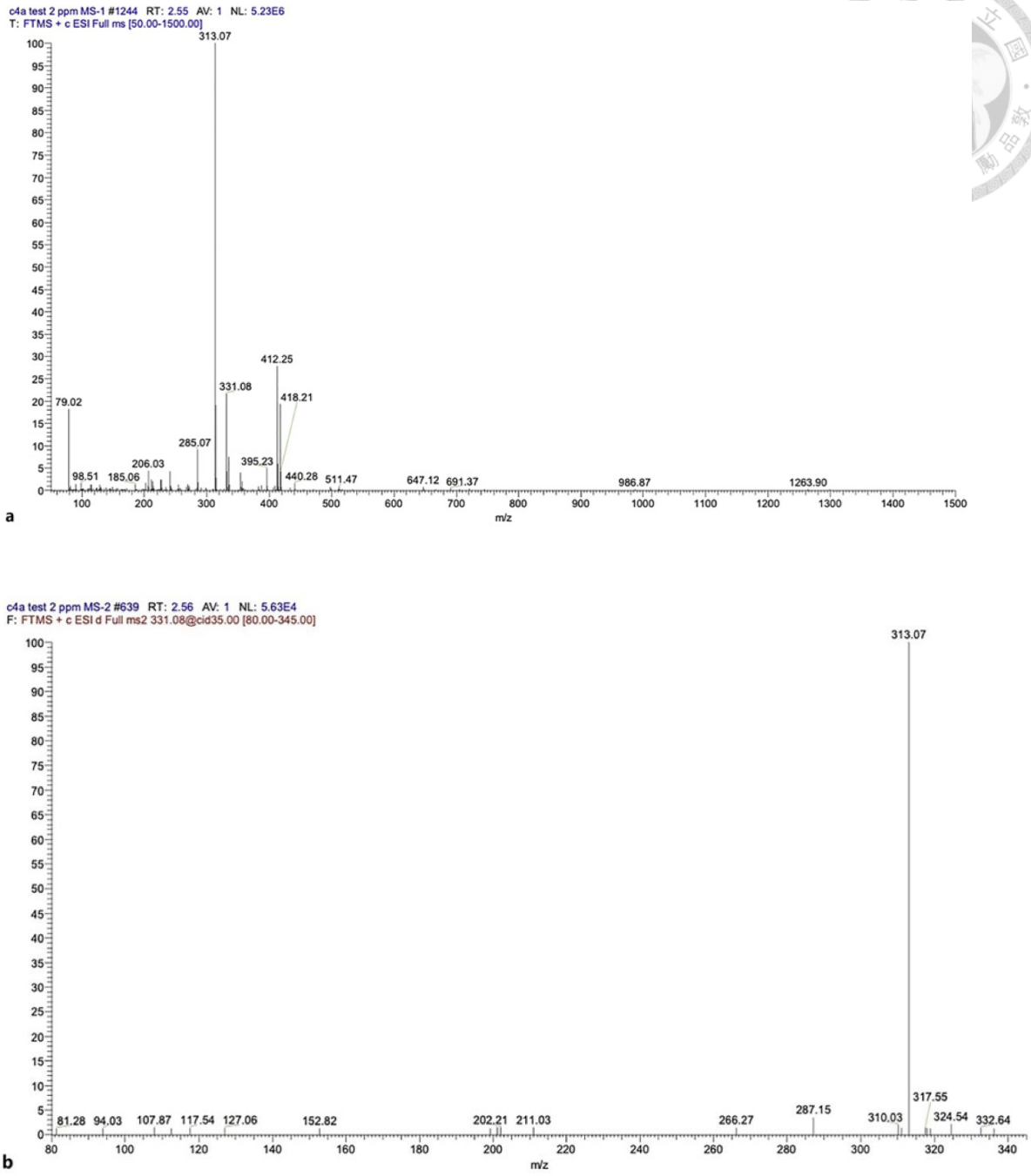


Figure 2-9. The AFB1 degradation pattern (m/z values) mediated by c4a strain. **a.** MS-1 profile of strain c4a-mediated AFB1 degradation. **b** MS-2 profile of ion fragment with m/z 331.08.

doi:10.6342/NTU202600056

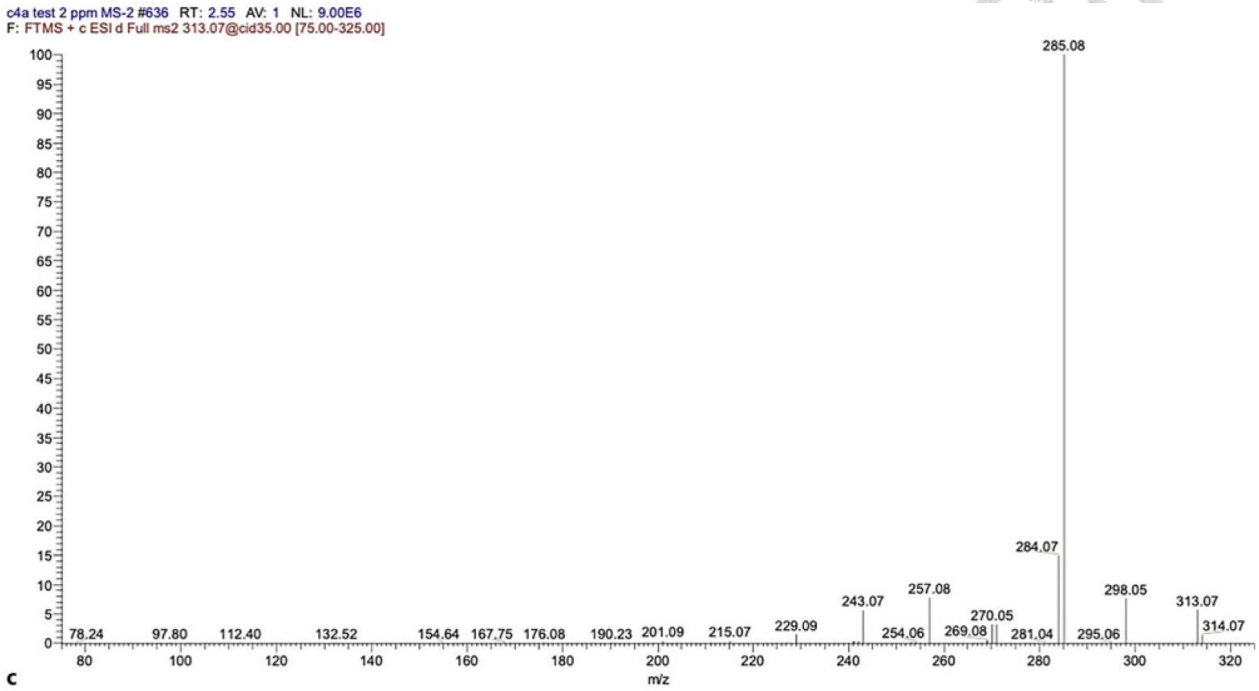


Figure 2-9. c MS-2 profile of ion fragment with m/z 313.07.

doi:10.6342/NTU202600056

Table 2-1 Biochemical characteristics of c4a strain

Substrate	Result	Substrate	Result
N-Acetyl-glucosamine	–	D-Lyxose	–
Adipic acid	–	Mallic acid	–
Adonitol	–	D-Maltose	+
Amygdalin	+	D-Mannitol	–
D-Arabinose	–	D-Mannose	+
L-Arabinose	–	Melezitose	–
D-Arabitol	–	Melibiose	–
L-Arabitol	–	α-Methyl-D-glucoside	–
Arbutin	–	α-Methyl-D-mannoside	–
L-Arginine	–	β-Methyl-xyloside	–
Capric acid	–	4-Nitrophenyl-β-D-glucopyranoside	–
Cellobiose	–	Phenylacetic acid	–
Dulcitol	–	Potassium gluconate	–
Erythritol	–	D-Raffinose	–
Esculin ferric citrate	+	Rhamnose	–
D-Fructose	–	Ribose	–
D-Fucose	–	Saccharose	–
L-Fucose	–	Salicin	–
Galactose	–	Sorbitol	–
Gelatin	+	L-Sorbose	–
β-Gentiobiose	+	Starch	–
Gluconate	–	D-Tagatose	–
D-Glucose	+	Trehalose	+
Glycerol	+	Tri-sodium citrate	+
Glycogen	+	L-Tryptophan	+
Inositol	–	D-Turanose	–
Inulin	–	Urea	+
5-Keto-gluconate	–	Xylitol	–
2-Keto-gluconate	–	D-Xylose	–
Lactose	–	L-Xylose	–

doi:10.6342/NTU202600056

Chapter III

Unpublished Data

In this chapter, experiments conducted during my doctoral program, following the completion of the previous studies, are compiled. I performed these experiments under the guidance of Dr. Je-Ruei Liu.

The results shared in this chapter are unpublished elsewhere in any journal or conference. Following the first confirmation of strain c4a's robust AFB1 breakdown capability, I investigated the genetic factors contributing to this anti-AFB1 phenomenon. By analyzing whole-genome sequencing data from this strain, candidate genes known to be anti-AFB1 were identified using bioinformatic tools. I recombinantly expressed these genes into expression vectors and analyzed the purified enzyme products against AFB1 and other mycotoxins (Deoxynivalenol and Zearalenone). Along with the anti-mycotoxin activity search, I also tested the bioconversion ability of the cloned gene AKR 15_78 against industrially important bulky ketones whose reaction metabolites can be used as important active pharmaceutical precursors.

Materials and Methods

Genome Sequencing and Assembly

Whole-genome sequencing and subsequent data analysis were performed at the NGS core lab in the Center for Biotechnology, National Taiwan University. A pure culture of strain c4a had been obtained earlier on sterile Luria agar plates. From there, a single isolated colony was transferred to liquid broth for overnight growth, and genomic DNA was then extracted

doi:10.6342/NTU202600056

using the QIAamp DNA Microbiome Kit from QIAGEN. The concentration and purity of the gDNA were checked with the Qubit dsDNA HS Assay Kit (Thermo Fisher Scientific), and integrity was further confirmed by running samples on agarose gel electrophoresis. Library preparation followed the standard protocol of the TruSeq Nano DNA Lib Prep Kit for Illumina. Sequencing itself was done as paired-end reads on the NextSeq Illumina platform, which generated roughly one gigabase of raw data in total. Adapter sequences were trimmed off using CASAVA from Illumina, and quality filtering removed reads falling below Q30, with FastQC used for the screening step. The resulting clean reads showed an average G+C content of about 45%. *De novo* assembly of these reads was carried out with the A5-Miseq pipeline. Gene prediction combined protein homology searches via the Exonerate program with ab initio predictions from Augustus. BUSCO was also run to benchmark the completeness of the predicted gene set. Functional annotation relied on BLAST2GO, and once everything was finalized, the whole genome sequence was deposited in NCBI GenBank under accession number WXVU00000000.

Native Activity Assay of Strain c4a

The strain c4a was inoculated into tubes containing the dyes Remazol brilliant blue and Congo red. Incubation was carried out at 30°C for 72 hours under static conditions. Dye concentrations were 100 mg/L for Remazol brilliant blue and 50 mg/L for Congo red (Velayutham et al., 2018). Control tubes without inoculation were run in parallel to account for any abiotic decolorization.

Identification of Anti-Mycotoxin Genes

To identify potential anti-mycotoxin genes in the assembled genome, a customized workflow was applied, the details of which are outlined in Figure 3-3. This workflow began with mapping the predicted proteins against the bacterial non-redundant database, followed by

doi:10.6342/NTU202600056

domain predictions using InterPro, particularly for candidates like the laccase sequence on scaffold 21_56. The conserved catalytic tetrad (Tyr-Lys-His-Asp) typical of aldo-keto reductases was identified in all AKR genes, as illustrated in Figure 3-5. A customized bioinformatics workflow was therefore developed to identify candidate anti-mycotoxin genes (Figure 3-3). Literature review identified reported enzymes active against aflatoxin B1 (AFB1), deoxynivalenol (DON), or zearalenone (ZEN). Candidate amino acid sequences were retrieved and BLAST-searched against UniProt. Resulting hits were pBLASTed against the c4a genome. Candidates underwent domain analysis using RedOxiBase, the Laccase Database (biocathnet LcCED v6.4.12), InterPro, Pfam, and PROSITE. Signal peptides were predicted with SignalP 5.0. Domain motifs (e.g., copper-binding sites, GXXDG heme motif, catalytic tetrad) were aligned using Clustal Omega. All primers designed and used for amplification and verification steps are listed in Table 3-5.

Cloning of Target Genes

Cloning of the selected target genes into the expression vector was done using the ligation-independent method described in the Novagen pET-32 Xa/LIC Vector Kit. The genes of interest included the laccase and three aldo-keto reductases designated AKR 1_282, AKR 4_167, and AKR 15_78. Primers were designed with the required 5' extensions for directional insertion: the forward primer carried 5'-GGTATTGAGGGTCGC-3' upstream of the gene-specific sequence, and the reverse primer had 5'-AGAGGAGAGTTAGAGCC-3' while omitting an in-frame stop codon so that the C-terminal fusion tags remained intact. Amplification was performed with KOD Hot Start DNA Polymerase. The cycling conditions started with 95°C for 2 min, then 35 cycles of 95°C for 20 s, 55°C for 10 s, and 70°C for 30 s per kb, ending with a final extension at 70°C for 5 min. The PCR products were cleaned up using the SpinPrep PCR Clean-Up Kit to remove leftover primers, nucleotides, and enzyme.

doi:10.6342/NTU202600056

Vector-compatible overhangs were generated by treating 0.2 pmol of each purified insert with LIC-qualified T4 DNA Polymerase in a 20 µL reaction that included 2 µL 10× buffer, 2 µL 25 mM dGTP, 1 µL 100 mM DTT, and 1 U of the enzyme. This mixture was incubated at 22°C for 30 min and then inactivated at 75°C for 20 min. Annealing was achieved by combining 0.02 pmol of the treated insert with 1 µL of the linearized pET-32 Xa/LIC vector, incubating at 22°C for 5 min, and then adding 1 µL of 25 mM EDTA for an additional 5 min. One microliter of the annealed product was transformed into NovaBlue GigaSingles competent cells through the usual heat-shock protocol: 5 min on ice, 30 s at 42°C, 2 min back on ice, followed by 1 h recovery in 250 µL SOC medium at 37°C with shaking. Cells were plated on LB agar supplemented with 50 µg/mL carbenicillin and grown overnight at 37°C. Positive colonies were screened by colony PCR using the pET Upstream Primer and T7 Terminator Primer. Clones were boiled in water for 5 min to release the template, and 10 µL of the lysate was used in a 50 µL reaction with NovaTaq DNA Polymerase, which was run for 35 cycles (94°C for 1 min, 55°C for 1 min, 72°C for 2 min). Insert sizes were checked on agarose gels. Plasmids from verified clones were purified using the Qiagen Plasmid Purification Kit, and full insert sequences were confirmed by primer walking. The correct recombinant plasmids were finally transformed into the expression host E. coli Rosetta-gami 2(DE3)pLysS under the same transformation conditions, selecting on LB agar containing 50 µg/mL carbenicillin and 34 µg/mL chloramphenicol. The basic plasmid map is shown in Figure 3-6. The overall cloning and transformation workflow is illustrated in Figure 3-7.

Recombinant Protein Expression and Purification

Recombinant protein expression was carried out in Rosetta-gami 2(DE3)pLysS cells harboring the individual constructs. Initial expression studies with AKR and laccase were performed at 17°C and 25°C using IPTG induction. A pre-culture was first prepared by

doi:10.6342/NTU202600056

inoculating 5 mL of LB at 37°C for 21 h, OD 1.105. This pre-culture was then used to build a seed culture in 10 mL of LB at 30°C for 18 h, with 1% glucose, OD 1.8. The seed culture was subsequently transferred to a 40 mL fermentation volume (4 flasks), 30°C, 1 mM IPTG, 190 rpm, induction for 24 h. Sonication followed. Binding buffer was 20 mM imidazole, 50 mM Tris Cl, pH 7.5. The elution buffer was 300 mM imidazole, 50 mM Tris Cl, pH 7.5. A HisTrap IMAC column was used for binding. The purification continued with FPLC elution from the His-trap IMAC column. Fractions containing the target protein were pooled, concentrated using Vivaspin centrifugal concentrators, and then dialyzed against 20 mM Tris-Cl, pH 8, to remove imidazole and prepare the enzyme for assays. This final buffer was selected because earlier tests showed the protein remained stable and active under those conditions. This step-wise scale-up and temperature shift were applied consistently across all targets, with the laccase construct additionally tested under copper supplementation in separate runs, which did not noticeably improve expression. Cells were lysed, and soluble and insoluble fractions were separated by centrifugation before running on SDS-PAGE. For the laccase construct, copper supplementation with 1.3 mM CuSO4 was tested in some inductions. The most promising AKR, 15_78, was purified by FPLC for downstream enzyme assays. The overall scheme for AKR 15_78 expression and downstream processing is shown in Figure 3-13.

Enzyme Assays and Functional Characterization

Enzyme assays for AKR 15_78 were performed as described by Ni et al., (2010), with slight modifications. For the assay with ethyl pyruvate at 340 nm, the reagents were: ethyl pyruvate 2 mM 2 µL, NADH 0.5 mM 12.5 µL, enzyme purified 30 µL, buffer 955.5 µL. OD was taken after 10 min of incubation at room temperature. Initial cofactor screening tested NADH,

doi:10.6342/NTU202600056

NADP, and NADPH against ethyl pyruvate as the substrate. Once the preferred cofactor was identified, optimum temperature and pH were determined using the FPLC-purified, concentrated, and dialyzed enzyme. Mycotoxin degradation potential was evaluated by incubating purified AKR 15_78 with AFB1 and ZEN at 1 ppm or DON at 30 ppm in suitable buffers, followed by extraction and quantification. When no activity was detected there, attention shifted to chiral ketone reduction, since optically active alcohols are valuable chiral building blocks in the pharmaceutical industry. Substrate screening and stereospecificity checks followed approaches based on Liang et al. (2018). For ethyl 4-chloroacetate, mobile phase n-hexane-isopropanol (9:1), 210 nm, 0.8 mL/min, 25°C, Chiralcel OB-H column; for ethyl 2-oxo-4-phenylbutyrate, mobile phase hexane/2-propanol (19:1), 210 nm, 0.8 mL/min, 25°C, Chiralcel OB-H column; for ethyl benzoyl acetate, mobile phase n-hexane-2-propanol (9:1), 220 nm, 25°C, OB-H Chiralcel column were used. Reduction was first monitored by a change in absorbance, and promising substrates were then analyzed by chiral HPLC after desalting on a Strata column and solvent evaporation by a cold trap (Eyela UT 2000). The general strategy for these conversions is summarized in Figure 3-19. The substrates were purchased from Sigma.

Results

GenomeAssembly and Annotation

The *de novo* assembly produced a draft genome whose basic statistics were compared to related BioProjects in Table 3-1. Contig and scaffold numbers were acceptable for the amount of data, though fragmentation remained in some regions, which was not unexpected given the sequencing depth. Mapping of predicted proteins to the bacterial nr database gave the rates shown in Table 3-2. A reasonable fraction found homologs, which later helped guide the functional annotation and candidate gene selection. BUSCO assessment of genome

doi:10.6342/NTU202600056

completeness is presented in Table 3-3. Most single-copy orthologs were recovered, though a small number were missing—possibly due to genuine absence or minor assembly issues that could be resolved with more data later. The overall sequencing and assembly pipeline is depicted step-by-step in Figure 3-1.

Native Activity Assay Outcomes

Whole-cell decolorization tests showed clear differences between tubes inoculated with c4a and uninoculated controls (Figure 3-2). Remazol brilliant blue was substantially decolorized in the presence of the strain, while c4a growth was observed in Congo red without decolorization, indicating that c4a possessed some dye-degrading capacity, potentially linked to the oxidoreductases flagged in the genome.

Identification and in silico Characterization of Anti-Mycotoxin Candidates

The list of putative anti-mycotoxin genes identified through the mining workflow is in Table 3-4. This included one laccase and several aldo-keto reductases that appeared promising on paper for roles in oxidative or reductive detoxification. The customized gene mining workflow that led to these candidates is illustrated in Figure 3-3. Domain architecture predicted by InterPro for the laccase on scaffold 21_56 is shown in Figure 3-4, confirming the presence of characteristic multicopper oxidase motifs. Alignment of the conserved catalytic tetrad in the AKRs is given in Figure 3-5; the residues matched well with known functional enzymes.

Cloning Verification

Cloning was verified by agarose gel electrophoresis of the purified plasmids. Figure 3-8 shows the results for the laccase insert, and Figure 3-9 shows the results for the three AKR

doi:10.6342/NTU202600056

inserts. Bands appeared at the expected sizes in each case, confirming successful ligation-independent cloning after minor primer adjustments in the early attempts.

Recombinant Protein Expression

Protein expression trials at 25°C revealed differences in solubility among the AKRs (Figure 3-10). AKR 15_78 consistently gave the strongest band in the soluble fraction, while the others partitioned more into inclusion bodies. The SDS-PAGE gel from the 17°C induction showed soluble (S) and insoluble (P) fractions for laccase and the three AKRs. Laccase lanes (LacS, LacP) showed no obvious overexpressed bands and appeared to match the background. AKR 1 and AKR 4 fractions were weak, mostly in pellets. AKR 15_78 stood out—the soluble lane (15S) had a strong band around 35–48 kDa (circled), while the pellet (15P) had much less. This confirmed AKR 15_78 gave the highest soluble expression at 17°C, far better than the other two AKR genes and laccase (Figure 3-11). This made it the main focus for purification and assays.

The SDS-PAGE gels compared laccase expression with and without 1.3 mM $CuSO_4$ supplementation. In the Coomassie-stained gel (Figure 3-12a), no clear band around 135 kDa appeared in any lane—even after 48 h of induction—whether copper was added or not; the background proteins dominated. Silver staining (Figure 3-12b) finally revealed a very faint band (circled) at the expected size only in the $CuSO_4$-supplemented samples after prolonged induction. Without copper, nothing showed up there either. Overall, expression remained low and the gene seemed somewhat toxic, as host proteins were suppressed post-induction. This poor yield was why laccase work was set aside early on.

The general scheme for the recombinant expression of AKR 15_78 was followed as outlined. Purification of AKR 15_78 by FPLC yielded a main peak in fraction 5, as seen in the chromatogram (Figure 3-14). The SDS-PAGE gel for AKR 15_78 showed clear differences

doi:10.6342/NTU202600056

across samples. Uninduced lanes (Sol and Ins) appeared as a typical host background, with no additional bands. After induction, the soluble fraction (Sol) had a strong band around 35–48 kDa (bracketed), matching the expected size for the His-tagged protein. The insoluble fraction (Ins) had only a faint trace of it, meaning most of the overexpressed AKR stayed soluble. The FPLC-eluted fraction and the Vivaspin-concentrated one both showed a single clean band at the same position, confirming good purity after purification. This gel verified that induction worked well and the purification steps effectively isolated soluble AKR 15_78 for the enzyme assays.

Biochemical Characterization of AKR 15_78

While testing for cofactor suitability, NADPH gave nearly 100% relative activity against ethyl pyruvate. NADH and NADP showed almost no activity—bars barely above zero. This confirmed that the enzyme strongly preferred NADPH as a cofactor. The optimum temperature assay for AKR 15_78 was run across a range from about 10°C to 90°C. Activity increased steadily up to around 30°C, where it peaked close to 100% relative activity. Then it held fairly high through 40°C before dropping off more sharply after 50°C, down to almost nothing by 90°C. The curve looked typical for a mesophilic enzyme. This set the working optimum at 30–40°C, which was used for the subsequent substrate tests. The pH assay covered from pH 4 to 11. Activity was low at acidic pH, began improving around pH 5–6, reached a maximum near pH 7, remained high through pH 8, then fell off steadily toward the alkaline side, dropping sharply after pH 9 to minimal levels at pH 11. The profile was bell-shaped, centered around neutral to slightly alkaline, with the highest point right at pH 7–8. Both assays used the standard ethyl pyruvate setup with NADPH as cofactor.

doi:10.6342/NTU202600056

Functional Assays

When purified AKR 15_78 was tested against the mycotoxins AFB1, ZEN, and DON at the specified concentrations, no measurable degradation occurred. That line of investigation was set aside.

Attention then turned to the reduction of chiral alcohols. Initial screening of bulky ketone substrates gave the activity summary in Table 3-6. Several showed a detectable decrease in OD, indicating turnover. The analytical strategy applied to the substrates is outlined in Figure 3-19. Chiral HPLC chromatograms for ethyl-2-oxo-4-phenylbutyrate and ethyl benzoyl acetate (Figure 3-20a and b) revealed that AKR metabolized both substrates. Ethyl-2-oxo-4-phenylbutyrate was converted into a new product with a retention time of 20.61 minutes. The S-form enantiomer of ethyl 2-hydroxy-4-phenyl butyrate was expected to be obtained by reacting AKR with this substrate, but the retention time (20.61 minutes) of the metabolized compound was found to differ (Liang et al., 2018). Interesting results were obtained with the substrate ethyl benzoyl acetate (Figure 3-20b)—the substrate was metabolized to a compound that eluted at 10.5 minutes. This matched very closely with the retention time of the important chiral compound 3-hydroxy-3-phenylpropionate (Liang et al., 2018). When AKR was reacted with the substrate ethyl-benzoyl acetate, no utilization was observed. In the reaction with ethyl 4–chloroacetate, the AKR metabolized product had a retention time of 16.29 minutes. The pure chiral product samples, ethyl-R-4-chloro 3-hydroxybutyrate and ethyl-S-4-chloro 3-hydroxybutyrate, showed retention times of 9.8 minutes and 10.50 minutes, respectively (Figure 3-21). These outcomes indicated that, while AKR 15_78 exhibited reductase activity, its stereospecificity and substrate range did not align perfectly with the targeted transformations, except for ethyl benzoyl acetate.

doi:10.6342/NTU202600056

Table 3-1. *De novo* assembly results compared with other BioProjects

		4.88 – 5.83	14 - 171	22188 - 371052
BioProject	Genome coverage	Total length	Contig (#)	N50
PRJNA281304	187.8x	5.83M	171	106549
PRJDB276	103x	4.75M	33	371052
PRJNA295461	79.48x	4.86M	82	240856
PRJEB12508	-	4.97M	381	22188
PRJEB17385	-	4.88M	14	676140
Our (c4a)	134-158x	5.41M	56	210711

doi:10.6342/NTU202600056

Table 3-2. Predictive genes mapping rate against the bacterial nr database

Mapping rate	Predictive genes
98.8%	3539

Mapping rate: Ratio of predictive genes mapped in bacteria non-redundant databases and the total 3579 predictive genes. (E-value $<10^{-6}$)

doi:10.6342/NTU202600056

Table 3-3. BUSCO benchmark assessment for predictive genes

Lineage	Completely found	Partially found	Missing
Bacteria	141 (95.27%)	1 (0.68%)	6 (4.05%)

BUSCO was performed in protein mode, with a total of 148 BUSCOsthe bacterial lineage

doi:10.6342/NTU202600056

Table 3-4. Anti-mycotoxin genes identified in the *C. timonianum* c4a genome

c4a gene	NCBI Accession Number	Reported Action Against	References
Laccase	WP_160139647	AFB1, ZEN	Gao et al., 2024; Zhang and Yang, 2025
DyP peroxidase	WP_160139647	AFB1, DON, ZEN, Azo dyes	Qin et al., 2021; An et al.,2023; Mangini et al., 2023
Aldo-keto reductase	WP_160139289, WP_160136907, WP_160136907	AFB1, DON	Abraham et al., 2022; Jiang et al,2024
Chitinase	WP_160136851	AFB1-producing fungus	Hawkins et al., 2015

doi:10.6342/NTU202600056

Table 3-5. Primers used in the study

Gene	Primer set (5' → 3')	Gene size
Laccase	Forward: GGTATTGAGGGTCGCAAAAAATTATTAATGTTTCTGGTGCTTTTG Reverse: AGAGGAGAGTTAGAGCCTTAATAGGTTAAGGTAATACCAGCTC	2814 bp
AKR 1_282	Forward: GGTATTGAGGGTCGCTATAATAATTTTGGAGAAGATTTAACAGAAAA Reverse: AGAGGAGAGTTAGAGCCTTAGTCATACCTTTCCTGATCGTTCT	1134 bp
AKR 4_167	Forward: GGTATTGAGGGTCGCAAATTTAAAAAATTAGGAAACACTGGTGAAC Reverse: AGAGGAGAGTTAGAGCCTTAGTTGTTGACCAGTTTCATTGAACCTT	984 bp
AKR 15_78	Forward: GGTATTGAGGGTCGCGAATATAGAAAATTAGGAAACACAGATTTAG Reverse: AGAGGAGAGTTAGAGCCTTAAATCTCGCTTAAAGCAGCGTTGAT	1002 bp
Kit specific primers	Forward: ATGCGTCCGGCGTAGA Reverse: GCTAGTTATTGCTCAGCGG-3	

doi:10.6342/NTU202600056

Table 3-6. AKR 15_78 action on selected chirally important substrates

Substrate + AKR	**Blank OD 340 nm**	**Test OD 340 nm**
Ethyl benzoyl acetate	3.85	2.14
Methyl benzoyl formate	1.54	0.35
Ethyl 2-oxo- 4 phenylbutyrate	3.8	0.34
1-benzyl-3-pyrrolidinone	1.73	1.50
Ethyl-4-chloroacetoacetate	1.49	0.35

doi:10.6342/NTU202600056

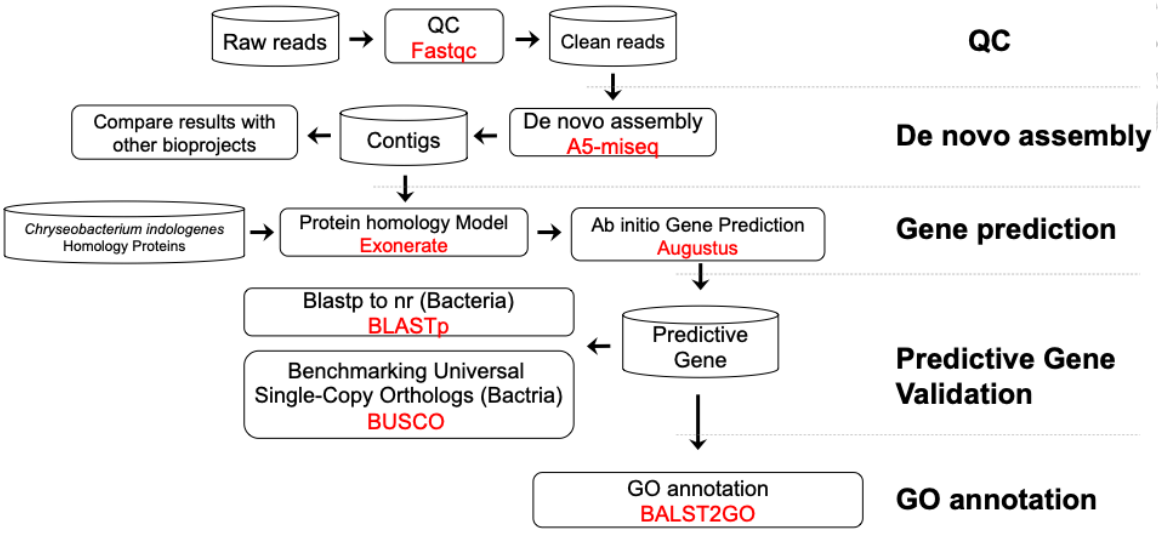


Figure 3-1. Workflow for whole-genome sequencing and assembly of *C. timonianum* c4a (Coil et al., 2015)

doi:10.6342/NTU202600056

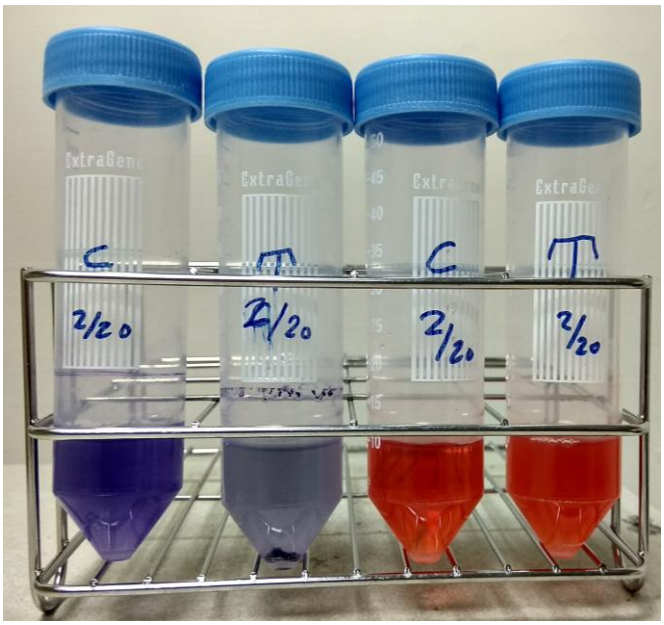


Figure 3-2. Decolorization of Remazol brilliant blue and growth in Congo red dye. C denotes the control tube without c4a colony inoculation, and T denotes the test tube inoculated with c4a strain dye by *C. timonianum* c4a

doi:10.6342/NTU202600056

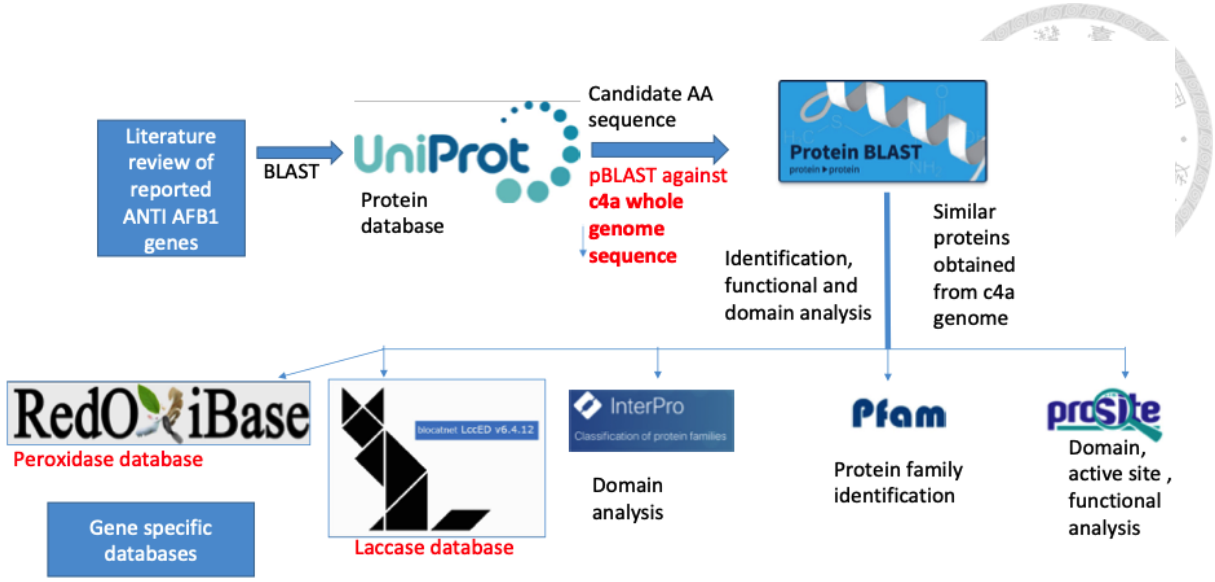


Figure 3-3. Customized workflow for genome-wide mining of anti-mycotoxin genes in *C. timonianum* c4a

doi:10.6342/NTU202600056

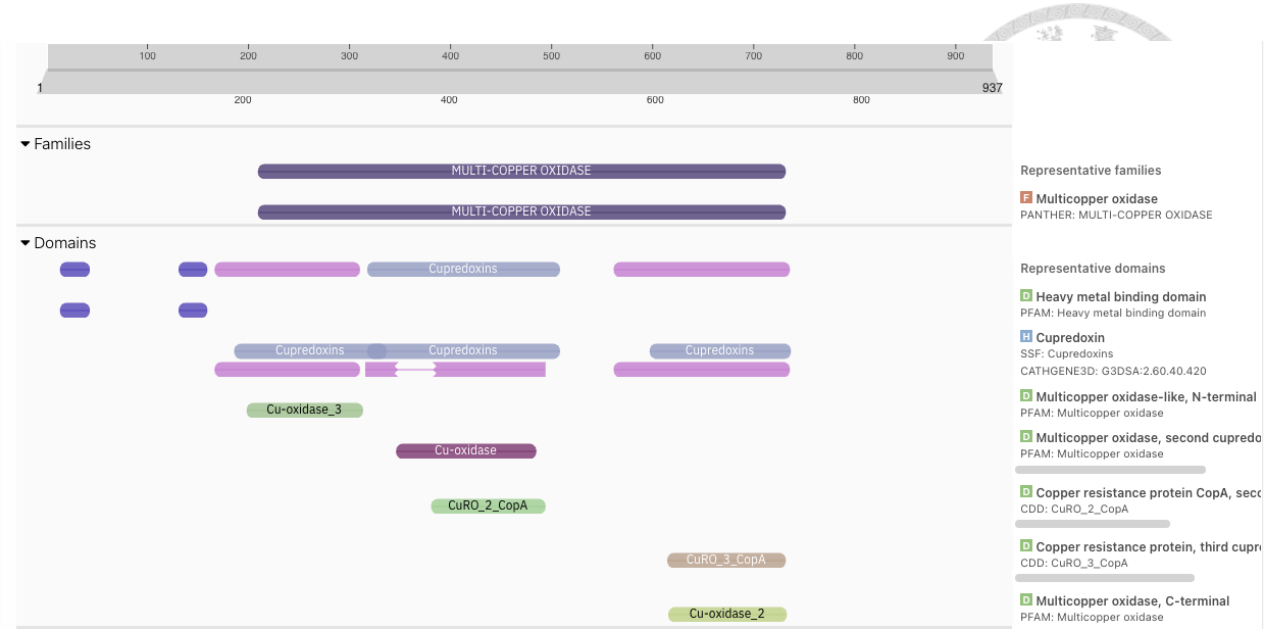


Figure 3-4. InterPro predicted domain organization of the protein sequence for scaffold 21_56 (Laccase)

doi:10.6342/NTU202600056

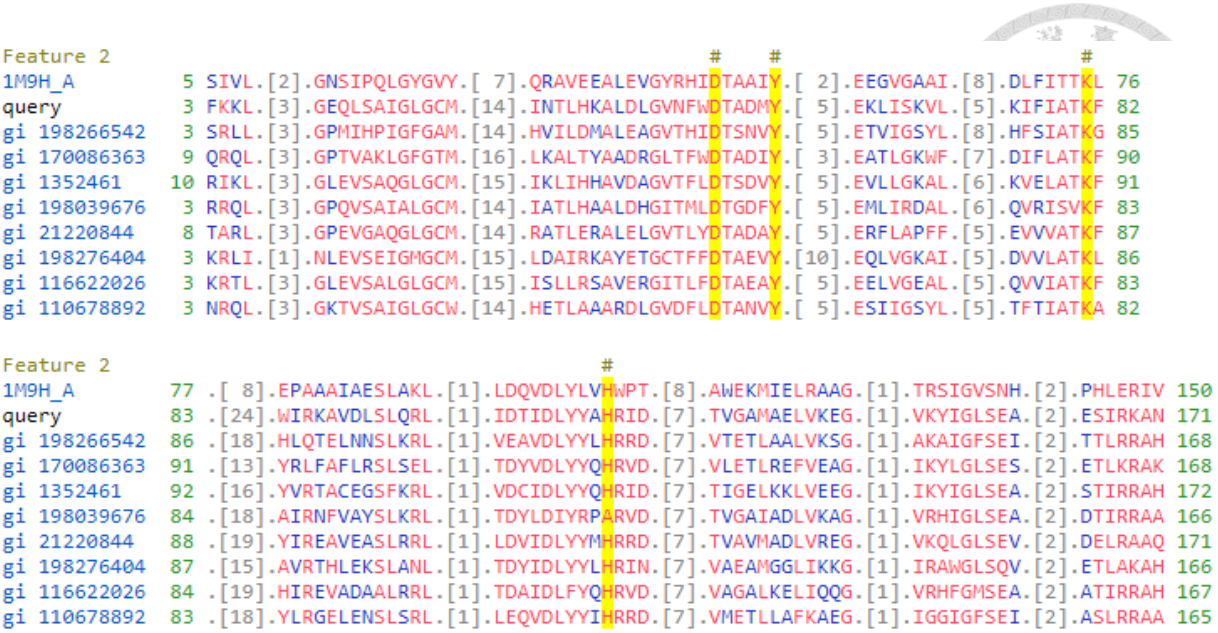


Figure 3-5. Conserved catalytic tetrad (Tyr-Lys-His-Asp) in aldo-keto reductases of c4a

doi:10.6342/NTU202600056

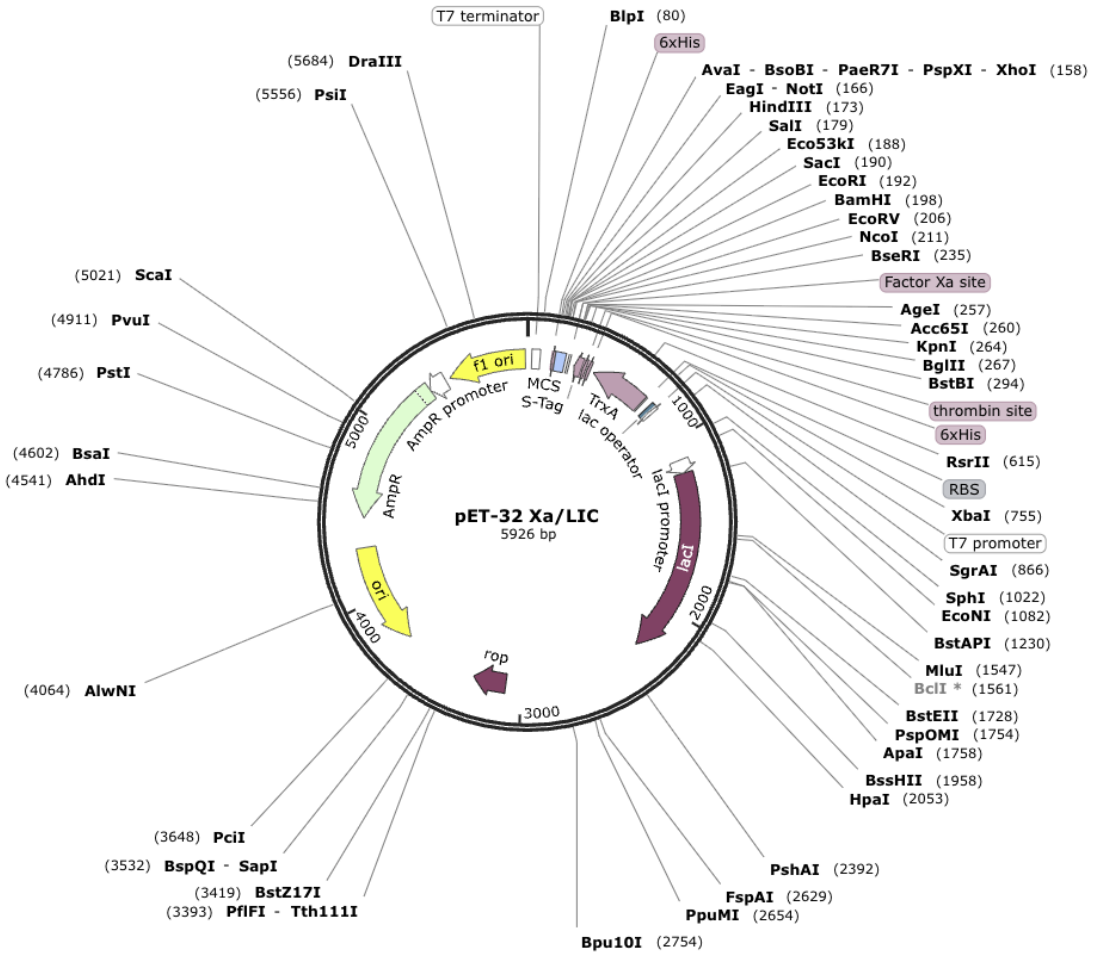


Figure 3-6. Plasmid pET32 Xa/LIC gene map

doi:10.6342/NTU202600056

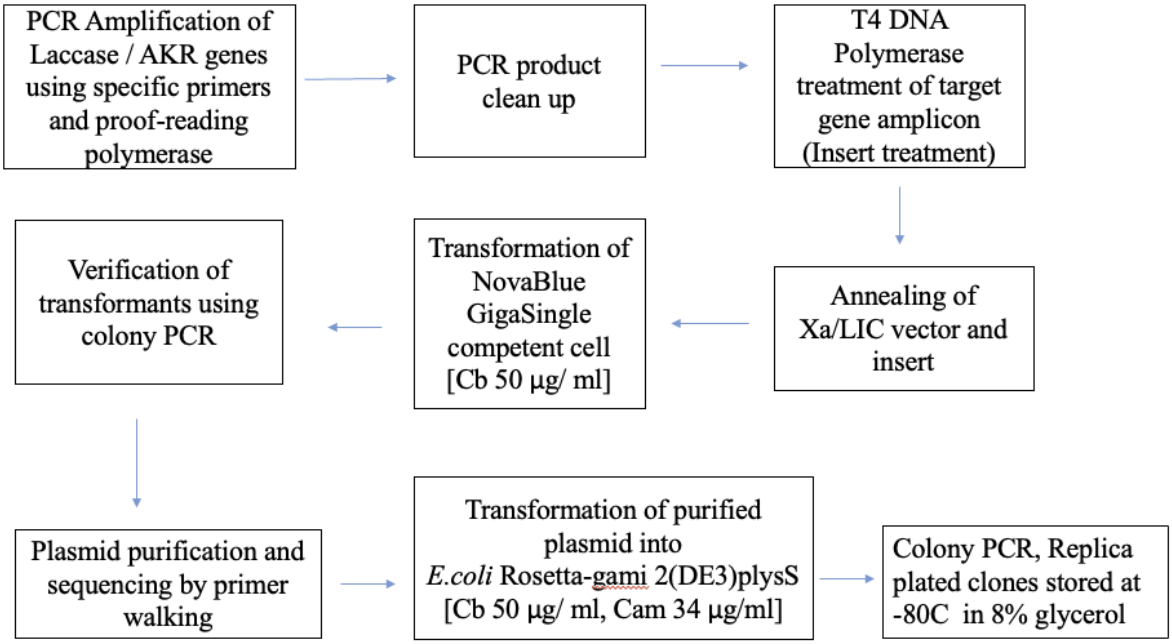
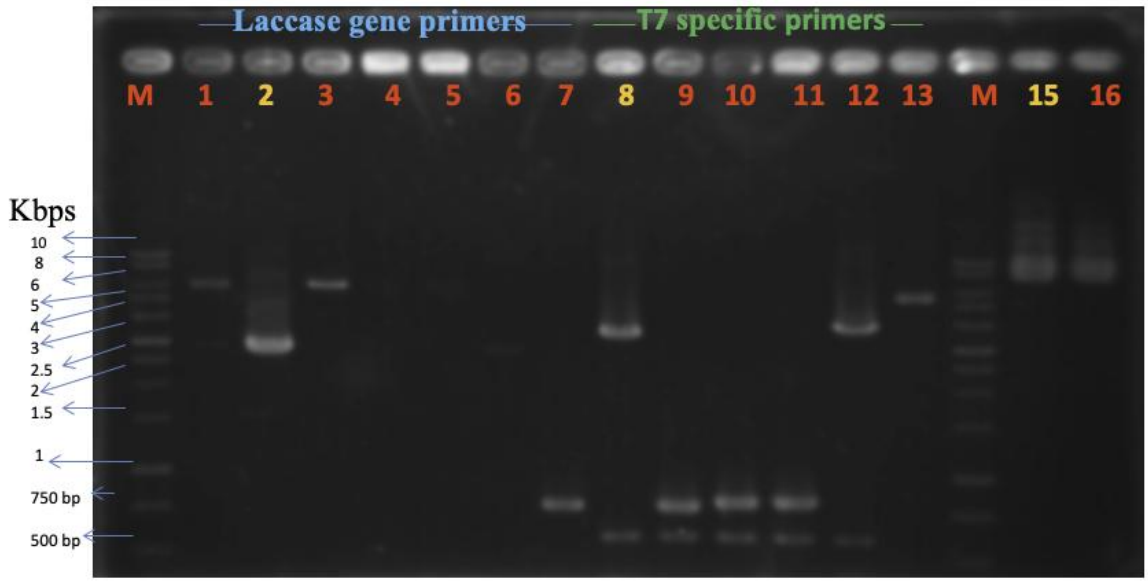


Figure 3-7. pET 32 Xa/LIC mediated gene cloning and transformation into an expression host

doi:10.6342/NTU202600056



Lane description: **M**: Marker, **lane 1**: clone 1 plasmid PCR product, **lane 2**: clone 2 plasmid PCR product, **lanes 3 to 6:** respective plasmid PCR products from selected clones. **Lane 7:** Positive control insert plasmid PCR product, **lane 8**: clone 2 plasmid PCR product, **lanes 9 to 11:** respective plasmid PCR products from selected clones, **lane 12**: Positive control insert plasmid PCR product, **lane 13:** *Plain purified plasmid* of clone 1, **lane 15:** *Plain purified plasmid* of clone 2, **lane 16:** *Plain purified plasmid* of positive control insert

Figure 3-8. Agarose gel electrophoresis of purified pET 32 Xa-LIC with Laccase gene inserts

doi:10.6342/NTU202600056

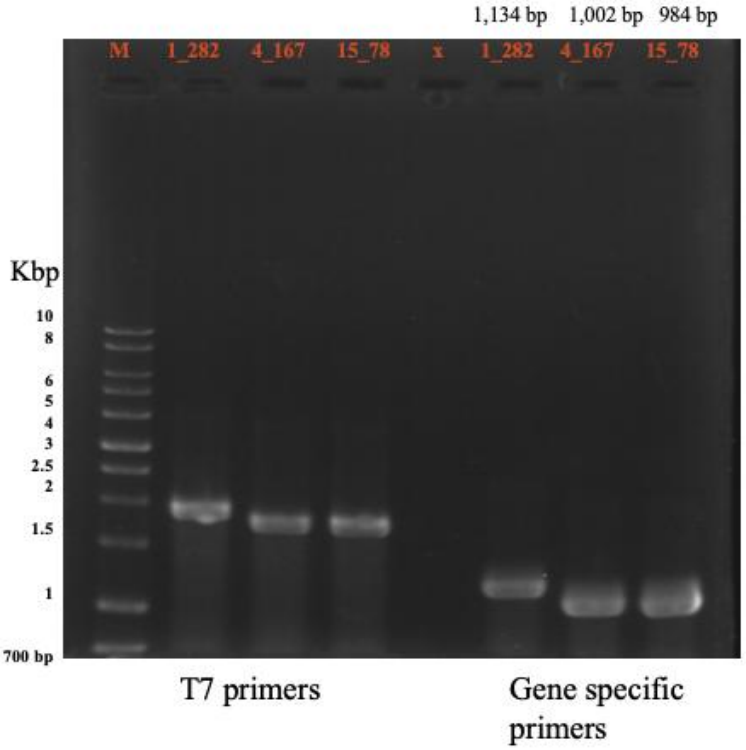


Figure 3-9. Agarose gel electrophoresis of purified pET 32 Xa-LIC with AKR gene inserts

doi:10.6342/NTU202600056

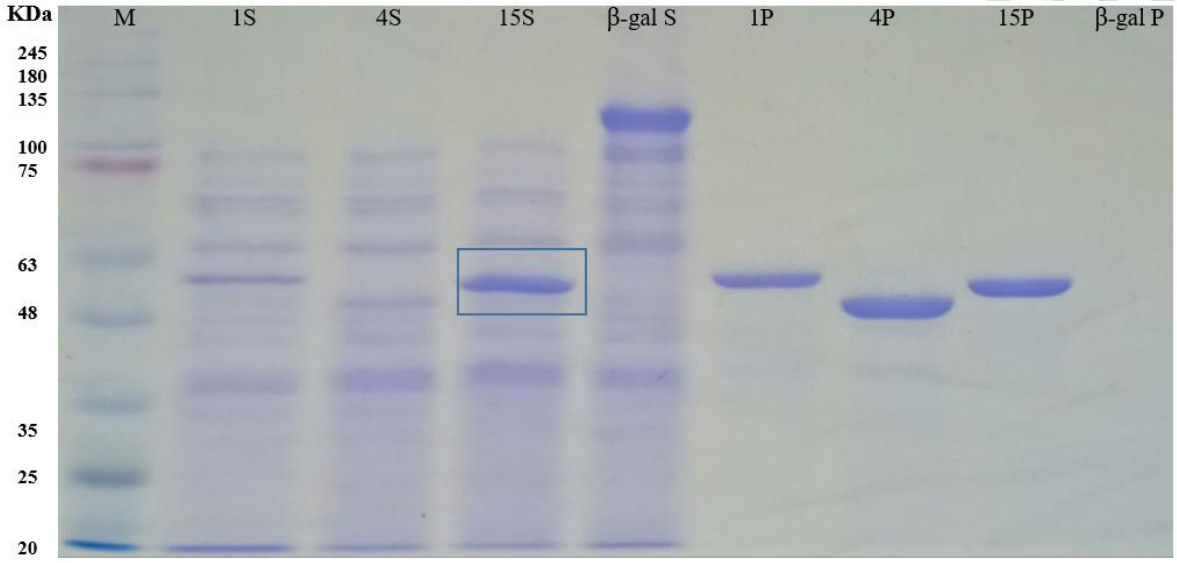


Figure 3-10. SDS PAGE showing protein expressions of AKR 1_282, 4_167, 15_78 genes in the soluble and insoluble fractions at 25°C. S: soluble fraction, P: Insoluble fraction

doi:10.6342/NTU202600056

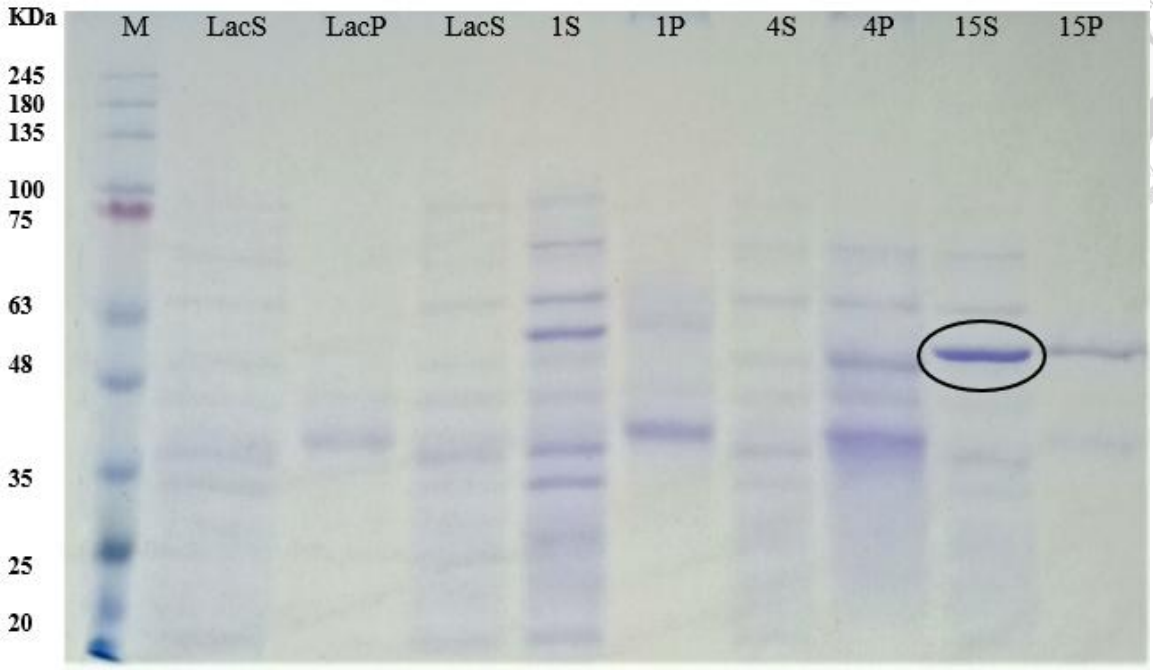
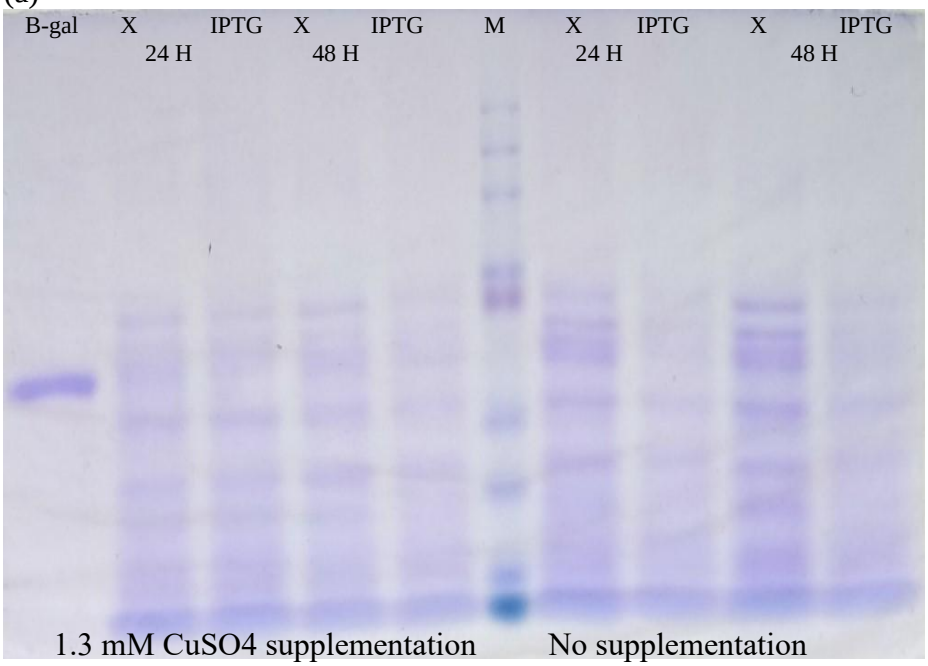


Figure 3-11. Protein expression in the soluble and insoluble fractions at 17°C after IPTG induction

doi:10.6342/NTU202600056

(a)



(b)

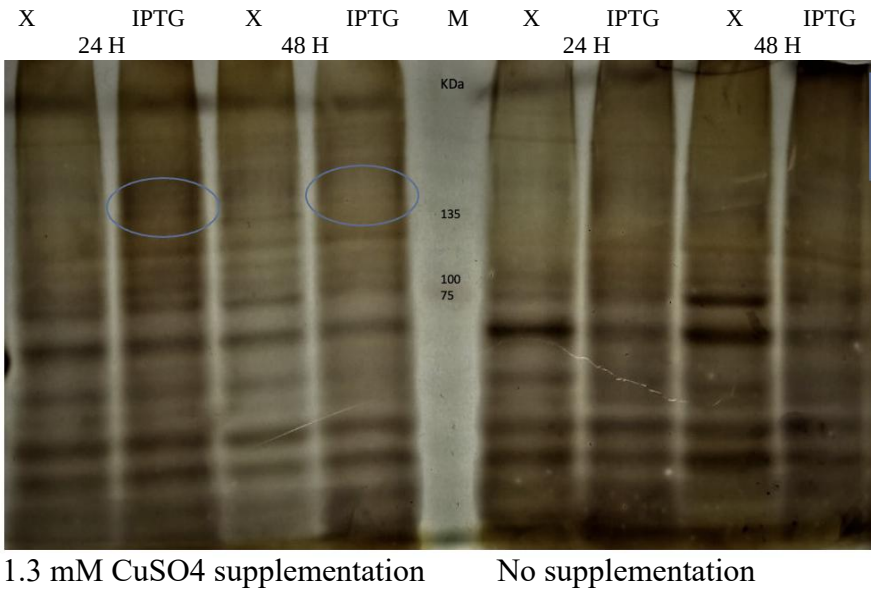


Figure 3-12. Laccase expression with CuSO4 supplementation (a) Supplementation of 1.3 mM CuSO4 gave a very faint band at about 135 kDa. In Coomassie blue staining, this band is not very well resolved. It was only visible when observed for the 24 H interval using silver stain (b) Silver stained SDS PAGE

doi:10.6342/NTU202600056

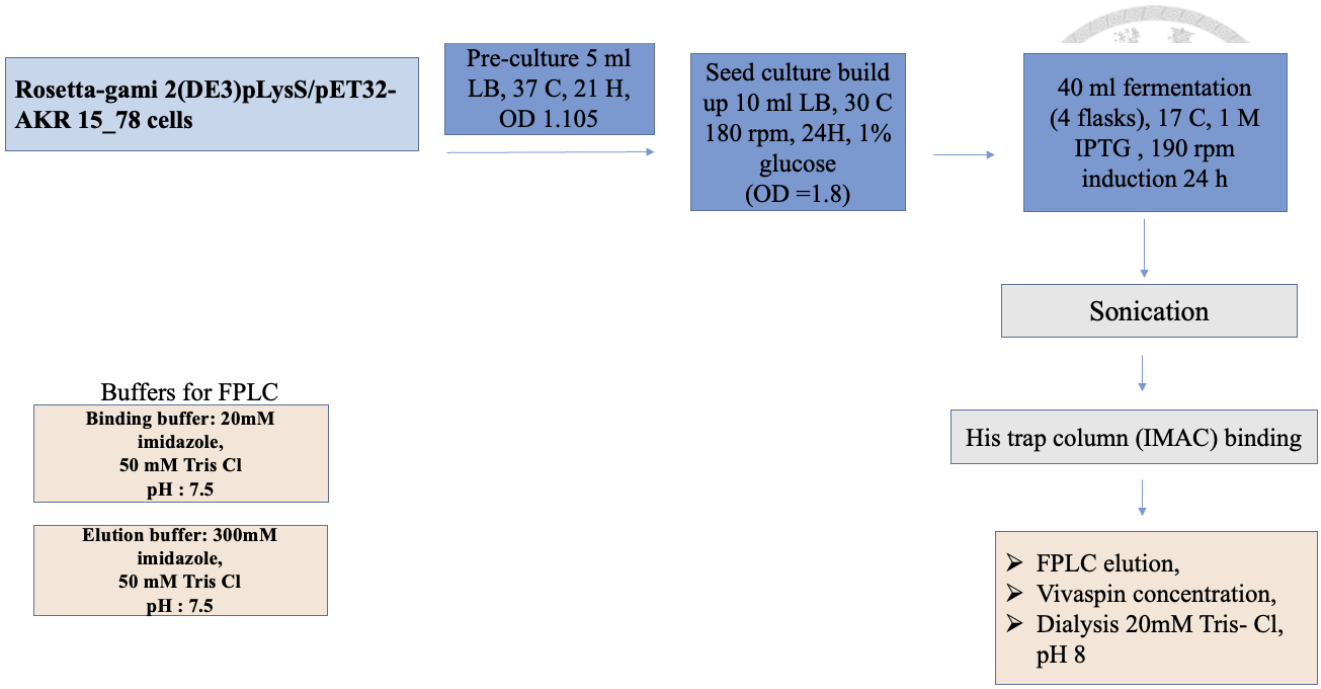


Figure 3-13. General scheme for the recombinant expression of AKR 15_78

doi:10.6342/NTU202600056

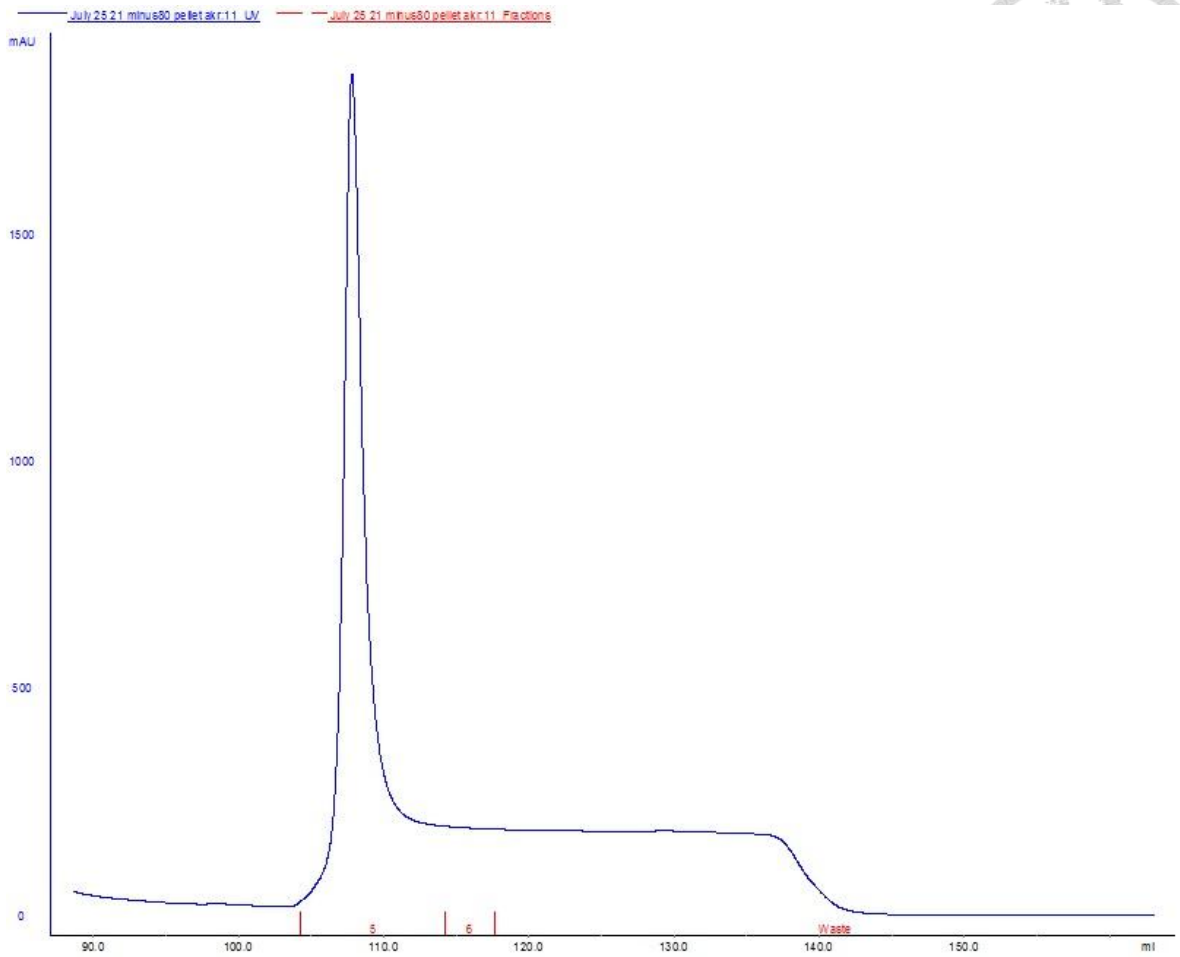


Figure 3-14. FPLC chromatogram of purified AKR 15_78 eluted in fraction number 5

doi:10.6342/NTU202600056

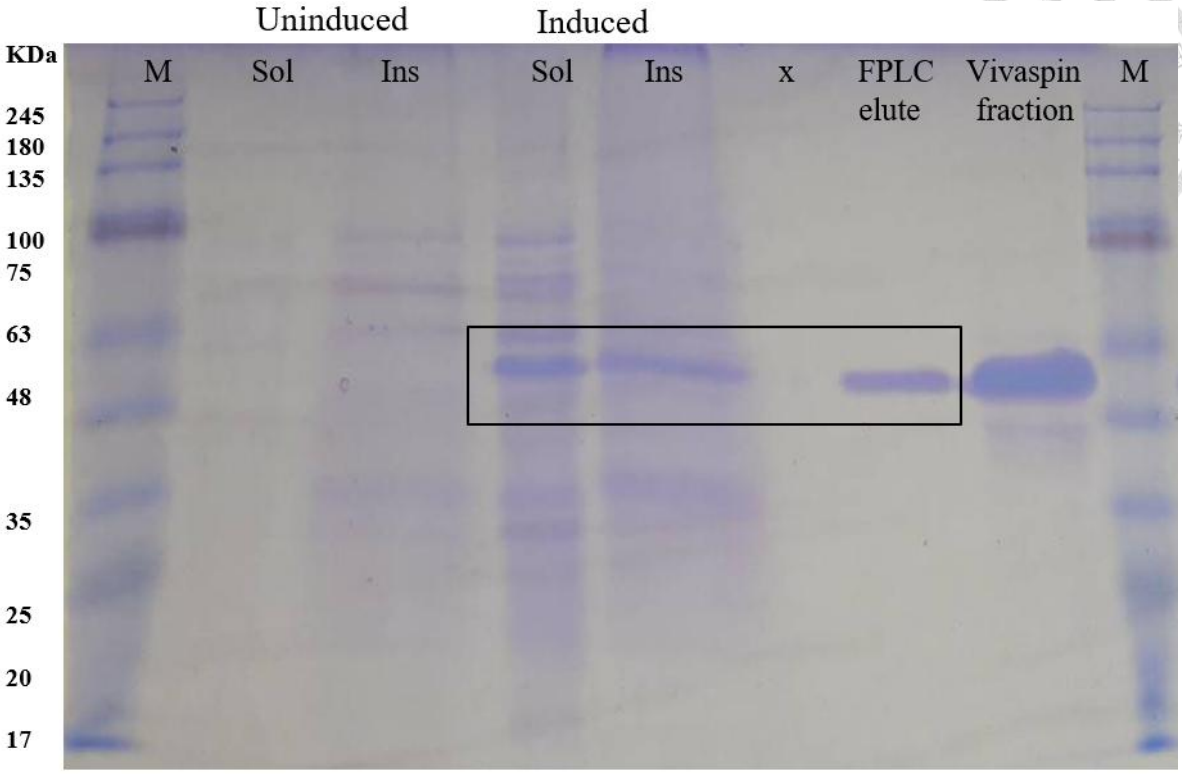


Figure 3-15. SDS PAGE showing AKR 15_78 expression in stages of purification
Sol: soluble fraction, Ins: insoluble fraction

doi:10.6342/NTU202600056

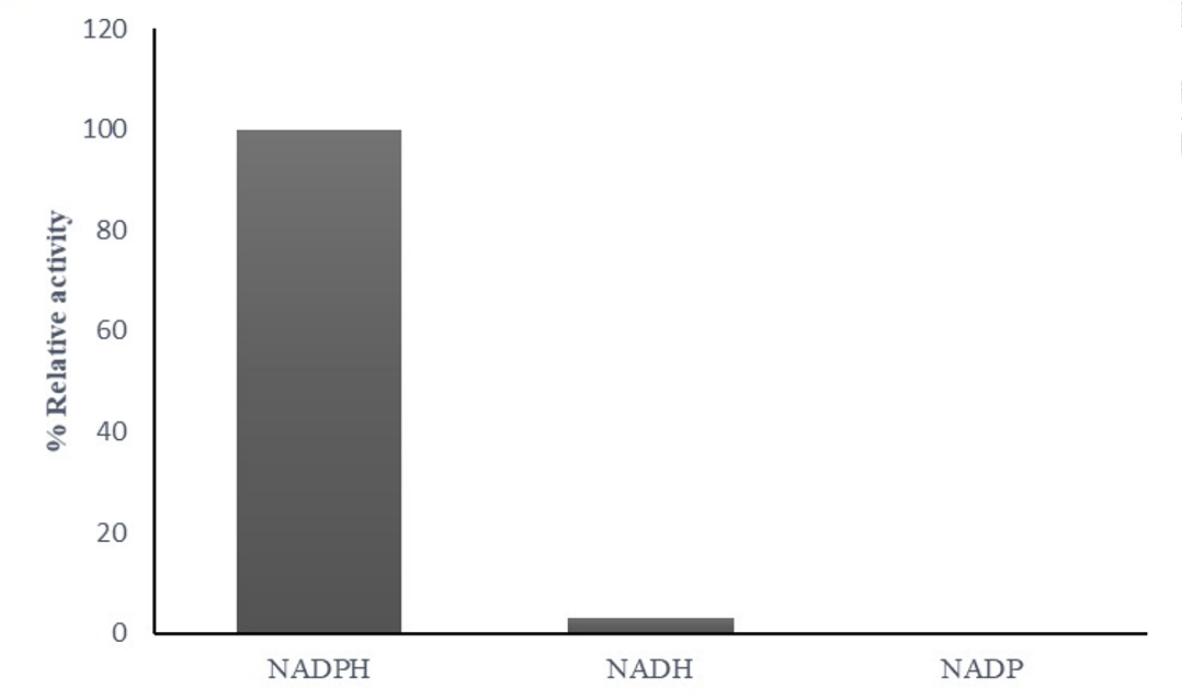


Figure 3-16. Cofactor suitability test for AKR 15_78 (NADH, NADP, and NADPH)

doi:10.6342/NTU202600056

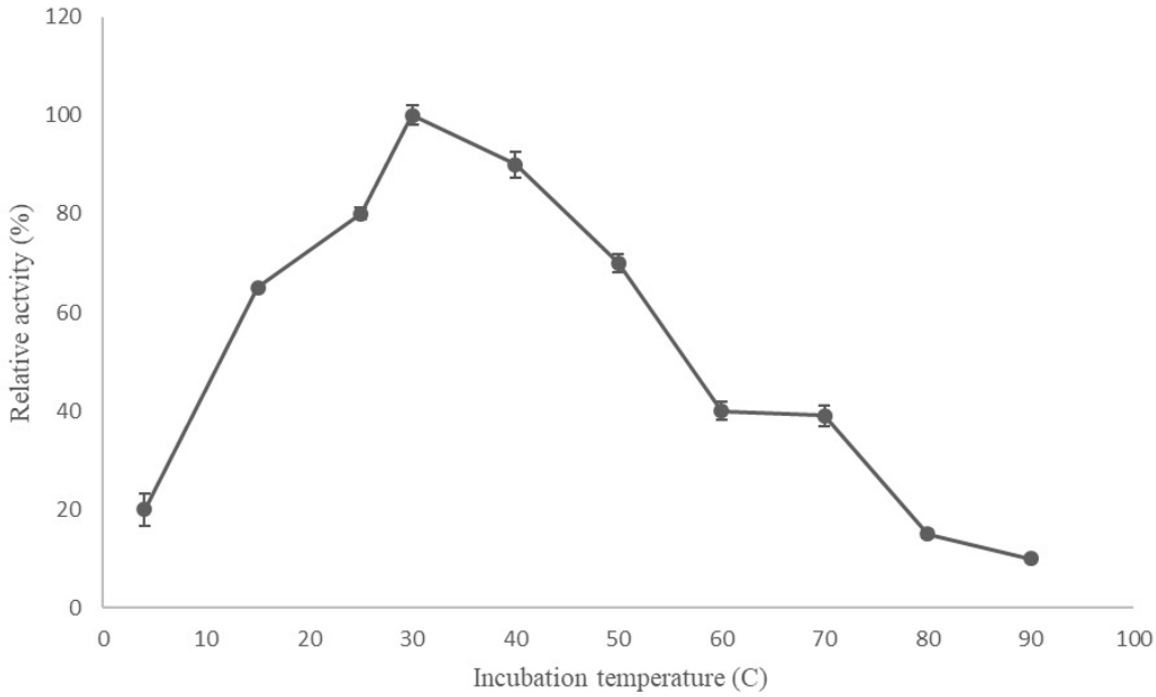


Figure 3-17. Optimum temperature assay for AKR 15_78

doi:10.6342/NTU202600056

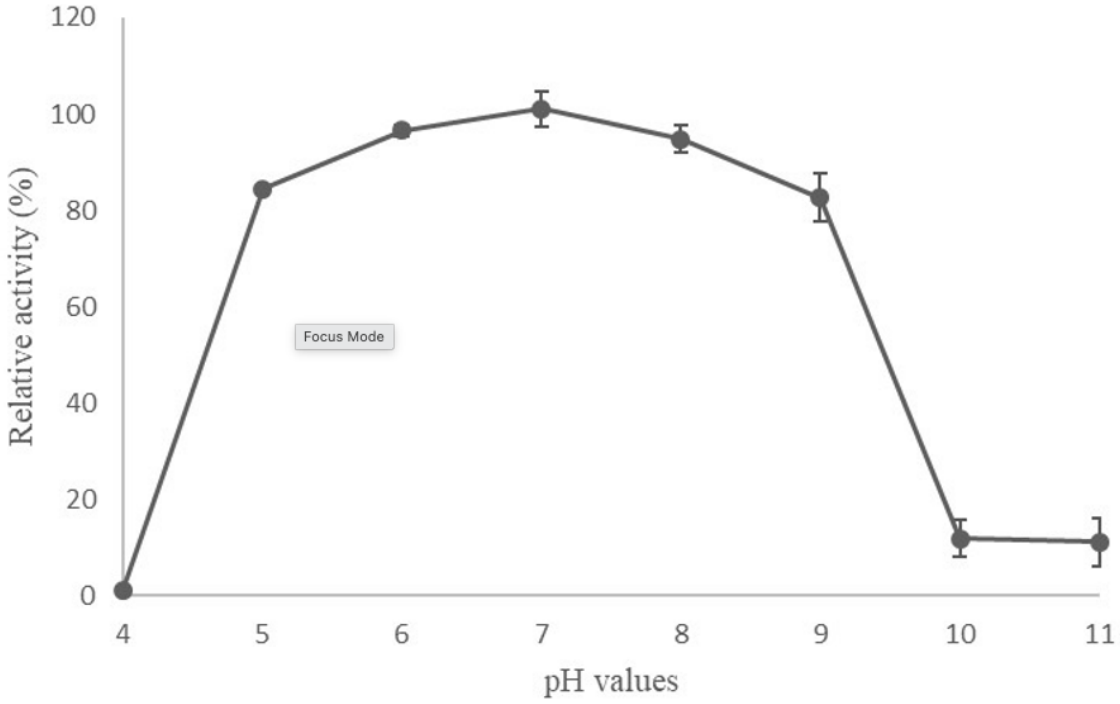


Figure 3-18. Optimum pH assay for AKR 15_78

doi:10.6342/NTU202600056

Reaction Components	Ethyl benzoyl formate (A)	Methyl benzoyl formate (B)	Ethyl 2-oxo- 4 phenylbutyrate (C)	Ethyl-4-chloroacetoacetate (D)
IPA			10 µL	
Substrates (1 g/L) (A to D)	1.8 µL	1.73 µL	1.83 µL	1.64 µL
0.2 mM NADPH (40 mM stock)			25 µL	
Tris-Cl (40 Mm, pH 8)			1.84 mL	
Pure AKR ENZYME (15 µg)			120 µL	

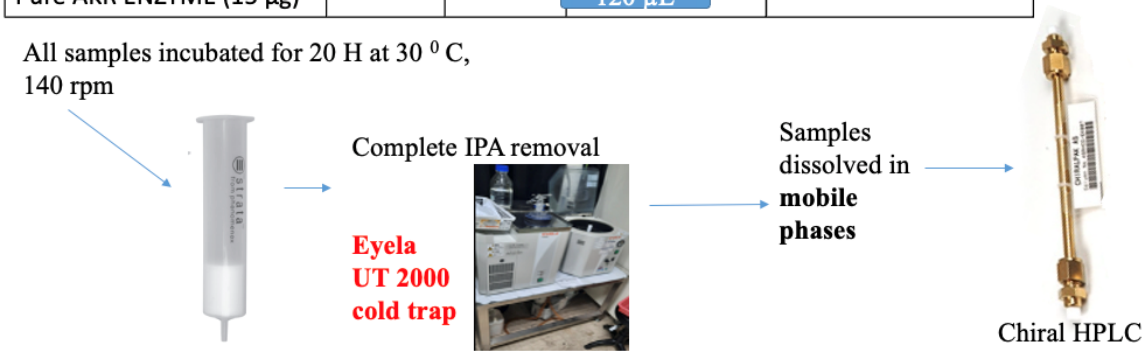


Figure 3-19. Schematic diagram showing the overall strategy for the conversion of bulky ketones using chiral HPLC

doi:10.6342/NTU202600056

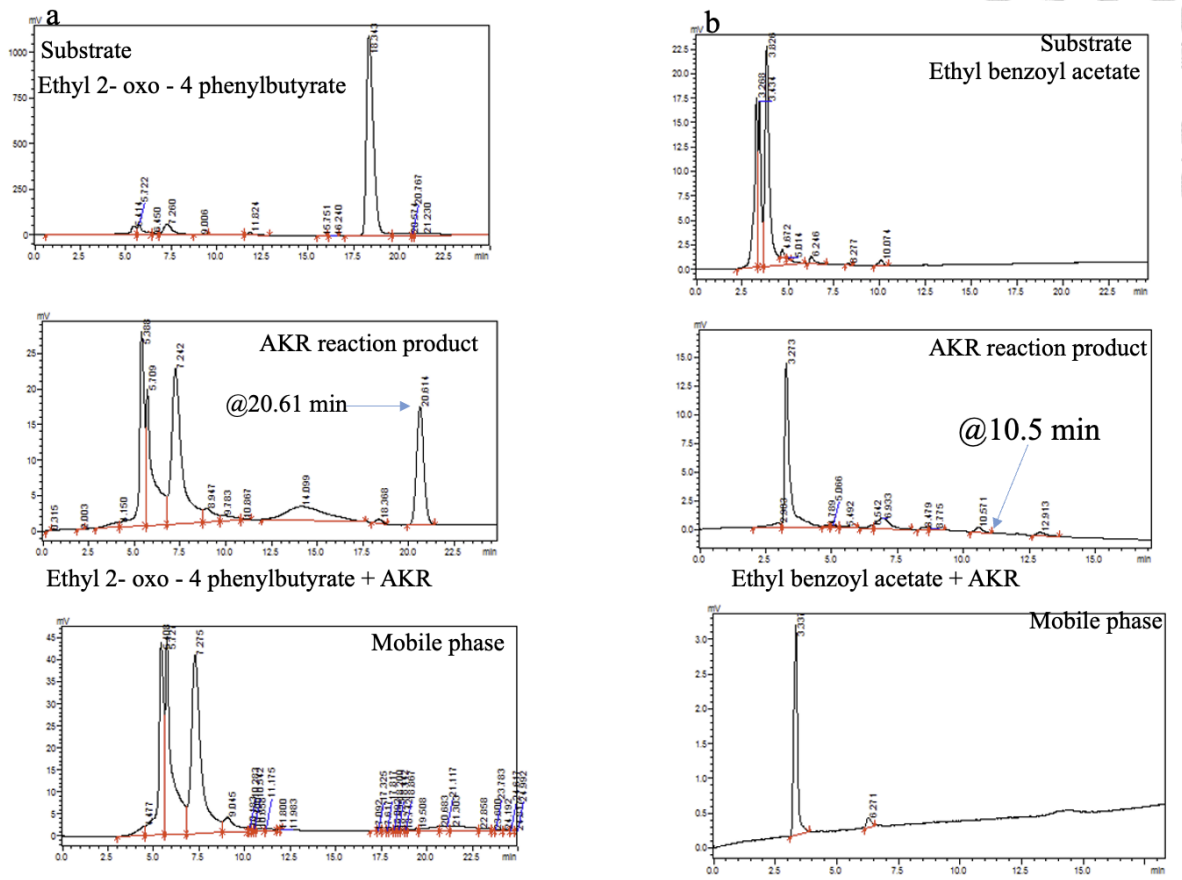


Figure 3-20. HPLC chromatograms of chiral products for the substrates **a.** Ethyl-2-oxo-4-phenylbutyrate and **b.** Ethyl benzoyl acetate. **a.** shows the transformation of substrate Ethyl-2–oxo–4 phenylbutyrate and **b.** shows the transformation of substrate ethyl benzoyl acetate. A pick at 10.5 minutes corresponding to 3-hydroxy-3-phenyl propionate

doi:10.6342/NTU202600056

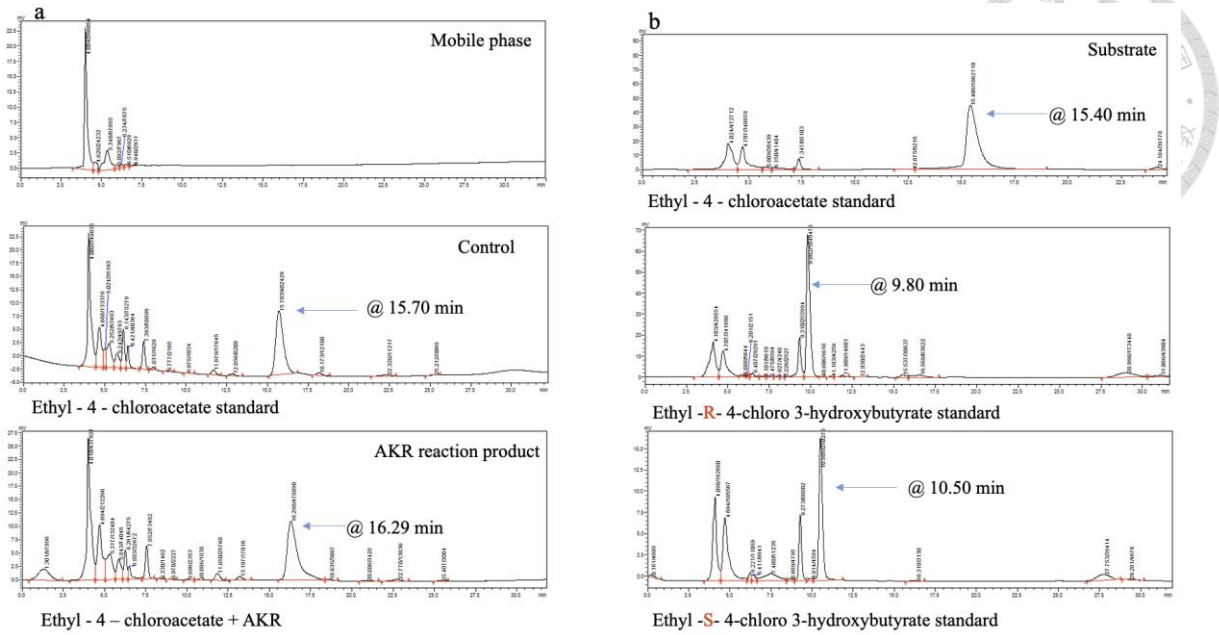


Figure 3-21. HPLC chromatograms of chiral products by AKR 15_78 enzyme against ethyl – chloroacetate as a substrate. Ethyl-R-4-chloro 3-hydroxybutyrate and Ethyl-S-4-chloro 3-hydroxybutyrate were pure desired target products.

doi:10.6342/NTU202600056

Protein sequences of c4a strain used in this study in FASTA format

Laccase

Scaffold 25_56

MKKLLMFLVLLFSVFTFAQTTKTYYTCPMHPEVVSSKPGDCPKCKMTLVKKTVVIQPKVV
AKPAVKTIPKVEAKTKPVEIKVNKTKVDVKKPKKTEEAKKVNAVKKAEPAQVAKPALKPI
SASPNISQSSPKTKASITYTCPMHPEVTSDKPGKCPKCGMELVEKEDHQHVVEDSKEEKS
ILKRNSENGKITFGGKTVRYDLYVKDTIVNFTGKNRRAIAINGKLQAPTLYFTEGDTAEI
YLHNMLKENTGLHWHGVILPNEHDGVPYLTTKPVTPGETHLYKFKISQNGTYWYHSHEAL
QEQIGMNGILVFKKREGEPKTEYNAEIPVLLGDWSDDDPMQIARRLHMANTDWYAVKKNA
VQSYWEAIKSGNFGTKALNEWKRMEAMDVSDVYYDKFLINGVPSSDYSNLKAGDKVRLRV
ANGGSSTYFWLNYGGGKIKVVGNDGNDVVPVEVDRLIVGVSETYDIEVTVPENKSFEFRA
TSEDRIGHASLWLGSGEKVEAPNLPRLMLFEGMKMMNGMMEMSGNMKPMTMTMGNQMMDM
NEVMYPEIPESQRKTTAKHINEMMGVKTKDEKKSEDHSQHAGMNMPEEKTIKRLSYNILK
SPEKTILPTDSIREMKFTLEGNMNHYLWTLDNKTVTETDKIMIKKGEILRIKLYNNSMMR
HPMHLHGHDFRLINSKGEYSPLKNVVDIMPMETVTLEFAANQDGDWFFHCHILYHMMAGM
GRIFSYENSKPNPQLPNRKLAWKNFLKDNKMISSMAMLDVASNKIHAETMTMFGPRWANL
NEFHTNWNFDHFEGSAKVGRFLGKFQWALPYAGVRVQKNHEIMERQMAEDMGMDFHGKKT
WFGQQKASKNKYAFIVGMQYVLPMLITADASVDHNGKVLLELSREDIPLSRRLRGNFSVN
SDGEFSTGIRYIVQKYLSISGNYDNEMGWGAGITLTY

Aldo-keto reductase

Scaffold 1_182

MYNNFGEDLTEKQIIMSVKDYRTLGKSGLRVSPLALGTMTFGEDWGWGTSPSDAYQILEY
YIHHGGNVIDTANIYTKGHSEKIIGDFLMKKKVRRDALVLSTKFWGNMFPHDPNGGGTGR
KAVIQSVEGSLKRLKTDYIDLYWMHAFDPYTPIEETISTLDHLVKQGKIRYIAISDTPAW
KITEAQMISKFRGWEAFIGLQLEYSLLERSVENELIPMALEMGLGVMPWSPLKEGILSGK
YIRGNKGEKISDRNDRINPEISESAYKIIDRLYELAKEKEVAVSAVAIAWVMLQRGVTST
LLGARTLSQLKENMKASMLELSTEELESLNVLSQPSLPFPYNLLEGAKDLLQAGTTINGV
TSNVAEILPQNDQERYD

Scaffold 4_167

MKFKKLGNTGEQLSAIGLGCMGMSFAYGPADEQESINTLHKALDLGVNFWDTADMYADGE
NEKLISKVLVPNRDKIFIATKFGFRFKDGKASHSGAPGTYFDGSPEWIRKAVDLSLQRLK
IDTIDLYYAHRIDPNVPVEETVGAMAELVKEGKVKYIGLSEASPESIRKANKIHPIAALQ
SEYSILTKDIENEILPTIRELGISLVPYSPLARGLFANISEVQNLDDNDFRKSLPRYQQE
YLENNTKLANEINEFAASKGVKGTQLALAWVLNQGDDIIPIPGTKRIKYLEENVAAANID
LSQSDLNMIDAILKKYPNVGERYNEGSMKLVNN

Scaffold 15_78

MEYRKLGNTDLELSTITHGAFAIGGNMWGGNEKQDSINSIHASLDHGVTSIDTAPFYGFG
LSEEMIGEAIKGKDRSKIQLLTKFGLVWDGSNNGKGEFFFDAEDEGKVIPVYKLASKANI
IKEVEESLKRLGTDYIDLLQLHWPDSTTAISETMEAMELLIQQGKVRAAGVSNYSVAQME
EANRTFKLASNQVSYSMLNRSIENDLVPYSLENNSGIIVYSPMERGLLTGKYFKDNKLKD
NDHRNGYFSQFDLNKVKTFLEKIEPIAQEKGASLSQLVLRWTTLQPAITVVLAGARNAEQ
AIDNAKAMDINLSQEELNFINAALSEI

doi:10.6342/NTU202600056

Chapter IV

Concluding remarks

Aflatoxin B1 (AFB1) contamination in feed and food crops continues to exact a heavy toll, affecting perhaps a quarter of global production while posing well-documented risks of hepatotoxicity and immunosuppression in livestock and humans alike (Eskola et al., 2020; Kumar et al., 2017). The toxin's difuranocoumarin structure, particularly the reactive double bond in the terminal furan ring, drives its carcinogenicity through epoxide formation (Smela et al., 2001). Although adsorption and chemical treatments offer partial solutions, microbial approaches—especially those relying on extracellular, thermostable activities—hold appeal for their specificity and minimal residue formation (Peng et al., 2018; Verheecke et al., 2016). Screening with a coumarin-based medium isolated several strains from chicken cecal contents and soil, but strain c4a stood out for its capacity to remove AFB1 (Figure 2-1). Colony morphology, biochemical tests, and multilocus phylogeny placed it firmly within *Chryseobacterium timonianum* (Hugo et al., 2015; Figures 2-4 and 2-6). Activity resided entirely in the extracellular fraction; intracellular extracts and cell pellet did not significantly contribute to this activity (Figure 2-3). Systematic optimization showed that supernatant from cultures grown in nutrient broth adjusted to a 4:1 gelatin peptone: beef extract ratio performed best, with peak removal at 60°C, pH 8, and in the presence of Mn^{2+} or Mg^{2+} (Figure 2-7, Figure 2-8). Retention of activity after autoclaving and loss upon protease or SDS treatment indicated the presence of a heat-stable proteinaceous component (Figure 2-7d). Mass spectrometry confirmed a structural change: addition of water across the furan double bond produced a metabolite of reduced toxicity. The ion fragmentation pattern (m/z values) for the

doi:10.6342/NTU202600056

c4a strain-mediated AFB1 degradation metabolite was found to be 417.21 → 412.25 → 331.08 → 313.07 → 285.08, with loss of H2O in the second last step, followed by loss of CO in the final step. An AFB1 biotransformation metabolite was observed at a retention time of 2.56 minutes with an m/z value of 331.08. The toxicity of this specific metabolite is reported to be significantly lower than that of pure AFB1 (Wang et al., 2021). This provided important validation of the significantly reduced cytotoxicity of the c4a-mediated AFB1 reaction metabolite.

Genome sequencing was then performed to identify the genes underlying this phenomenon. The draft assembly proved adequate for annotation, and targeted searches flagged a multicopper oxidase (laccase, scaffold 21_56) with typical copper-binding motifs alongside three aldo-keto reductases carrying the expected catalytic tetrad (unpublished data, Figures 3-3 to 3-5). Whole-cell assays confirmed oxidoreductase activity by decolorizing Remazol brilliant blue (Figure 3-2). Cloning of laccase and aldo-keto reductase genes was successfully done in the pET-32 XA/LIC vector. However, expression of the laccase gene in *Escherichia coli* Rosetta-gami 2(DE3)pLysS yielded negative results, with very low protein expression. The laccase construct gave almost no soluble protein, even when copper was supplemented during induction (Figure 3-12). This failure does not rule out a role—bacterial laccases have degraded AFB1 elsewhere (Alberts et al., 2009; Wang et al., 2019)—but it does highlight familiar obstacles with multicopper oxidases in heterologous systems. Shifting to a yeast host (like *Pichia pastoris* or *Kluveromyces marxianus*), codon-optimizing the gene, or expressing individual cupredoxin domains separately could circumvent folding and copper-loading issues that often plague full-length constructs in prokaryotes.

AKR 15_78 expressed well and purified cleanly (Figure 3-11, Figure 3-14), displaying NADPH preference and reasonable stability between 30–40°C and pH 7–8. Incubation with

doi:10.6342/NTU202600056

AFB1, zearalenone, and deoxynivalenol, however, produced no degradation. Screening for bulky ketones revealed some reductase activity, yet chiral analysis using the column employed did not detect the anticipated pharmaceutical intermediates exactly (Figure 3-20a; Table 3-6). However, when ethyl benzoyl acetate was used as the substrate (Figure 3-20b), a distinct product peak was observed at 10.5 min, a retention time that closely matched the reported elution of the chiral compound 3-hydroxy-3-phenyl propionate (Liang et al., 2018). A switch to alternative stationary phases, such as Chiralcel OD-H, might still reveal minor enantiomers or side products worth pursuing (Liang et al., 2018).

Taken together, the work establishes *C. timonianum* c4a as a source of robust, extracellular, and unusually heat-stable AFB1-transforming activity—a trait that sets it apart from many previously described degraders (Shu et al., 2018; Cai et al., 2020). The genomic and expression studies, while falling short of assigning precise molecular responsibility, underscore the persistent difficulties in moving from sequence prediction to functional validation. Identifying the actual effector(s) will likely require direct proteomic analysis of the active supernatant, followed by targeted gene disruption in the native strain. Such steps remain crucial if the system is to be engineered or deployed reliably. Nonetheless, the phenotypic characterization alone provides a solid foundation for further development of *Chryseobacterium*-based strategies for AFB1 mitigation.

doi:10.6342/NTU202600056

References

Abou Abdallah R, Cimmino T, Baron S, Cadoret F, Michelle C, Raoult D, et al. Description of *Chryseobacterium timonianum* sp. nov., isolated from a patient with pneumonia. Antonie Van Leeuwenhoek. 2017;110(9):1121-32. doi:10.1007/s10482-017-0885-8.

Abraham N, Schroeter KL, Zhu Y, Chan J, Evans N, Kimber MS, Carere J, Zhou T, Seah SY. Structure–function characterization of an aldo–keto reductase involved in detoxification of the mycotoxin, deoxynivalenol. Sci Rep. 2022;12(1):14737. doi:10.1038/s41598-022-19040-8.

Abrar M, Anjum FM, Butt MS, Pasha I, Randhawa MA, Saeed F, et al. Aflatoxins: biosynthesis, occurrence, toxicity, and remedies. Crit Rev Food Sci Nutr. 2013;53(8):862-74. doi:10.1080/10408398.2011.563154.

Adegoke GO, Babalola AK, Akanni AO. Effects of sodium metabisulphite, hydrogen peroxide and heat on aflatoxin B1 in lafun and gari: two cassava products. Nahrung. 1991;35(10):1041-5. doi:10.1002/food.19910351009.

Alassane-Kpembi I, Schatzmayr G, Taranu I, Marin D, Puel O, Oswald IP. Mycotoxins co-contamination: methodological aspects and biological relevance of combined toxicity studies. Crit Rev Food Sci Nutr. 2017;57(16):3489-3507. doi:10.1080/1040841X.2016.1197539.

Alberts JF, Engelbrecht Y, Steyn PS, Holzapfel WH, van Zyl WH. Biological degradation of aflatoxin B1 by *Rhodococcus erythropolis* cultures. Int J Food Microbiol. 2006;109(1–2):121–126. doi:10.1016/j.ijfoodmicro.2006.01.019.

Alberts JF, Gelderblom WCA, Botha A, van Zyl WH. Degradation of aflatoxin B1 by fungal laccase enzymes. Int J Food Microbiol. 2009;135(1):47–52. doi:10.1016/j.ijfoodmicro.2009.07.022.

Alshannaq A, Yu JH. Occurrence, toxicity, and analysis of major mycotoxins in food. Int J Environ Res Public Health. 2017;14(6):632. doi:10.3390/ijerph14060632.

An X, Yi C, Ningjian L, Shulin Z, Liuwei W, Qinghua Z. Green and sustainable approach for decoloration and detoxification of azo dye by bacterial-mediated thermo-halotolerant dye-decolorizing peroxidase (DyP). Process Biochem. 2023;130:334-46. doi:10.1016/j.procbio.2023.04.025.

Andrade PD, Caldas ED. Aflatoxins in cereals: worldwide occurrence and dietary risk assessment. World Mycotoxin J. 2015;8(4):415-431. doi:10.3920/WMJ2014.1847

Atehnkeng J, Ojiambo PS, Ikotun T, Sikora RA, Cotty PJ, Bandyopadhyay R. Evaluation of atoxigenic isolates of *Aspergillus flavus* as potential biocontrol agents for aflatoxin in maize. Food Addit Contam Part A. 2008;25(10):1264–1271. doi:10.1080/02652030802112635.

Battilani P, Toscano P, Van der Fels-Klerx HJ, et al. Aflatoxin B1 contamination in maize in Europe increases due to climate change. Sci Rep. 2016;6:24328. doi:10.1038/srep24328.

Bennett JW, Klich M. Mycotoxins. Clin Microbiol Rev. 2003;16(3):497-516. doi:10.1128/CMR.16.3.497-516.2003.

Berthiller F, Crews C, Dall'Asta C, et al. Masked mycotoxins: a review. Mol Nutr Food Res. 2013;57(1):165-86. doi:10.1002/mnfr.201200764.

Bhatnagar D, Ehrlich KC, Cleveland TE. Molecular genetic analysis and regulation of aflatoxin biosynthesis. Appl Microbiol Biotechnol. 2003;61(2):83-93. doi:10.1007/s00253-002-1199-x.

doi:10.6342/NTU202600056

Branà MT, Sergio L, Haidukowski M, Logrieco AF, Altomare C. Degradation of aflatoxin B1 by an enzymatic extract from spent mushroom substrate of *Pleurotus eryngii*. Toxins (Basel). 2020;12(1):49. doi:10.3390/toxins12010049.

Cai M, Qian Y, Chen N, Ling T, Wang J, Jiang H, et al. Detoxification of aflatoxin B1 by *Stenotrophomonas* sp. CW117 and characterization of the thermophilic degradation process. Environ Pollut. 2020;261:114178. doi:10.1016/j.envpol.2020.114178.

Chang PK. Creating large chromosomal segment deletions in *Aspergillus flavus* by a dual CRISPR/Cas9 system: deletion of gene clusters for production of aflatoxin, cyclopiazonic acid, and ustiloxin B. Microbiol Spectr. 2024;12(1):e0332723. doi:10.1128/spectrum.03327-23.

Chen R, Ma F, Li PW, Zhang W, Ding XX, Zhang Q, et al. Effect of ozone on aflatoxins detoxification and nutritional quality of peanuts. Food Chem. 2014;146:284–288. doi:10.1016/j.foodchem.2013.09.059.

Choi H, Lee SA, Kim JH. Aflatoxin B1: Challenges and strategies for the intestinal microbiota and intestinal health of monogastric animals. Toxins (Basel). 2025;17(1):43. doi:10.3390/toxins17010043.

Codex Alimentarius Commission. Code of practice for the reduction of aflatoxin B1 in raw materials and supplementary feeding stuffs for milk-producing animals (CXC 45-1997). Rome: FAO/WHO; 1997.

Coil D, Jospin G, Darling AE. A5-miseq: an updated pipeline to assemble microbial genomes from Illumina MiSeq data. Bioinformatics. 2015;31(4):587-9. doi:10.1093/bioinformatics/btu661

Cotty PJ. Influence of field application of an atoxigenic strain of *Aspergillus flavus* on the populations of *A. flavus* infecting cotton bolls and on the aflatoxin content of cottonseed. Phytopathology. 1994;84:1270-7.

Diao E, Li X, Zhang Z, Ma W, Ji N, Dong H. Ultraviolet irradiation detoxification of aflatoxins. Trends Food Sci Technol. 2015;42(1):64-9. doi:10.1016/j.tifs.2014.12.001.

Eaton DL, Gallagher EP. Mechanisms of aflatoxin carcinogenesis. Annu Rev Pharmacol Toxicol. 1994;34:135-72. doi:10.1146/annurev.pa.34.040194.001031.

Eskola M, Kos G, Elliott CT, Hajšlová J, Mayar S, Krska R. Worldwide contamination of food-crops with mycotoxins: validity of the widely cited 'FAO estimate' of 25%. Crit Rev Food Sci Nutr. 2020;60(16):2773-2789. doi:10.1080/10408398.2019.1658570.

European Commission. Directive 2002/32/EC of the European parliament and of the council of 7 May 2002 on undesirable substances in animal feed. Off J Eur Communities. 2002;L140:10-21.

European Commission. Directive 2003/100/EC of 31 October 2003 amending Annex I to directive 2002/32/EC of the European parliament and of the council on undesirable substances in animal feed. Off J Eur Union. 2003;L285:33-37.

Fountain JC, Scully BT, Ni X, Kemerait RC, Lee RD, Chen ZY, Guo B. Environmental influences on maize-*Aspergillus flavus* interactions and aflatoxin production. Front Microbiol. 2014;5:40. doi:10.3389/fmicb.2014.00040.

Frisvad JC, Skouboe P, Samson RA. Taxonomic comparison of three different groups of aflatoxin producers and a new efficient producer of aflatoxin B1, sterigmatocystin and 3-O-methylsterigmatocystin, *Aspergillus rambellii* sp. nov. Syst Appl Microbiol. 2005;28(5):442-53. doi:10.1016/j.syapm.2005.02.009.

Gao B, An W, Wu J, Wang X, Han B, Tao H, Liu J, Wang Z, Wang J. Simultaneous degradation of AFB1 and ZEN by CotA laccase from *Bacillus subtilis* ZJ-2019-1 in the mediator-assisted or immobilization system. Toxins (Basel). 2024;16(10):445. doi:10.3390/toxins16100445.

doi:10.6342/NTU202600056

Gelaye Y, Luo H. Green-synthesized nanomaterials for aflatoxin mitigation: a review. Nanotechnol Sci Appl. 2025;18:211-223. doi:10.2147/NSA.S520121.

Gratz S, Wu QK, El-Nezami H, Juvonen RO, Mykkänen H, Turner PC. *Lactobacillus rhamnosus* GG reduces aflatoxin B1 transport, metabolism, and toxicity in Caco-2 cells. Appl Environ Microbiol. 2007;73(12):3958–3964. doi:10.1128/AEM.02945-06.

Groopman JD, Kensler TW, Wild CP. Protective interventions to prevent aflatoxin-induced carcinogenesis in developing countries. Annu Rev Public Health. 2008;29:187-203. doi:10.1146/annurev.publhealth.29.020907.090859.

Guan S, Ji C, Zhou T, Li J, Ma Q, Niu T. Aflatoxin B(1) degradation by *Stenotrophomonas maltophilia* and other microbes selected using coumarin medium. Int J Mol Sci. 2008;9(8):1489-503. doi:10.3390/ijms9081489.

Haque MA, Wang Y, Shen Z, et al. Mycotoxin contamination and control strategy in human, domestic animal and poultry: a review. Microb Pathog. 2020;142:104095. doi:10.1016/j.micpath.2020.104095.

Haskard CA, El-Nezami HS, Kankaanpää PE, Salminen S, Ahokas JT. Surface binding of aflatoxin B1 by lactic acid bacteria. Appl Environ Microbiol. 2001;67(7):3086–3091. doi:10.1128/AEM.67.7.3086-3091.2001.

Hawkins LK, Mylroie JE, Oliveira DA, Smith JS, Ozkan S, Windham GL, Williams WP, Warburton ML. Characterization of the maize chitinase genes and their effect on *Aspergillus flavus* and aflatoxin accumulation resistance. PLoS One. 2015;10(6):e0126185. doi:10.1371/journal.pone.0126185.

Hugo C, Bernardet J-F, Nicholson A, Kämpfer *P. Chryseobacterium* in: Bergey's manual of systematics of archaea and bacteria. John Wiley & Sons; 2015. p. 1-107. doi:10.1002/9781118960608.gbm01170.

Hussain I, Anwar J. A study on contamination of aflatoxin M1 in raw milk in the Punjab province of Pakistan. Food Control. 2008;19(4):393-395. doi:10.1016/j.foodcont.2007.04.019.

Hussein HS, Brasel JM. Toxicity, metabolism, and impact of mycotoxins on humans and animals. Toxicology. 2001;167(2):101-134. doi:10.1016/s0300-483x(01)00471-1.

Iqbal SZ, Jinap S, Pirouz AA, Faizal ARA. Aflatoxin M1 in milk and dairy products, occurrence and recent challenges: a review. Trends Food Sci Technol. 2015;46(1):110-119. doi:10.1016/j.tifs.2015.08.005.

Iram W, Anjum T, Iqbal M, Ghaffar A, Abbas M. Structural elucidation and toxicity assessment of degraded products of aflatoxin B1 and B2 by aqueous extracts of *Trachyspermum ammi*. Front Microbiol. 2016;7:346. doi:10.3389/fmicb.2016.00346.

Jiang T, Li F, Li F, Xie C, Liu D, Yao D. Degradation of aflatoxin B1 by the *Armillariella tabescens*-derived aldo-keto reductase AtAKR. Food Biosci. 2024;58:103768. doi:10.1016/j.fbio.2024.103768.

Jowsey IR, Jiang Q, Itoh K, Yamamoto M, Hayes JD. Expression of the aflatoxin B1-8,9-epoxide-metabolizing murine glutathione S-transferase A3 subunit is regulated by the Nrf2 transcription factor through an antioxidant response element. Mol Pharmacol. 2003;64(5):1018-28. doi.org/10.1124/mol.64.5.1018.

Kavitha P, Mounika N, Ramana JV, Sreedevi B. Aflatoxicosis in livestock and poultry. J Anim Feed Sci Technol. 2015;3:21-26.

Khan R. Mycotoxins in food: Occurrence, health implications, and control strategies-a comprehensive review. Toxicon. 2024;248:108038. doi:10.1016/j.toxicon.2024.108038.

Klich MA. *Aspergillus flavus*: the major producer of aflatoxin. Mol Plant Pathol. 2007;8(6):713-22. doi:10.1111/j.1364-3703.2007.00436.x.

doi:10.6342/NTU202600056

Köppen R, Koch M, Siegel D, Merkel S, Maul R, Nehls I. Determination of mycotoxins in foods: current state of analytical methods and limitations. Appl Microbiol Biotechnol. 2010;86(6):1595-612. doi:10.1007/s00253-010-2535-1.

Kumar P, Mahato DK, Kamle M, Mohanta TK, Kang SG. Aflatoxins: a global concern for food safety, human health and their management. Front Microbiol. 2017;7:2170. doi:10.3389/fmicb.2016.02170.

Kutasi K, Recek N, Zaplotnik R, Mozetič M, Krajnc M, Gselman P, Primc G. Approaches to inactivating aflatoxins - a review and challenges. Int J Mol Sci. 2021;22(24):13322. doi:10.3390/ijms222413322.

Kutsuna R, Mashima I, Miyoshi-Akiyama T, Muramatsu Y, Tomida J, Kawamura Y. *Chryseobacterium lecithinasegens* sp. nov., a siderophore-producing bacterium isolated from soil at the bottom of a pond. Int J Syst Evol Microbiol. 2021;71(12). doi:10.1099/ijsem.0.005135.

Lahtinen SJ, Haskard CA, Ouwehand AC, Salminen SJ, Ahokas JT. Binding of aflatoxin B1 to cell wall components of *Lactobacillus rhamnosus* strain GG. Food Addit Contam. 2004;21(2):158–164. doi:10.1080/02652030310001639551.

Latham RL, Boyle JT, Barbano A, Loveman WG, Brown NA. Diverse mycotoxin threats to safe food and feed cereals. Essays Biochem. 2023;67(5):797-809. doi:10.1042/EBC20220221.

Leggieri MC, Battilani P, Pietri A, Toscano P. Modelling aflatoxin risk in maize under climate change scenarios in Europe. World Mycotoxin J. 2021;14(2):139-150. doi:10.3920/WMJ2020.2639.

Liang C, Nie Y, Mu X, Xu Y. Gene mining-based identification of aldo–keto reductases for highly stereoselective reduction of bulky ketones. Bioresour Bioprocess. 2018;5(1):33. doi:10.1186/s40643-018-0219-4.

Liew WP, Mohd-Redzwan S. Mycotoxin: its impact on gut health and microbiota. Front Cell Infect Microbiol. 2018;8:60. doi:10.3389/fcimb.2018.00060.

Mangini V, Rosini E, Caliandro R, Mangiatordi GF, Delre P, Sciancalepore AG, Pollegioni L, Haidukowski M, Mazzorana M, Sumarah MW, Renaud JB. DypB peroxidase for aflatoxin removal: new insights into the toxin degradation process. Chemosphere. 2024;349:140826. doi:10.1016/j.chemosphere.2023.140826.

McKenzie KS, Kubena LF, Denvir AJ, Rogers TD, Hitchens GD, Bailey RH, et al. Aflatoxicosis in Turkey poults is prevented by treatment of naturally contaminated corn with ozone generated by electrolysis. Poult Sci. 1998;77(8):1094-102. doi:10.1093/ps/77.8.1094.

Medina A, Akbar A, Baazeem A, Rodriguez A, Magan N. Climate change, food security and mycotoxins: challenges and opportunities. Curr Opin Food Sci. 2017;17:120-125. doi:10.1016/j.cofs.2017.10.008.

Meissonnier GM, Pinton P, Laffitte J, et al. Immunotoxicity of aflatoxin B1: impairment of the cell-mediated response to vaccine antigen and modulation of cytokine expression. Toxicol Appl Pharmacol. 2008;231(2):142-9. doi:10.1016/j.taap.2008.04.004.

Mitchell NJ, Bowers E, Hurburgh C, Wu F. Potential economic losses to the US corn industry from aflatoxin contamination. Food Addit Contam Part A Chem Anal Control Expo Risk Assess. 2016;33(3):540-550. doi:10.1080/19440049.2016.1138544.

Mughal MJ, Peng X, Kamboh AA, Chen P, Zhou Y, Fang J. Aflatoxin B1 induced systemic toxicity in poultry and rescue effects of selenium and zinc. Biol Trace Elem Res. 2017;178(2):292-300. doi:10.1007/s12011-016-0923-9.

doi:10.6342/NTU202600056

Mwakinyali SE, Ming Z, Xie H, Zhang Q, Li P. Investigation and characterization of *Myroides odoratimimus* strain 3J2MO aflatoxin B1 degradation. J Agric Food Chem. 2019;67(16):4595-602. doi:10.1021/acs.jafc.8b06810.

Ni Y, Li CX, Ma HM, Zhang J, Xu JH. Biocatalytic properties of a recombinant aldo-keto reductase with broad substrate spectrum and excellent stereoselectivity. Appl Microbiol Biotechnol. 2011;89(4):1111-8. doi:10.1007/s00253-010-2895-9.

Ning M, Zhang S, Xie Y, Wang W, Gao Y. Aflatoxin B1 removal by three bacterial strains and optimization of fermentation process parameters. Biotechnol Appl Biochem. 2019;66(6):930-8. doi:10.1002/bab.1807.

Ogwuegbu MC, Mthiyane DMN. Molecular antioxidant and immunological mechanisms of phytogenics in the mitigation of aflatoxicosis in poultry. J Appl Poult Res. 2024;33(3):100457. doi:10.1016/j.japr.2024.100457.

Omotayo OP, Omotayo AO, Mwanza M, Babalola OO. Prevalence of mycotoxins and their consequences on human health. Toxicol Res. 2019;35(1):1-7. doi:10.5487/TR.2019.35.1.001.

Owuor Lalah J, Omwoma S, Orony DAO. Aflatoxin B1: chemistry, environmental and diet sources and potential exposure in human in Kenya. IntechOpen; 2020. doi:10.5772/intechopen.88773.

Payne GA. Process of contamination by aflatoxin-producing fungi and their impact on crops. Mycotoxins in agriculture and feed safety. In: The Toxicology of Aflatoxins. Academic Press. 1998.

Peles F, Sipos P, Győri Z, Pfliegler WP, Giacometti F, Serraino A, et al. Adverse effects, transformation and channeling of aflatoxins into food raw materials in livestock. Front Microbiol. 2019;10:2861. doi:10.3389/fmicb.2019.02861.

Peng Z, Chen L, Zhu Y, Huang Y, Hu X, Wu Q, et al. Current major degradation methods for aflatoxins: a review. Trends Food Sci Technol. 2018;80:155-66. doi:10.1016/j.tifs.2018.08.009.

Petchkongkaew A, Taillandier P, Gasaluck P, Lebrihi A. Isolation of *Bacillus* spp. from Thai fermented soybean (Thua-nao): screening for aflatoxin B1 and ochratoxin A detoxification. J Appl Microbiol. 2008;104(5):1495-502. doi:10.1111/j.1365-2672.2007.03700.x.

Phillips TD, Lemke SL, Grant PG. Characterization of clay-based enterosorbents for the prevention of aflatoxicosis. Adv Exp Med Biol. 2002;504:157-71. doi:10.1007/978-1-4615-0629-4_16.

Pitt JI, Wild CP, Baan RA, Gelderblom WCA, Miller JD, Riley RT, Wu F, editors. Improving public health through mycotoxin control. IARC Scientific Publication No. 158. Lyon: International Agency for Research on Cancer; 2012.

Popescu RG, Borda D, Spinu M, Sandru CD. Aflatoxins in feed: types, metabolism, health consequences in swine and mitigation strategies. Toxins (Basel). 2022;14(12):853. doi:10.3390/toxins14120853.

Probst C, Njapau H, Cotty PJ. Outbreak of an unusual aflatoxin-producing strain of *Aspergillus* in Kenya. Appl Environ Microbiol. 2012;78(18):6796-8. doi:10.1128/AEM.01212-12.

Qin X, Su X, Tu T, Zhang J, Wang X, Wang Y, Wang Y, Bai Y, Yao B, Luo H, Huang H. Enzymatic degradation of multiple major mycotoxins by dye-decolorizing peroxidase from *Bacillus subtilis*. Toxins (Basel). 2021;13(6):429. doi:10.3390/toxins13060429.

Raksha Rao K, Vipin AV, Hariprasad P, Anu Appaiah KA, Venkateswaran G. Biological detoxification of aflatoxin B1 by *Bacillus licheniformis* CFR1. Food Control. 2017;71:234-41. doi:10.1016/j.foodcont.2016.06.040.

doi:10.6342/NTU202600056

Raruang Y, Omolehin O, Hu D, Wei Q, Han ZQ, Rajasekaran K, et al. Host-induced gene silencing targeting *Aspergillus flavus* aflM reduced aflatoxin contamination in transgenic maize under field conditions. Front Microbiol. 2020;11:754. doi:10.3389/fmicb.2020.00754.

Raters M, Matissek R. Thermal stability of aflatoxin B1 and ochratoxin A. Mycotoxin Res. 2008;24(3):130–134. doi:10.1007/s12550-008-0015-5.

Rustom IY. Aflatoxin in food and feed: occurrence, legislation and inactivation by physical methods. Food Chem. 1997;59:57-67. doi.org/10.1016/S0308-8146(96)00096-9.

Samarajeewa U, Sen AC, Cohen MD, Wei CI. Detoxification of aflatoxins in foods and feeds by physical and chemical methods. J Food Prot. 1990;53(6):489-501. doi:10.4315/0362-028X-53.6.489.

Sánchez-Bravo P, Noguera-Artiaga L, Gómez-López VM, Carbonell-Barrachina ÁA, Gabaldón JA, Pérez-López AJ. Impact of non-thermal technologies on the quality of nuts: a review. Foods (Basel). 2022;11:3891.doi: 10.3390/foods11233891.

Sargeant K, Sheridan A, O'Kelly J, Carnaghan RB. Toxicity associated with certain samples of groundnuts. Nature. 1961;192:1096-7. doi:10.1038/1921096a0.

Sen Y, Onal-Ulusoy B, Mutlu M. Detoxification of hazelnuts by different cold plasmas and gamma irradiation treatments. Innov Food Sci Emerg Technol. 2019;54:252-9. doi:10.1016/j.ifset.2019.05.002.

Shu X, Wang Y, Zhou Q, Li M, Hu H, Ma Y, et al. Biological degradation of aflatoxin B1 by cell-free extracts of *Bacillus velezensis* DY3108 with broad pH stability and excellent thermostability. Toxins (Basel). 2018;10(8):330. doi:10.3390/toxins10080330.

Singh J, Mehta A. The main aflatoxin B1 degrading enzyme in *Pseudomonas putida* is thermostable lipase. Heliyon. 2022;8(10):e10809. doi:10.1016/j.heliyon.2022.e10809.

Sipos P, Peles F, Brassó DL, Béri B, Pusztahelyi T, Pócsi I, Győri Z. Physical and chemical methods for reduction in aflatoxin content of feed and food. Toxins (Basel). 2021;13(3):204. doi:10.3390/toxins13030204.

Smela ME, Currier SS, Bailey EA, Essigmann JM. The chemistry and biology of aflatoxin B(1): from mutational spectrometry to carcinogenesis. Carcinogenesis. 2001;22(4):535-45. doi:10.1093/carcin/22.4.535.

Tessari ENC, Oliveira CAF, Cardoso ALSP, Ledoux DR, Rottinghaus GE. Effects of aflatoxin B1 and fumonisin B1 on blood biochemical parameters in broilers. Toxicon. 2006;48(6):643-9.

Thakare D, Zhang J, Wing RA, Cotty PJ, Schmidt MA. Aflatoxin-free transgenic maize using host-induced gene silencing. Sci Adv. 2017;3(3):e1602382. doi:10.1126/sciadv.1602382.

Thakur S, Singh RK, De PS, Dey A. Aflatoxins in feeds: issues and concerns with safe food production. Indian J Anim Health. 2022;61(1):1-13. doi:10.36062/ijah.2022.14421-411.

Toopaang W, Panyawicha K, Srisuksam C, Hsu WC, Lin CC, Tanticharoen M, et al. Metabolomic analysis demonstrates the impacts of polyketide synthases PKS14 and PKS15 on the production of beauvericins, bassianolide, enniatin A, and ferricrocin in entomopathogen *Beauveria bassiana*. Metabolites. 2023;13(3):425. doi:10.3390/metabo13030425.

U.S. Food and Drug Administration. CPG Sec. 683.100 Action levels for aflatoxins in animal feeds. 2024.

van Egmond HP, Schothorst RC, Jonker MA. Regulations relating to mycotoxins in food: perspectives in a global and European context. Anal Bioanal Chem. 2007;389(1):147-57. doi:10.1007/s00216-007-1317-9.

Varga J, Frisvad JC, Samson RA. Two new aflatoxin producing species, and an overview of *Aspergillus* section *Flavi*. Stud Mycol. 2011;69(1):57-80. doi:10.3114/sim.2011.69.05.

doi:10.6342/NTU202600056

Vekiru E, Fruhauf S, Rodrigues I, Ottner F, Krska R, Schatzmayr G, et al. In vitro binding assessment and in vivo efficacy of several adsorbents against aflatoxin B1. World Mycotoxin J. 2015;8(4):477-88. doi:10.3920/WMJ2014.1800.

Verheecke C, Liboz T, Mathieu F. Microbial degradation of aflatoxin B1: current status and future advances. Int J Food Microbiol. 2016;237:1-9. doi:10.1016/j.ijfoodmicro.2016.07.028.

Wang L, Wu J, Liu Z, Shi Y, Liu J, Xu X, et al. Aflatoxin B1 degradation and detoxification by *Escherichia coli* CG1061 isolated from chicken cecum. Front Pharmacol. 2018;9:1548. doi:10.3389/fphar.2018.01548.

Wang X, Bai Y, Huang H, Tu T, Wang Y, Wang Y, et al. Degradation of aflatoxin B1 and zearalenone by bacterial and fungal laccases in the presence of mediators. Toxins (Basel). 2019;11(10):609. doi:10.3390/toxins11100609.

Wang YD, Song CG, Yang J, Zhou T, Zhao YY, Qin JC, et al. Accurate identification of degraded products of aflatoxin B1 under UV irradiation based on UPLC-Q-TOF-MS/MS and NMR Analysis. Front Chem. 2021;9:789249. doi:10.3389/fchem.2021.789249.

Williams JH, Phillips TD, Jolly PE, Stiles JK, Jolly CM, Aggarwal D. Human aflatoxicosis in developing countries: a review of toxicology, exposure, potential health consequences, and interventions. Am J Clin Nutr. 2004;80(5):1106-22. doi:10.1093/ajcn/80.5.1106.

Yue X, Ren X, Fu J, Wei N, Altomare C, Haidukowski M, et al. Characterization and mechanism of aflatoxin degradation by *Trichoderma reesei* CGMCC3.5218. Front Microbiol. 2022;13:1003039. doi:10.3389/fmicb.2022.1003039.

Zhang C, Qu Z, Hou J, Yao Y. Contamination and control of mycotoxins in grain and oil crops. Microorganisms. 2024;12(3):567. doi:10.3390/microorganisms12030567.

Zhang Y, Wang P, Kong Q, Cotty PJ. Biotransformation of aflatoxin B1 by *Lactobacillus helveticus* FAM22155 in wheat bran by solid-state fermentation. Food Chem. 2021;341(Pt 1):128180. doi:10.1016/j.foodchem.2020.128180.

Zhang A, Yang J. A review of research progress on the microbial or enzymatic degradation and mechanism of aflatoxin B1. J Microbiol Biotechnol. 2025 Aug 18;35:e2504044. doi: 10.4014/jmb.2504.04044.

Chung TK, Erdman JW Jr, Baker DH. Hydrated sodium calcium aluminosilicate: effects on zinc, manganese, vitamin A, and riboflavin utilization. Poult Sci. 1990;69(8):1364-70. doi:10.3382/ps.0691364.

Tomasevic-Canovic M, Dakovic A, Markovic V, Radosavljevic-Mihajlovic A, Vukicevic J. Adsorption effects of mineral adsorbents, Part III: adsorption behaviour in the presence of vitamin B6 and microelements. Acta Vet (Beograd). 2000;50:23-30.

Velayutham K, Madhava AK, Pushparaj M, Thanarasu A, Devaraj T, Periyasamy K, Subramanian S. Biodegradation of Remazol Brilliant Blue R using isolated bacterial culture (Staphylococcus sp. K2204). Environ Technol. 2018;39(22):2900-2907. doi:10.1080/09593330.2017.1369579.

Wang Y, Zhao C, Zhang D, Zhao M, Zheng D, Lyu Y, et al. Effective degradation of aflatoxin B1 using a novel thermophilic microbial consortium TADC7. Bioresour Technol. 2017;224:166-73. doi:10.1016/j.biortech.2016.11.033.

Zhao C, Dong L, Zhang F, Luo Y, Yang Z, Zhang X, et al. Screening and characterization of a salt-tolerant aflatoxin B1-degrading strain isolated from Doubanjiang, a Chinese typical red pepper paste. Food Sci Technol. 2022;42:e122621. doi:10.1590/fst.122621.

doi:10.6342/NTU202600056

Appendix

Limaye A, Liu JR. Screening and Characterization of a *Chryseobacterium timonianum* Strain with Aflatoxin B1 Removal Ability. Microb Physiol. 2024;34(1):182–196. doi:10.1159/000540803.

doi:10.6342/NTU202600056

Microbial Physiology

Research Article

Microbial Physiol 2024;34:182–196
DOI: 10.1159/000540803

Received: April 15, 2023
Accepted: August 1, 2024
Published online: August 13, 2024

Screening and Characterization of a *Chryseobacterium timonianum* Strain with Aflatoxin B1 Removal Ability

Aniket Limaye[a] Je-Ruei Liu[a, b, c, d]

[a]Institute of Biotechnology, National Taiwan University, Taipei, Taiwan; [b]Department of Animal Science and Technology, National Taiwan University, Taipei, Taiwan; [c]Center for Biotechnology, National Taiwan University, Taipei, Taiwan; [d]Agricultural Biotechnology Research Center, Academia Sinica, Taipei, Taiwan

Downloaded from http://karger.com/mip/article-pdf/34/1/182/4276784/000540803.pdf by guest on 31 December 2025

Keywords
Aflatoxin B1 · Removal activity · *Chryseobacterium timonianum* · Metabolite analysis

Abstract
Introduction: Aflatoxin B1 (AFB1) is a potent hepatocarcinogenic mycotoxin found in animal feed and human food components. AFB1 contamination poses severe food safety and economic consequences. ***Methods:*** In this study, we used a coumarin-selective medium to isolate bacterial strains that can remove AFB1. Among the isolated bacterial strains, strain c4a exhibited the highest AFB1 removal activity. This strain was subjected to biochemical and phylogenetic characterization. The AFB1 removal activity of the extracellular supernatant of this strain was optimized for growth medium, reaction temperature, pH, and metal ions. The degradation products were analyzed using UPLC-ESI MS/MS. ***Results:*** Strain c4a was found to be most closely related to *Chryseobacterium timonianum*. The extracellular supernatant of *C. timonianum* c4a grown in a modified nutrient broth (with gelatin peptone and beef extract in a 4:1 ratio) demonstrated the highest AFB1 removal activity when incubated with 1 ppm AFB1 at 60°C, pH 8, and Mn^{2+} or Mg^{2+} supplementation for 72 h. Surprisingly, the autoclaved extracellular supernatant also retained AFB1 removal activity. UPLC-ESI MS/MS analysis suggested that AFB1 was transformed into a metabolite (m/z value 285.08) by water molecule addition on furan ring double bond. ***Conclusion:*** The AFB1 removal activity of *C. timonianum* c4a was extracellular, constitutive, and highly thermostable, structurally transforming AFB1 into a much less toxic product. Herein, we present the first evidence of thermostable AFB1 removal activity of a strain belonging to *C. timonianum*.

© 2024 The Author(s).
Published by S. Karger AG, Basel

Introduction

Aflatoxins belong to the family of structurally related mycotoxins secreted by *Aspergillus flavus* and *A. Parasiticus*. The four main aflatoxins are B1, B2, G1, and G2. The letters represent blue or green ultraviolet (UV) fluorescence, while the numbers represent their migration distance across a thin-layer chromatographic plate [1]. These secondary metabolites are difuranocoumarin derivatives produced by a common polyketide pathway involving seventeen genes encoding twelve enzymatic conversions [2, 3].

AFB1 has a core structure comprising dihydrofuro [2,3-b] furan and a coumarin ring, with the key toxic

karger@karger.com
www.karger.com/mip

© 2024 The Author(s).
Published by S. Karger AG, Basel

This article is licensed under the Creative Commons Attribution-NonCommercial-4.0 International License (CC BY-NC) (http://www.karger.com/Services/OpenAccessLicense). Usage and distribution for commercial purposes requires written permission.

Correspondence to:
Je-Ruei Liu, jrliu@ntu.edu.tw

doi:10.6342/NTU202600056

component being the furan ring's double bond. In the liver, this double bond (C-8/C-9) gets converted to AFB1-8,9-epoxide, forming highly toxic adducts with DNA, glutathione S-transferase, or N7 guanine [4]. The International Agency for Research on Cancer (IARC) has announced aflatoxins as Class 1 carcinogens, which are highly poisonous toxic substances. Among the aflatoxins, aflatoxin B1 (AFB1) is the most potent. The Food and Agriculture Organization (FAO) of the United Nations has estimated that about 25% or more of the world's food crops are affected and destroyed by AFB1 contamination each year.

Aspergillus species thrive in humid, warm tropical and subtropical areas where aflatoxin destroys crops. During preharvest to storage, aflatoxin can contaminate peanuts, corn, wheat, and soybeans [3]. AFB1 metabolism and toxicity in livestock depend on species, age, sex, feed mix, dosage, and exposure time. Resulting conditions include induced immunosuppression with poor cellular and humoral immunity, liver bleeding, renal necrosis, pancreatic cancer, and decreased body weight gain, milk and egg production [5]. Thus, AFB1-mediated livestock toxicity and further AFB1 carryover can be restricted by physical, chemical, or biological means. AFB1 can be physically adsorbed by bentonite or yeast cell walls [6] or chemically degraded by ozone, hydrogen peroxide, acidic electrolyzed water solution, and gamma and UV radiation [7–10]. Existing physical and chemical methods do not fully meet commercial productivity, safety, and cost standards [11]. Research indicates that AFB1-metabolizing bacteria or their derived metabolites effectively eliminate AFB1 [12–17]. However, this approach, while relatively safe, may yield toxic biotransformed metabolites, necessitating assessment of AFB1 biodegradation and metabolite profiles.

Coumarin has been used as a carbon source in selective media for screening AFB1-removing bacteria [18]. In this study, we employed a coumarin-selective medium to isolate AFB1-removing bacteria. Bacterial strains capable of growing in a coumarin-selective medium were selected for further analysis. Our laboratory-isolated bacterium, the c4a strain, was included in the screening because its genome contains important AFB1-degrading enzyme genes, including multicopper oxidase (NCBI accession number: WP_228452318) and DyP-peroxidase (NCBI accession number: WP_160139647). Given its high growth rate in the coumarin medium, we investigated whether the c4a strain can metabolize AFB1. The c4a strain demonstrated the highest AFB1 degradation among the selected coumarin-degrading strains. The c4a strain was identified as *C. timonianum* through physiologically, biochemically, and phylogenetically. The AFB1 removal activity of the c4a strain was optimized by adjusting the medium composition, reaction temperature, pH, and metal ion supplementation. The final transformed metabolites were subjected to LC-MS/MS analysis to determine possible structural changes in the AFB1 molecule, followed by a comparative toxicity study. Here, we report a novel, highly thermostable, extracellular AFB1 removal phenomenon by the *C. timonianum* c4a strain, resulting in structural modification of the furan ring of AFB1, which is linked to its toxicity.

Materials and Methods

Chemicals and Media

Luria-Bertani (LB) broth, nutrient broth, tryptone-yeast extract (TYE) broth, and M9 medium were purchased from Acumedia (Lansing, MI, USA), while coumarin and AFB1 were purchased from Sigma-Aldrich, Inc. (St. Louis, MO, USA). A coumarin medium, which contained coumarin as the sole carbon source, was prepared according to the method described by Guan et al. [18]. Each liter of coumarin medium contained 10.0 g coumarin, 0.25 g KH_2PO_4, 1.0 g NH_4NO_3, 1.0 g $CaCl_2$, 0.25 g $MgSO_4$, 1.0 mg $FeSO_4$, and 15.0 g agar, while the pH was adjusted to 7.0.

Experimental Samples

Forty Arbor Acres broilers (1 day old) were randomly divided into two groups: group A birds were not fed mycotoxin, and group B birds were given feed containing 200 ppb of AFB1. On day 35, the cecal digesta samples of one bird from group A and two from group B were subjected to bacterial screening. A soil sample enriched with chicken feathers obtained from the experimental farm of National Taiwan University (Taipei, Taiwan) was also used for bacterial screening.

Bacterial Screening and Isolation

The cecal digesta and soil samples (1 g each) were homogenized with 9 mL of sterile phosphate-buffered saline (PBS buffer, 0.1 M, pH 7.0) and serially diluted from 10^{-1}–10^{-4} fold before plating onto coumarin agar. The plates were incubated at 37°C aerobically and anaerobically for 4–7 days until colonies appeared. The colonies were transferred to new coumarin plates three consecutive times, following which single colonies were inoculated in coumarin broth and cultured at 37°C and 220 rpm, with bacterial growth monitored using a spectrophotometer at 600 nm. All isolated bacterial strains were further determined for their AFB1 removal activity.

Downloaded from http://karger.com/mpp/article-pdf/34/1/182/4277674/000540803.pdf by guest on 31 December 2025

doi:10.6342/NTU202600056

AFB1 Removal Activities of the Isolated Bacterial Strains

Overnight cultures of the isolated bacterial strains were inoculated into 10 mL sterile LB broth containing 1 ppm of AFB1 and incubated at 37°C at 220 rpm agitation for 72 h. A 450 µL aliquot of culture media was centrifuged at 10,000 *g* for 10 min at 4°C, and the amount of residual AFB1 in the LB broth was analyzed by high-performance liquid chromatography (HPLC). The bacterial strain, c4a, showing the maximum AFB1 biodegradation, was subjected to further characterization studies.

AFB1 Removal Activities of the Extracellular Supernatant, Intracellular Extract, and Cell Wall Fraction of the c4a Strain

A single colony of the c4a strain was inoculated into 3 mL LB broth and incubated at 30°C with 220 rpm agitation. After 7.5 h, the exponentially growing culture was added to 10 mL of sterile LB broth to obtain a final bacterial concentration of 1×10^9 CFU/mL. After 24 h under the same incubation regime, extracellular supernatant and cell pellets were separately obtained by centrifugation at 13,000 *g* for 10 min at 4°C. The cell pellet was washed twice with sterile PBS (0.1 M, pH 7.0), resuspended in 5 mL of sterile PBS, and sonicated on ice for 10 min with an ultrasonicator (Model XL, Misonix, Farmingdale, NY, USA). The intracellular extracts and cell wall fractions were obtained by centrifuging the sonicated cells at 13,000 *g* for 10 min at 4°C. The cell wall fraction was redissolved in sterile PBS with 1 ppm AFB1, while the extracellular supernatant and intracellular extract were mixed with 1 ppm AFB1, and all mixtures were incubated at 30°C and 220 rpm agitation for 96 h. During the incubation, 450 µL of aliquots were collected every 24 h for HPLC analysis of AFB1 concentration.

HPLC Analysis of AFB1 Concentrations

After filtration through a 0.2 µm membrane syringe filter (Pall Corporation, New York, NY, USA), 15 µL of each sample was subjected to HPLC analysis using an LC-20 AT delivery system (Shimadzu, Kyoto, Japan) equipped with an RF-10AXL fluorescence detector (Shimadzu), a Cosmosil 5C18-ARII column (Nacalai Tesque Inc., Kyoto, Japan; 250 × 4.6 mm i.d., particle size 5 µm) with a guard column (4 × 4 mm, 5 µm particle size), and a SIL-10A autoinjector (Shimadzu). The binary gradient HPLC protocol was adopted [19] with slight modifications. It involved a fluorescence (RF) detector (λ ex = 364 nm; λ em = 440 nm) and an UV detector (λ = 225 nm and 362 nm solvents, 0.1% phosphoric acid and acetonitrile: methanol, in a ratio of 1:1 [v/v]). The organic solvent concentration was increased from 0 to 100% over 35 min, with a flow rate of 1 mL/min and column temperature of 30°C. Commercial AFB1 standards were used to generate a standard curve to quantify the AFB1 concentration, and the AFB1-residual rate was obtained using the following formula:

$$\frac{\text{AFB1 peak area in treatment}}{\text{AFB1 peak area in control}} \times 100\%$$

Phenotypic and Biochemical Characterization of the c4a Strain

The c4a strain showed the highest AVB1 removal activity among the isolated strains and thus was subjected to further morphological and biochemical characterization. The c4a strain was streaked onto a sterile LB agar plate and incubated overnight at 30°C to observe colony morphology. The c4a cells were Gram stained and then observed under a microscope. The biochemical characterization and carbohydrate metabolism profiling of the c4a strain was performed using API 20 NE and API 50 CH kits (bioMerieux Inc., Marcy l'Etoile, France) according to the manufacturer's instructions.

Phylogenetic Characterization of the c4a Strain

Phylogenetic trees were constructed using single genes (*16S rRNA* and *gyrB*) and concatenated gene sequences (*rpoB*, *gyrB*, and *rpoD*). The *16S rRNA*, *gyrB*, *rpoB*, and *rpoD* gene sequences of the c4a strain (GenBank assembly accession number GCA_009900745.1) and selected type strains, including *Chryseobacterium balustinum* DSM 16775, *C. culicis* DSM 23031, *C. glaciei* IHBB 10212, *C. gleum* ATCC 35910, *C. indologenes* NBRC 14944, *C. nakagawai* G0041 (GCF_900637665.1), *C. piscium* CCUG 51923 (GCA_003385415.1), *C. scophthalmum* DSM 16779 (GCA_900143185.1), *C. timonianum* G972 (GCA_900078205.2), and *Riemerella anatipestifer* ATCC 11845 (GCA_000252855.1), were obtained from the NCBI whole genome sequence data. For the type strain, *Chryseobacterium lecithinasegens* PAGU 2197, the NCBI database contained the housekeeping genes used in this study; but the whole genome sequence was unavailable. Upon sequence alignment with BioEdit, MEGA 10.0.4 software was used to construct phylogenetic trees with 1,000 bootstrap replications using neighbor-joining and maximum likelihood algorithms.

Effect of Growth Medium Composition on AFB1 Removal Activity of the c4a Strain

The extracellular supernatant of the c4a strain grown in nutrient broth, LB broth, TYE broth, and M9 medium was tested for AFB1 removal. 1% overnight c4a culture was inoculated into 100 mL growth media and incubated for

Downloaded from http://karger.com/mpp/article-pdf/34/1/182/4276784/000540803.pdf by guest on 31 December 2025

doi:10.6342/NTU202600056

72 h in an orbital shaker at 30°C and 220 rpm. The extracellular supernatant was collected by centrifuging the bacterial culture at 10,000 *g* for 10 min at 4°C. The extracellular supernatant was mixed with 1 ppm AFB1 stock solution and incubated at 30°C for 72 h. The extracellular supernatant of the c4a strain grown in nutrient broth with gelatin peptone and beef extract in a 5:3 ratio had maximum AFB1 removal activity, so the ratio was optimized. The modified nutrient broth contained gelatin peptone and beef extract in a ratio of 1:9, 3:7, 1:1, 5:3, 7:3, 4:1, or 9:1, and the final total concentration of gelatin peptone and beef extract in the modified nutrient broth was 8 g/L. Based on AFB1 removal activity, the modified nutrient broth (modified NB) with gelatin peptone and beef extract in a 4:1 ratio was chosen as the final growth medium.

Effects of Reaction Temperature and pH, Mineral Ions, Heat Treatment, Protease Inhibitors, and SDS on AFB1 Removal Activity of the Extracellular Supernatant of the c4a Strain

The extracellular supernatant of the c4a strain was prepared as described above. To study the effects of reaction temperature on AFB1 removal activity, the extracellular supernatant of the c4a strain was mixed with AFB1 stock solution to achieve a final concentration of 1 ppm AFB1 and then incubated at 15, 20, 30, 40, 50, or 60°C for 72 h on an orbital shaker at 220 rpm. To study the effects of reaction pH on AFB1 removal activity, the extracellular supernatant of the c4a strain was mixed with AFB1 stock solution to achieve a final concentration of 1 ppm AFB1, and then the pH values of the mixtures were adjusted to 6, 7, 8, or 9 using 1 N HCl or 1 N NaOH and then incubated at 30°C for 72 h on an orbital shaker at 220 rpm. To study the effects of mineral ions on AFB1 removal activity, the extracellular supernatant of the c4a strain was mixed with $MgCl_2$, $ZnSO_4$, $CuSO_4$, $MnCl_2$, LiCl, or $FeCl_3$ stock solution to achieve a final concentration of 10 mM of each mineral ion. Then, the mixture was mixed with AFB1 stock solution to achieve a final concentration of 1 ppm AFB1 and incubated at 30°C for 72 h on an orbital shaker at 220 rpm. To study the effects of heat treatment on AFB1 removal activity, the extracellular supernatant of the c4a strain was autoclaved at 121°C for 15 min and then mixed with AFB1 stock solution to achieve a final concentration of 1 ppm AFB1 and incubated at 30°C for 72 h on an orbital shaker at 220 rpm. To study the effects of protease inhibitors and SDS on AFB1 removal activity, the extracellular supernatant of the c4a strain was mixed with an EDTA-free protease inhibitor (cOmplete ULTRA Tablets, Mini, Roche Diagnostics, Basel, Switzerland) or SDS (5%). Then, the mixture was mixed with AFB1 stock solution to achieve a final concentration of 1 ppm AFB1 and incubated at 30°C for 72 h on an orbital shaker at 220 rpm. At the end of the experiment, aliquots of 450 µL from each sample were taken to analyze AFB1 concentration.

Analysis of AFB1 Degradation Metabolites

The high-resolution LC-MS and LC-MS/MS data were collected by a Thermo UPLC-ESI Orbitrap Elite mass spectrometer equipped with an ACQUITY UPLC system (0–6 min 5–99.5% ACN, 6–8 min 99.5% ACN, 8–8.2 min 99.5–5% ACN, 8.2–10 min 5% ACN, both ACN and H2O contain 0.1% formic acid; ACQUITY UPLC BEH C18, 1.7 µm, 2.1 × 100 mm; flow rate: 0.4 mL/min). The extracellular fraction of the c4a strain and sterile growth media were dosed with 2 ppm AFB1 under optimum reaction conditions. The sample injection volume was 10 µL. Positive ion mode mass data were acquired between m/z 100–1,500 at 15,000 resolution. The top four intense ions from each full mass scan were selected for collision-induced dissociation. The selected ions were fragmented with normalized collision energy 35.0, activation Q 0.250, activation time 10.0, and 15,000 resolution for collision-induced dissociation. The isolation width was 2.5 Da [20]. MS/MS data were obtained in duplicates utilizing data-dependent acquisition. MS scan was performed using Thermo Xcalibur 2.2 SP 1.48 software over mass-to-charge (m/z) range 100–1,500.

Statistical Analyses

All AFB1 removal experiments were performed in triplicate, and the generated data were analyzed via one-way analysis of variance (ANOVA) using RStudio version 1.2.5. Duncan's multiple range test was performed to detect statistical differences, and a p value <0.05 was considered statistically significant.

Results

Isolation of Bacterial Strains with Potential for Removal of AFB1

Bacterial strains with AFB1 removal potential were isolated from chicken digesta and soil samples using the coumarin-selective medium. Three bacterial strains, 3PB1, BN5, and 4CW, were isolated from mycotoxin-fed chicken digesta; one bacterial strain, IL1, was isolated from non-mycotoxin-fed chicken digesta; and one bacterial strain, c4a, was isolated from the soil. As shown in Figure 1, the c4a strain was the most effective AFB1 remover of the five isolated strains, so it was chosen for

Downloaded from: http://karger.com/mmp/article-pdf/34/1/182/4270784/000540803.pdf by guest on 31 December 2025

doi:10.6342/NTU202600056

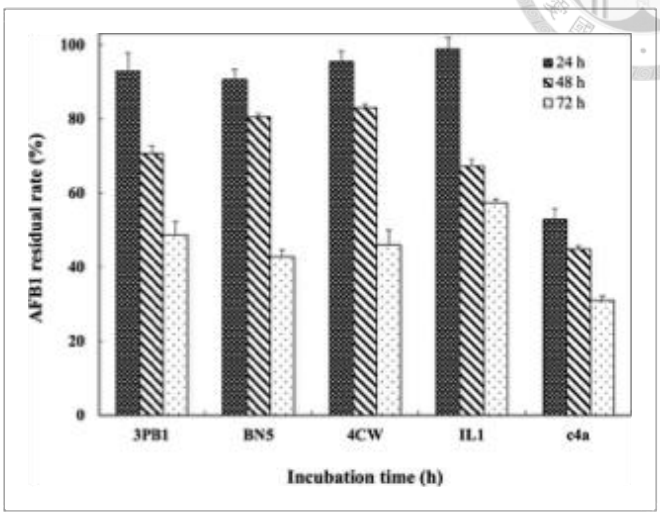


Fig. 1. AFB1 removal activity of the isolated bacterial strains. All data are expressed as mean ± SD (n = 3).

further investigation. Figure 2 represents the HPLC profile of AFB1 removal by extracellular supernatant of strain c4a, demonstrating AFB1 removal activity. The AFB1 removal activities of the intracellular extract and cell wall fraction of the c4a strain were also tested. As shown in Figure 3, the intracellular extract and cell wall fraction of the c4a strain had negligible AFB1 removal activity, implying that c4a-mediated AFB1 removal occurs exclusively extracellularly.

Phenotypic, Biochemical, and Genomic Characteristics of the c4a Strain

When grown on LB or nutrient agar, the c4a strain produced bright yellow colonies (1–3 mm). After 18–24 h of incubation at 30°C, the isolated colonies become elevated and smooth, with a buttery consistency (Fig. 4a). The yellow-orange convex colonies indicated the presence of flexirubin pigment, which turns red when 20% KOH is added. When grown on LB agar, these colonies also emit a fruity odor. Microscopic examination of the Gram-stained c4a cells revealed red-colored rods (Fig. 4b), which were Gram-negative and exhibited no motility or endospore formation.

The biochemical properties of the c4a strain were investigated using the API 20 NE system. The substrate assimilation profile of strain c4a revealed that it produced indole (tryptophan positive), urease, oxidase, hydrolyzed esculin, gelatin, assimilated glucose, mannose, maltose, and citrate. The c4a strain could not reduce nitrate to nitrogen, ferment glucose, produce arginine dihydrolase, and assimilate arabinose, N-acetylglucosamine, potassium gluconate, capric acid, adipic acid, malic acid, and phenylacetic acid. Based on these findings, the c4a strain was 99.4% identical to *C. indologenes*. However, the API database listed *C. indologenes* as the only species of the *Chryseobacterium* genus. The API 50 CH system was used to investigate further carbohydrate substrate utilization in the c4a strain. The results revealed that the c4a strain metabolized glycerol, amygdalin, esculin, D-trehalose, amidon, glycogen, gentiobiose, and xylitol (Table 1).

Figure 5 shows phylogenetic trees based on *16S rRNA* and *gyrB* gene sequences. In the 16S rRNA phylogenetic tree, the c4a strain is located on a distinct branch with closely related neighbors, *C. timonianum* and *C. lecithinasegens* (Fig. 5a). In the gyrB phylogenetic tree, the c4a strain shared a phylogenetic branch with *C. nakagawai* and *C. lecithinasegens* (Fig. 5b). These phylogenetic trees could not determine the phylogenetic placement of the c4a strain. To improve phylogenetic resolution, multilocal sequence alignment (MLSA) was performed with a concatenated sequence of three housekeeping genes (*rpoB-gyrB-rpoD*) (Fig. 6). The c4a strain formed a direct branch with its closest neighbor, *C. timonianum*, suggesting that it might belong to *C. timonianum*.

Downloaded from: http://harper.com/mp/article-pdf/34/1/182/4270784/000540803.pdf by guest on 31 December 2025

doi:10.6342/NTU202600056

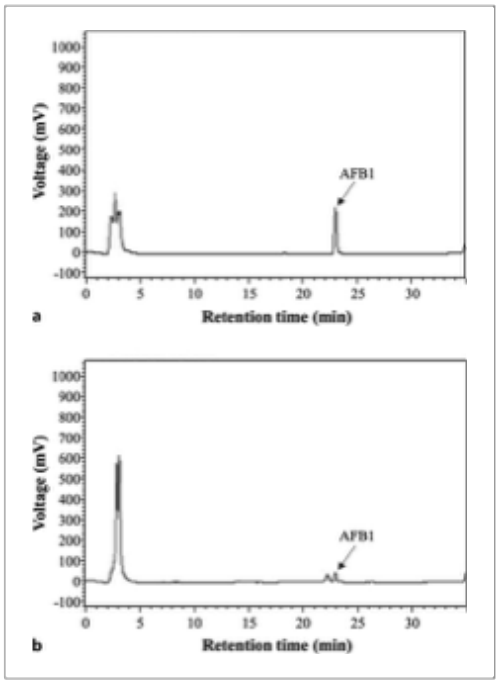


Fig. 2. High-performance liquid chromatography (HPLC) profile of AFB1 removal by the c4a strain. **a** HPLC profile of AFB1 in nutrient broth. **b** HPLC profile of AFB1 removal by the extracellular supernatant of the c4a strain.

Effect of Growth Medium Composition on AFB1 Removal Activity of the c4a Strain

To improve the AFB1 removal activity, the c4a strain was cultured in different growth media, and the AFB1 removal activity of the extracellular supernatants of the c4a strain was compared. As shown in Figure 7a, the extracellular supernatant of the c4a strain cultured in nutrient broth showed the highest AFB1 removal activity, followed by those cultured in LB broth and TYE broth. The extracellular supernatant of the c4a strain cultured in M9 minimal salt (M9) medium showed the lowest AFB1 removal activity. Figure 7b shows the effects of varied combinations of gelatin peptone and beef extract on the AFB1 removal activity of the extracellular supernatant of the c4a strain. The extracellular supernatant of the c4a strain cultured in the modified nutrient broth containing gelatin peptone and beef extract in a ratio 4:1 showed the highest AFB1 removal activity.

Effect of Reaction Temperature on AFB1 Removal Activity of the Extracellular Supernatant of the c4a Strain

The effect of reaction temperature on AFB1 removal activity of the extracellular supernatant of the c4a strain was determined after 72 h of incubation of the extracellular supernatant of c4a with 1 ppm of AFB1 at 15, 20, 30, 40, 50, or 60°C. As shown in Figure 8a, the AFB1 removal activity of the extracellular supernatant of the c4a strain was favored at higher temperatures, reaching a maximum at 60°C.

Effect of Reaction pH on AFB1 Removal Activity of the Extracellular Supernatant of the c4a Strain

The effect of reaction pH on AFB1 removal activity of the extracellular supernatant of the c4a strain was determined after 72 h of incubation of the CFF of c4a with 1 ppm of AFB1 at pH 6, 7, 8, or 9. As shown in Figure 8b, the AFB1 removal activity of the extracellular supernatant of the c4a strain was more effective in the alkaline range and maximal at pH 8.

Effect of Mineral Ions on AFB1 Removal Activity of the Extracellular Supernatant of the c4a Strain

The addition of metal ions in the extracellular supernatant of the c4a strain altered the AFB1 removal activity. As shown in Figure 8c, the addition of Mn^{2+} and Mg^{2+} ions significantly increased the AFB1 removal activity of the extracellular supernatant of the c4a strain while adding Fe^{3+} ions in the extracellular supernatant of the c4a strain decreased the AFB1 removal activity.

Effect of Protease Inhibitors, SDS, and Autoclaved Treatments on AFB1 Removal Activity of the Extracellular Supernatant of the c4a Strain

The addition of the protease inhibitor cocktails in the extracellular supernatant of the c4a strain significantly reduced the AFB1 removal activity, and the addition of SDS completely deactivated the AFB1 removal activity of the extracellular supernatant of the c4a strain, thus suggesting that the molecule(s) in the extracellular supernatant of the c4a strain-mediated the AFB1 removal is proteinic. The AFB1 removal activity of the autoclaved extracellular supernatant of the c4a strain was retained, indicating that heat treatment did not affect the AFB1 removal activity of the extracellular supernatant of the c4a strain (Fig. 8d).

Analysis of AFB1 Degradation Metabolites

The AFB1 degradation pattern (m/z values) by the c4a strain was found to be 417.21 → 412.25 → 331.08 → 313.07 → 285.08, with loss of H_2O in the second last step, followed by loss of CO in the final step. The final degradation

Downloaded from http://karger.com/mpp/article-pdf/34/1/182/4276784/000540803.pdf by guest on 31 December 2025

doi:10.6342/NTU202600056

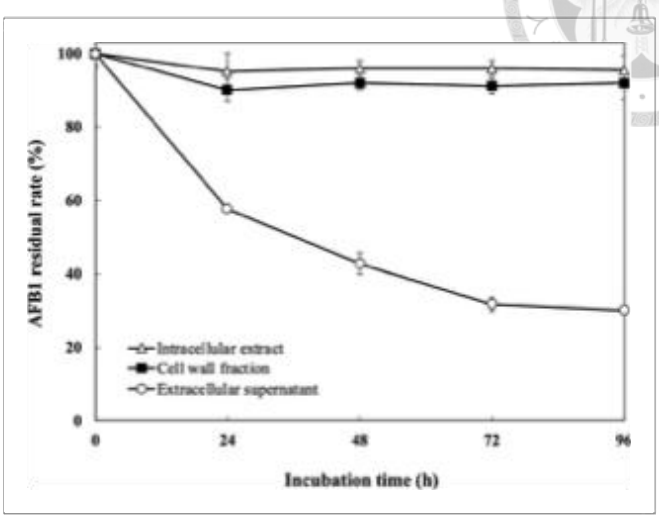


Fig. 3. Removal of AFB1 by intracellular extract, cell wall fraction, and extracellular supernatant of the c4a strain. All data are expressed as mean ± SD (n = 3).

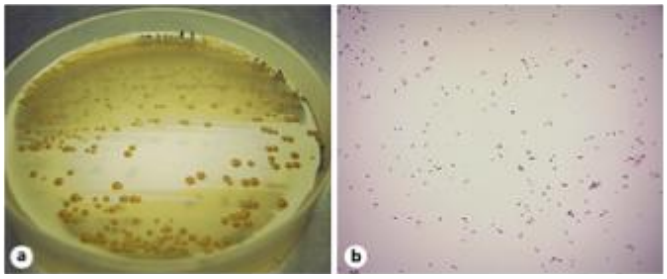


Fig. 4. Macroscopic and microscopic examinations of the c4a strain. **a** The colony morphologies of the c4a strain on LB agar plate. **b** Gram-stained c4a cells observed under a phase-contrast microscope (×1,000).

product had the molecular formula $C_{17}H_{14}O_7$. Figure 9a shows the MS-1 profile of strain c4a-mediated AFB1 degradation. It showed the predominant presence of an ion fragment of m/z 313.07. Figure 9b shows the MS-2 profile at m/z 331. 08, which shows the dominant presence of ion fragment m/z 313.07. Figure 9c shows the MS-2 profile at m/z 313.07 having an ion fragment of m/z 285.08.

Discussion

Coumarin is a phenolic compound derived from cis-*O*-hydroxycinnamic acid with a structure similar to that of AFB1, and so has been used in the selection media to screen for AFB1-degrading microbial strains [18, 21, 22]. Coumarin media was thus employed to selectively isolate bacterial strains with the potential to remove AFB1 in the present study. Five bacterial strains, 3PB1, BN5, 4CW, IL1, and c4a, were obtained following coumarin-selective screening. The c4a strain, isolated from the chicken feather enriched soil sample, showed the highest AVB1 removal activity among the isolated strains and thus was subjected to further study.

The primary morphological and biochemical characteristics of the c4a strain were similar to the other members of the genus *Chryseobacterium*. A comparative analysis of the biochemical profiles to understand the unique metabolic capabilities of the c4a strain and its close neighbors, *C. timonianum* G972 [23] and *C.*

Downloaded from http://karger.com/mpr/article-pdf/34/1/182/4276784/000540803.pdf by guest on 31 December 2025

doi:10.6342/NTU202600056

Table 1. Biochemical characteristics of the c4a strain

Substrate	Result	Substrate	Result
N-Acetyl-glucosamine	–	D-Lyxose	–
Adipic acid	–	Mallic acid	–
Adonitol	–	D-Maltose	+
Amygdalin	+	D-Mannitol	–
D-Arabinose	–	D-Mannose	+
L-Arabinose	–	Melezitose	–
D-Arabitol	–	Melibiose	–
L-Arabitol	–	α-Methyl-D-glucoside	–
Arbutin	–	α-Methyl-D-mannoside	–
L-Arginine	–	β-Methyl-xyloside	–
Capric acid	–	4-Nitrophenyl-β-D-glucopyranoside	–
Cellobiose	–	Phenylacetic acid	–
Dulcitol	–	Potassium gluconate	–
Erythritol	–	D-Raffinose	–
Esculin ferric citrate	+	Rhamnose	–
D-Fructose	–	Ribose	–
D-Fucose	–	Saccharose	–
L-Fucose	–	Salicin	–
Galactose	–	Sorbitol	–
Gelatin	+	L-Sorbose	–
β-Gentiobiose	+	Starch	–
Gluconate	–	D-Tagatose	–
D-Glucose	+	Trehalose	+
Glycerol	+	Tri-sodium citrate	+
Glycogen	+	L-Tryptophan	+
Inositol	–	D-Turanose	–
Inulin	–	Urea	+
5-Keto-gluconate	–	Xylitol	–
2-Keto-gluconate	–	D-Xylose	–
Lactose	–	L-Xylose	–

lecithinasegens CCUG 17150 [24], was carried out. All three strains tested positive for acid production using D-glucose, D-mannose, esculin, D-maltose, D-trehalose, and gentibiose. *C. lecithinasegens* and the c4a strain utilized amygdalin and produced indole, whereas *C. timonianum* did not. These comparisons revealed that the c4a strain and *C. timonianum* have a more varied metabolic profile than *C. lecithinasegens*. Unlike *C. lecithinasegens* and *C. timonianum*, the c4a strain could not metabolize glycogen or glycerol.

The 16S rRNA-based phylogenetic tree showed that the c4a strain formed a monophyletic branch with *C. timonianum* (99.21%) and *C. lecithinasegens* (98.92%). To understand the differentiation of strain c4a within this genus, another phylogenetic tree was created using *gyrB* gene sequences. The most similar sequences to strain c4a were *C. lecithinasegens* (92.92%), followed by *C. nakagawai* (92.87%) and *C. timonianum* (91.58%). The c4a strain's gyrB sequence was less than 89% similar to other *Chryseobacterium* strains. We created an additional

Downloaded from http://karger.com/mip/article-pdf/34/1/182/4276784/000540803.pdf by guest on 31 December 2025

doi:10.6342/NTU202600056

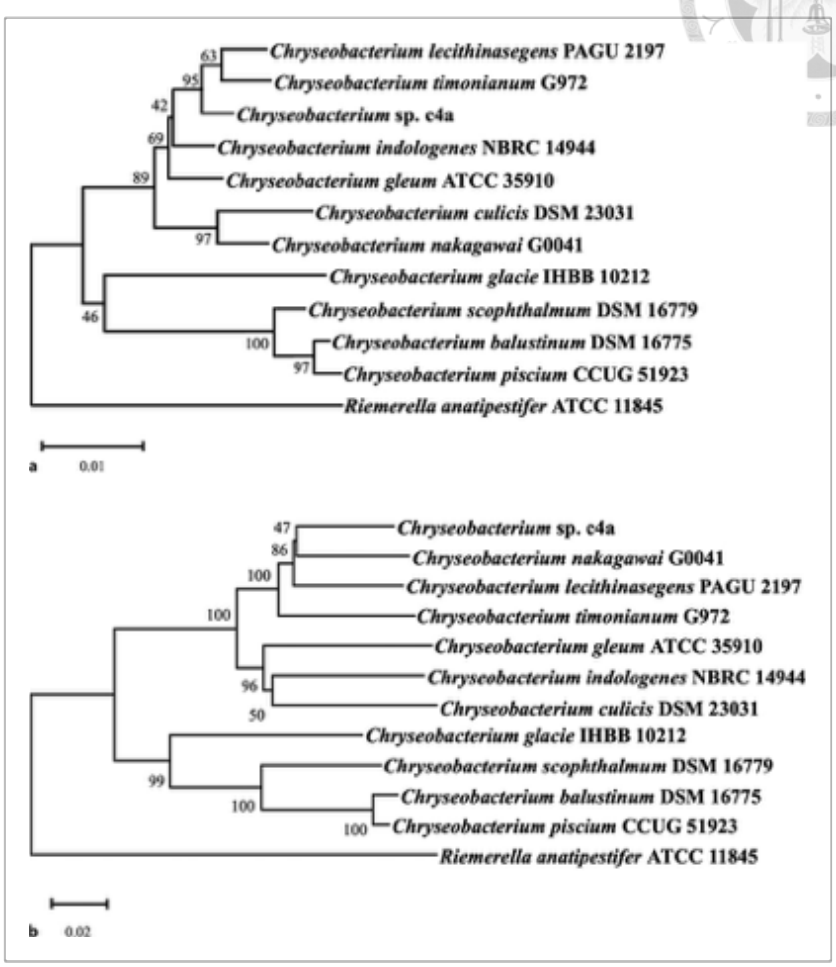


Fig. 5. Neighbor-joining phylogenetic tree-based analyses of the 16S rRNA and DNA gyrase B (*gyrB*) genes of *Chryseobacterium* species. **a** Neighbor-joining phylogenetic tree based on *16S rRNA* gene sequences. The scale bar represents 0.01 nucleotide substitution per nucleotide position. **b** Neighbor-joining phylogenetic tree based on *gyrB* gene sequences. The scale bar represents 0.02 nucleotide substitution per nucleotide position. At major nodes, bootstrap percentages for 1,000 re-samplings are shown.

phylogenetic tree using a rpoB-gyrB-rpoD concatenated sequence of conserved housekeeping genes and found that the c4a strain and *C. timonianum* shared a close phylogenetic relationship, implying that it may belong to *C. timonianum*.

The *Chryseobacterium* genus is classified within the Flavobacteriaceae family, Flavobacteriales order, and in the *Flavobacteriia* class. The majority of *Chrsyeobacterium* species were found in soil, freshwater or saltwater, insects, biofilms, and industrial sources like

Downloaded from http://karger.com/mpr/article-pdf/34/1/182/4276784/000540803.pdf by guest on 31 December 2025

doi:10.6342/NTU202600056

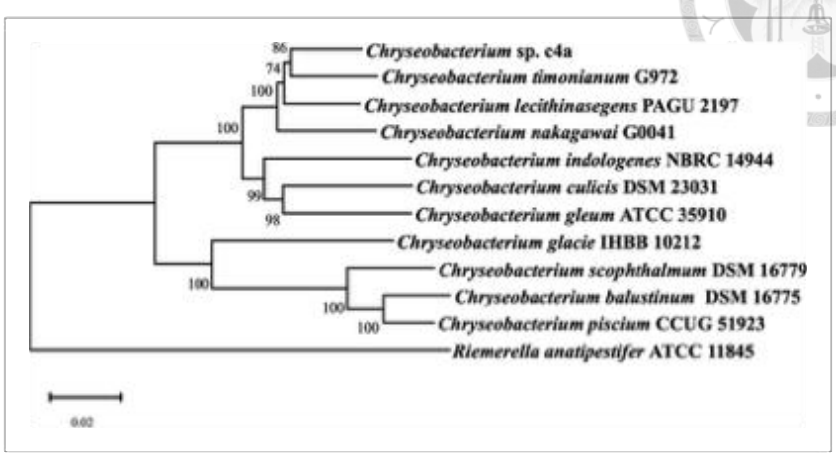


Fig. 6. Neighbor-joining phylogenetic tree-based analyses of the RNA polymerase β subunit (rpoB), DNA gyrase B (*gyrB*), and σ factor of RNA polymerase (rpoD) of *Chryseobacterium* species. The scale bar represents 0.02 nucleotide substitution per nucleotide position. At major nodes, bootstrap percentages for 1,000 re-samplings are shown.

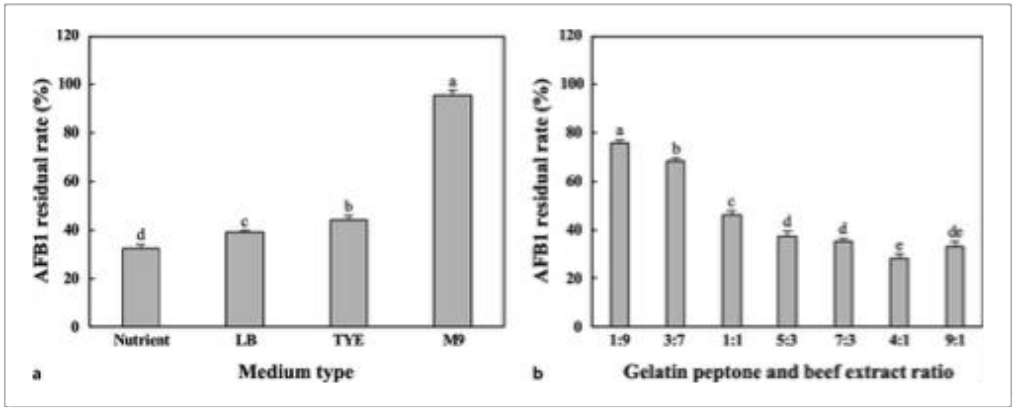


Fig. 7. Effect of growth medium composition on the AFB1 removal activity of the c4a strain. **a** Effect of nutrient broth, LB broth, TYE broth, and M9 medium on the AFB1 removal activity of the c4a strain. **b** Effect of the ratio of gelatin peptone and beef extract in the nutrient broth on the AFB1 removal activity of the c4a strain. All data are expressed as mean ± SD (n = 3). Bars marked with the same letter are not significantly different (p > 0.05).

beer bottling factories. Although some *Chryseobacterium species* have been isolated from human clinical samples, it is difficult to determine whether they are direct or opportunistic pathogens or merely contaminants [25]. Similarly, the c4a strain was isolated from farm soil that had not been fertilized or treated with chemicals, whereas *C. timonianum* was isolated from sputum.

Downloaded from http://karger.com/mpr/article-pdf/34/1/182/4276784/000540803.pdf by guest on 31 December 2025

doi:10.6342/NTU202600056

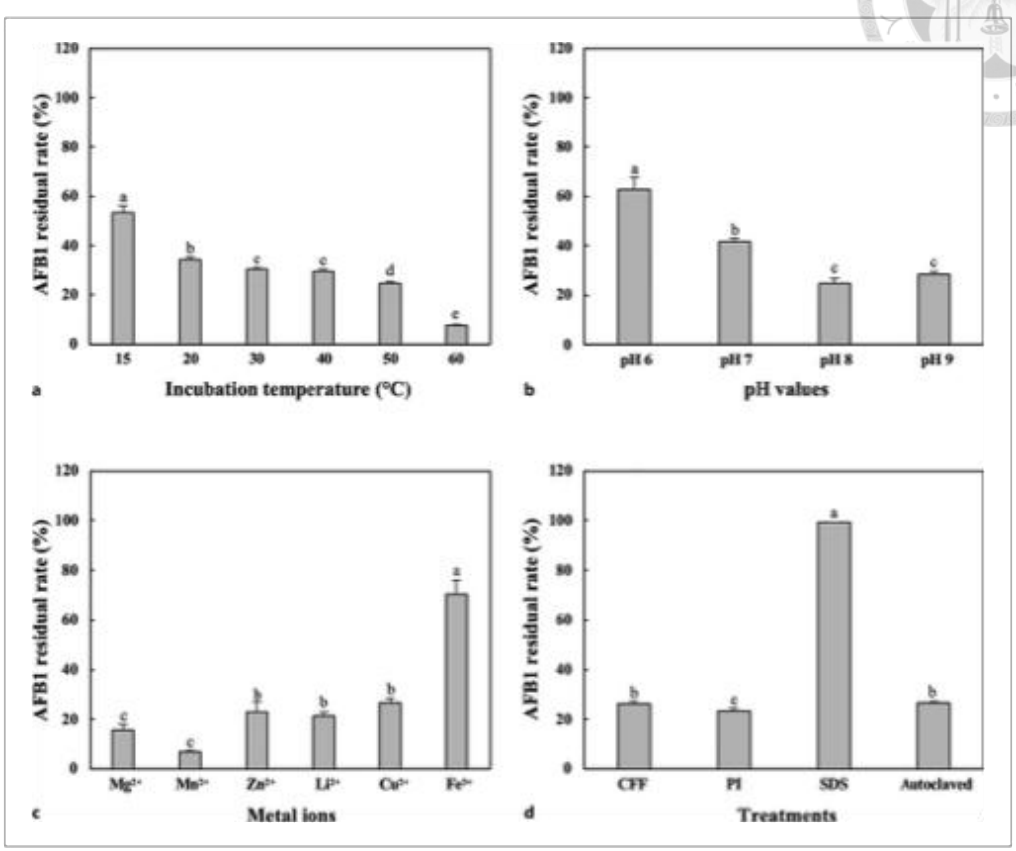
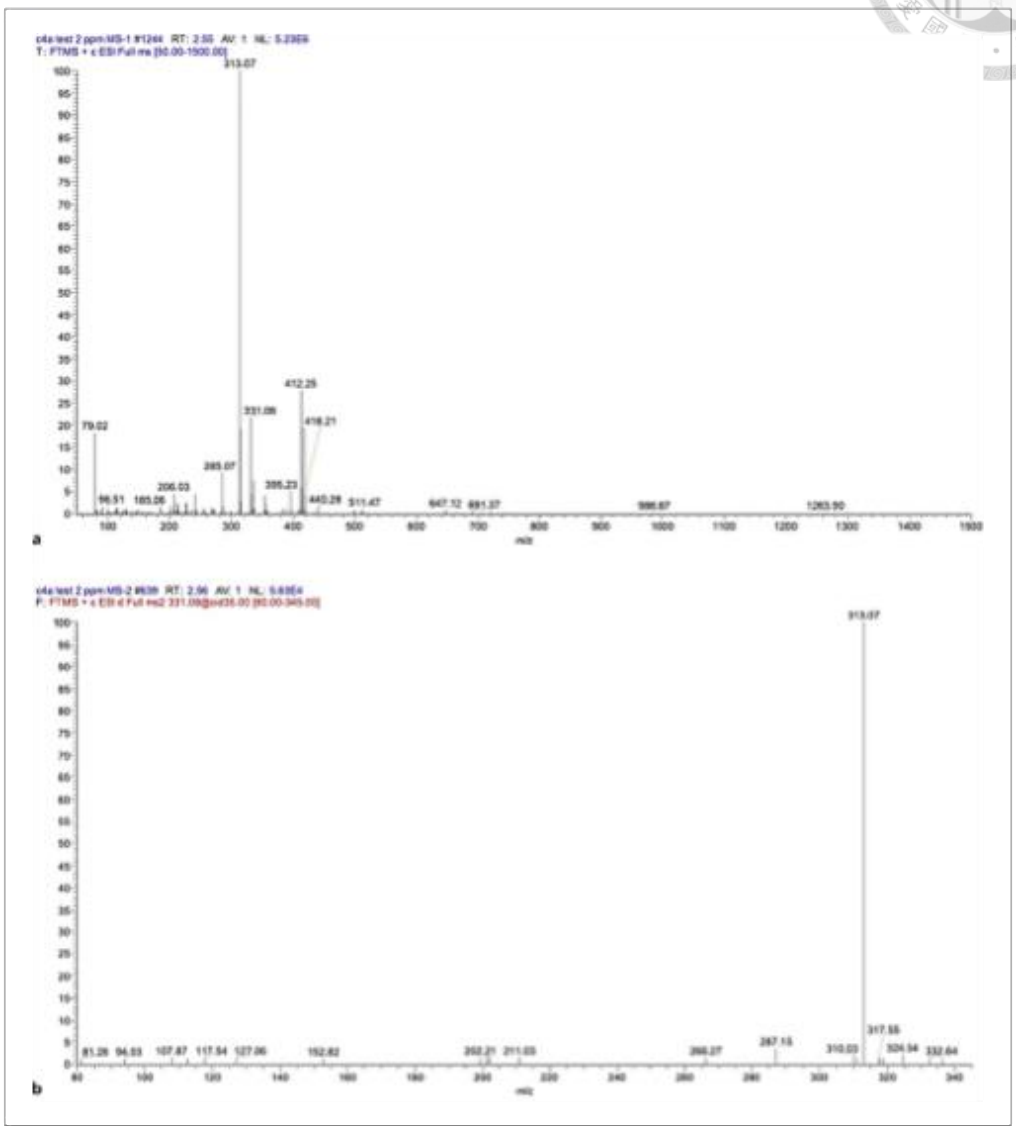


Fig. 8. Effects of reaction temperature (**a**), reaction pH (**b**), supplementation of mineral Ions (**c**), and protease inhibitors, SDS, and autoclave treatment (**d**) on the AFB1 removal activity of the extracellular supernatant of c4a strain. Effects of incubation temperatures, pH values, mineral ions, heat, and proteinase inhibitor on AFB 1 biodegradation by the c4a strain. All data are expressed as mean ± SD ($n = 3$). Bars marked with the same letter are not significantly different ($p > 0.05$).

Characterization studies showed that the c4a strain-mediated AFB1 removal was constitutive and extracellular. There is abundant evidence of microbial degradation across multiple genera, and physical AFB1 binding to bacterial and yeast cell walls has been widely reported [12]. This surface binding may not be specific, leading to binding minerals and trace nutrients like vitamins [26, 27]. Enzymatic degradation is a more effective and targeted biocontrol strategy for AFB1 contamination. After 72 h, the c4a strain's extracellular supernatant removed the highest AFB1 in this study. The growth media components affected the c4a strain's AFB1 removal activity, with gelatin peptone being a critical media component. AFB1 removal activity of strain c4a spanned a wide temperature range and was found to be highly thermotolerant. We observed that autoclaving did not affect this phenomenon. A microbial consortium with dominant *Geobacillus* and *Tepidimicrobium* species [28] and single bacterial strains like *Escherichia coli* CG1061 [15], *Bacillus velezensis* DY3108 [13], and *Stenostrophomonas* sp. CW117 [16] have shown thermostable AFB1 removal activity at 80°C–100°C.

Downloaded from http://karger.com/mpr/article-pdf/34/1/182/4276784/000540803.pdf by guest on 31 December 2025

doi:10.6342/NTU202600056



9

(Figure continued on next page.)

The pH dependence and metal cofactor specificity for the AFB1 removal activity of the c4a strain were observed, with acidic pH significantly reducing the AFB1 removal activity of the c4a strain, similar to *B. velezensis* AD8 [29]. The highest AFB1 removal activity of the c4a strain was found at pH 8, similar to that observed for *E. coli* CG1061

Downloaded from: http://karger.com/mip/article-pdf/34/1/182/4276784/000540803.pdf by guest on 31 December 2025

doi:10.6342/NTU202600056

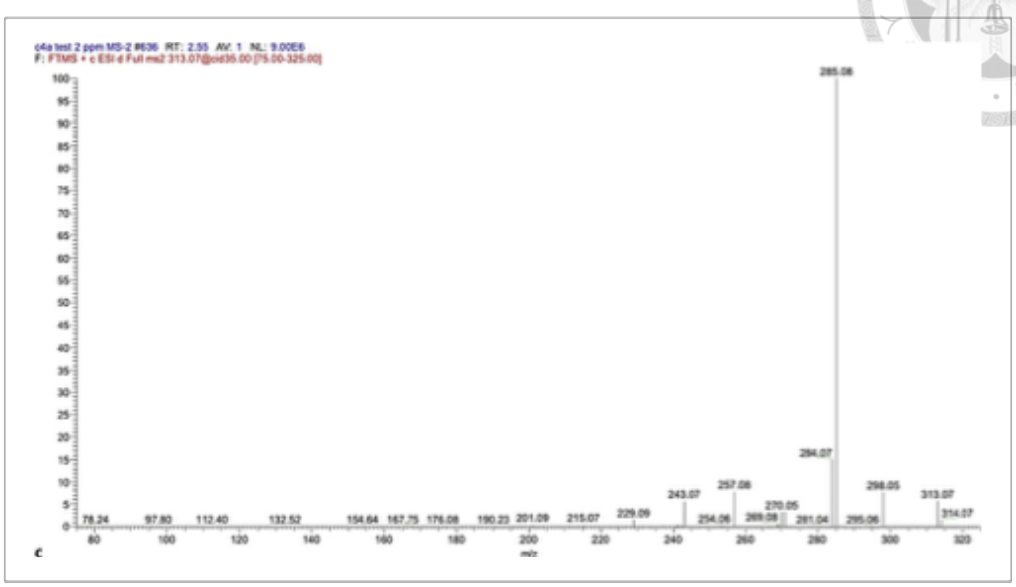


Fig. 9. The AFB1 degradation pattern (m/z values) mediated by c4a strain. **a** MS-1 profile of strain c4a-mediated AFB1 degradation. **b** MS-2 profile of ion fragment with m/z 331.08. **c** MS-2 profile of ion fragment with m/z 313.07.

[15]. The addition of a protease inhibitor caused a reduction in AFB1 removal activity of the c4a strain, which implied that the presence of protease positively affected AFB1 removal activity. The proteinic AFB1 removal activity was completely inhibited after SDS addition, as SDS causes the structural disintegration of proteins in the extracellular cell-free fraction. The AFB1 removal activity of the c4a strain was dependent on metal ions supplementation, with Fe^{3+} ion addition reducing AFB1 removal activity, whereas Mn^{2+} and Mg^{2+} ions significantly improved AFB1 removal activity. Fe^{3+} induced inhibition of AFB1 removal activity was found to be similar to the case of the bacterium *Myroides odoratimimus* [14]. AFB1 removal improvement effect in the case of Mn^{2+} and Mg^{2+} ion additions was found to be identical to that reported for *Stenotrophomonas* sp. CW117 [16]. These characterization results indicate that the AFB1 removal activity of the c4a strain resulted from complex protein interactions with excellent thermotolerance and a specific preference for pH and metal ions.

UPLC-ESI MS/MS analysis gave insight into strain c4a-mediated AFB1 degradation. At 2.55 s, a metabolite peak of various ionic fragments emerged. The MS-1 and MS-2 analyses of this peak showed that ion 313.07 m/z disintegrated into a final transformed product of 285.08. Recently, an interesting work documented all AFB1 breakdown products after UV irradiation using UPLC-Q-TOF-MS/MS and NMR [4]. This report revealed the same degradation product with chemical formula C17H14O7 as the c4a strain (285.08 m/z). The transformation pattern suggested water molecule addition on the double bond (C-8/C-9) of AFB1. The article assayed degradation product toxicity on LO-2, Hep-G2, and MCF-7 cell lines [4]. The cytotoxic activity (μM) of the transformed product (m/z 285.08) was much lower (>100 μM) than pure AFB1(22.47, 29.08, 36.57 μM) against LO-2, HepG2, and MCF-7 cell lines. These findings showed that strain c4a extracellular supernatant may target the C8-C9 double bond of AFB1's furan ring, lowering its cytotoxicity.

Based on the relevant literature review, AFB1 removal activity of any *Chrsyeobacterium* species has not been reported yet. To the best of our knowledge, this is the first report of the AFB1 removal potential of a bacterial strain belonging to *C. timonianum*. This evidence makes the current study a promising reference for future studies concerning the environmental biocontrol of AFB1 by *C. timonianum*.

Downloaded from http://karger.com/mpr/article-pdf/34/1/182/4276784/000540803.pdf by guest on 31 December 2025

doi:10.6342/NTU202600056

Acknowledgments

We are grateful to Dr. Yu Liang Yang for guidance in LC-MS/MS experimentation and analysis. This study was conducted in the metabolomics core facility, ABRC, Academica Sinica, Taipei, Taiwan.

Funding Sources

The work was supported by a grant from the Ministry of Science and Technology (Grant No. MOST 110-2313-B-002-052-MY2).

Statement of Ethics

The animal procedures were approved by the Institutional Animal Care and Use Committee of National Taiwan University, Approval No. NTU105-EL-00027.

Author Contributions

All authors contributed to the study's conception and design. Material preparation, data collection, and analysis were performed by Aniket Limaye. The first draft of the manuscript was written by Aniket Limaye and Dr. Je Ruei Liu. All authors commented on previous versions of the manuscript. All authors read and approved the final manuscript.

Conflict of Interest Statement

The authors have no competing interests to declare that are relevant to the content of this article.

Data Availability Statement

All data generated or analyzed during this study are included in this article. Further inquiries can be directed to the corresponding author.

References

1 Klich MA. *Aspergillus flavus*: the major producer of aflatoxin. Mol Plant Path. 2007;8(6):713–22. https://doi.org/10.1111/j.1364-3703.2007.00436.x

2 Bhatnagar D, Ehrlich KC, Cleveland TE. Molecular genetic analysis and regulation of aflatoxin biosynthesis. Appl Microbiol Biotechnol. 2003;61(2):83–93. https://doi.org/10.1007/s00253-002-1199-x

3 Abrar M, Anjum FM, Butt MS, Pasha I, Randhawa MA, Saeed F, et al. Aflatoxins: biosynthesis, occurrence, toxicity, and remedies. Crit Rev Food Sci Nutr. 2013;53(8):862–74. https://doi.org/10.1080/10408398.2011.563154

4 Wang Y-D, Song C-G, Yang J, Zhou T, Zhao YY, Qin JC, et al. Accurate identification of degraded products of aflatoxin B1 under UV irradiation based on UPLC-Q-TOF-MS/MS and NMR Analysis. Front Chem. 2021;9:789249. https://doi.org/10.3389/fchem.2021.789249

5 Peles F, Sipos P, Győri Z, Pfliegler WP, Giacometti F, Serraino A, et al. Adverse effects, transformation and channeling of aflatoxins into food raw materials in livestock. Front Microbiol. 2019;10:2861. https://doi.org/10.3389/fmicb.2019.02861

6 Vekiru E, Fruhauf S, Rodrigues I, Ottner F, Krska R, Schatzmayr G, et al. In vitro binding assessment and in vivo efficacy of several adsorbents against aflatoxin B1. World Mycotoxin J. 2015;8(4):477–88. https://doi.org/10.3920/wmj2014.1800

7 Adegoke GO, Babalola AK, Akanni AO. Effects of sodium metabisulphite, hydrogen peroxide and heat on aflatoxin B1 in lafun and gari: two cassava products. Nahrung. 1991;35(10):1041–5. https://doi.org/10.1002/food.19910351009

8 McKenzie KS, Kubena LF, Denvir AJ, Rogers TD, Hitchens GD, Bailey RH, et al. Aflatoxicosis in Turkey poults is prevented by treatment of naturally contaminated corn with ozone generated by electrolysis. Poult Sci. 1998;77(8):1094–102. https://doi.org/10.1093/ps/77.8.1094

9 Diao E, Li X, Zhang Z, Ma W, Ji N, Dong H. Ultraviolet irradiation detoxification of aflatoxins. Trends Food Sci Technol. 2015;42(1):64–9. https://doi.org/10.1016/j.tifs.2014.12.001

10 Sen Y, Onal-Ulusoy B, Mutlu M. Detoxification of hazelnuts by different cold plasmas and gamma irradiation treatments. Innov Food Sci Emerg Technol. 2019;54:252–9. https://doi.org/10.1016/j.ifset.2019.05.002

11 Verheecke C, Liboz T, Mathieu F. Microbial degradation of aflatoxin B1: current status and future advances. Int J Food Microbiol. 2016;237:1–9. https://doi.org/10.1016/j.ijfoodmicro.2016.07.028

12 Peng Z, Chen L, Zhu Y, Huang Y, Hu X, Wu Q, et al. Current major degradation methods for aflatoxins: a review. Trends Food Sci Technol. 2018;80:155–66. https://doi.org/10.1016/j.tifs.2018.08.009

13 Shu X, Wang Y, Zhou Q, Li M, Hu H, Ma Y, et al. Biological degradation of aflatoxin B1 by cell-free extracts of *Bacillus velezensis* DY3108 with broad pH stability and excellent thermostability. Toxins. 2018;10(8):330. https://doi.org/10.3390/toxins10080330

14 Mwakinyali SE, Ming Z, Xie H, Zhang Q, Li P. Investigation and characterization of *Myroides odoratimimus* strain 3J2MO aflatoxin B1 degradation. J Agric Food Chem. 2019;67(16):4595–602. https://doi.org/10.1021/acs.jafc.8b06810

15 Wang L, Wu J, Liu Z, Shi Y, Liu J, Xu X, et al. Aflatoxin B1 degradation and detoxification by *Escherichia coli* CG1061 isolated from chicken cecum. Front Pharmacol. 2018;9:1548. https://doi.org/10.3389/fphar.2018.01548

16 Cai M, Qian Y, Chen N, Ling T, Wang J, Jiang H, et al. Detoxification of aflatoxin B1 by *Stenotrophomonas* sp. CW117 and characterization of the thermophilic degradation process. Environ Pollut. 2020;261:114178. https://doi.org/10.1016/j.envpol.2020.114178

17 Zhang Y, Wang P, Kong Q, Cotty PJ. Biotransformation of aflatoxin B1 by *Lactobacillus helveticus* FAM22155 in wheat bran by solid-state fermentation. Food Chem. 2021;341(Pt 1):128180. https://doi.org/10.1016/j.foodchem.2020.128180

18 Guan S, Ji C, Zhou T, Li J, Ma Q, Niu T. Aflatoxin B(1) degradation by *Stenotrophomonas maltophilia* and other microbes selected using coumarin medium. Int J Mol Sci. 2008;9(8):1489–503. https://doi.org/10.3390/ijms9081489

19 Petchkongkaew A, Taillandier P, Gasaluck P, Lebrihi A. Isolation of *Bacillus* spp. from Thai fermented soybean (Thua-nao): screening for aflatoxin B1 and ochratoxin A detoxification. J Appl Microbiol. 2008;104(5):1495–502. https://doi.org/10.1111/j.1365-2672.2007.03700.x

20 Toopaang W, Panyarycha K, Srisuksam C, Hsu WC, Lin CC, Tanticharoen M, et al. Metabolomic analysis demonstrates the impacts of polyketide synthases PKS14 and PKS15 on the production of beauvericins, bassianolide, enniatin A, and ferricrocin in entomopathogen Beauveria bassiana. Metabolites. 2023;13(3):425. https://doi.org/10.3390/metabo13030425

Downloaded from http://karger.com/mpi/article-pdf/34/1/182/4276784/000540803.pdf by guest on 31 December 2025

21 Raksha Rao K, Vipin AV, Hariprasad P, Anu Appaiah KA, Venkateswaran G. Biological detoxification of aflatoxin B1 by *Bacillus licheniformis* CFR1. Food Control. 2017;71:234–41. https://doi.org/10.1016/j.foodcont.2016.06.040
22 Ning M, Zhang S, Xie Y, Wang W, Gao Y. Aflatoxin B1 removal by three bacterial strains and optimization of fermentation process parameters. Biotechnol Appl Biochem. 2019;66(6):930–8. https://doi.org/10.1002/bab.1807
23 Abou Abdallah R, Gimmino T, Baron S, Cadoret F, Michelle C, Raoult D, et al. Description of *Chryseobacterium timoniarum* sp. nov., isolated from a patient with pneumonia. Antonie van Leeuwenhoek. 2017;110(9):1121–32. https://doi.org/10.1007/s10482-017-0885-8
24 Kutsuna R, Mashima I, Miyoshi-Akiyama T, Muramatsu Y, Tomida J, Kawamura Y. *Chryseobacterium lecithinasegens* sp. nov., a siderophore-producing bacterium isolated from soil at the bottom of a pond. Int J Syst Evol Microbiol. 2021;71(12). https://doi.org/10.1099/ijsem.0.005135
25 Hugo C, Bernardet J-F, Nicholson A, Kämpfer PC. Bergey's manual of systematics of archaea and bacteria. p. 1–107.
26 Chung TK, Erdman JW Jr, Baker DH. Hydrated sodium calcium aluminosilicate: effects on zinc, manganese, vitamin A, and riboflavin utilization. Poult Sci. 1990;69(8):1364–70. https://doi.org/10.3382/ps.0691364
27 Tombaevi anovj M, Dakovj A, Markovi V, Radosavljevi -Mihajlovj A, Vukicevic J. Adsorption effects of mineral adsorbents. Part III: adsorption behaviour in the presence of vitamin B6 and microelements. Acta Vet-Beograd. 2000;50:23–30.
28 Wang Y, Zhao C, Zhang D, Zhao M, Zheng D, Lyu Y, et al. Effective degradation of aflatoxin B1 using a novel thermophilic microbial consortium TADC7. Bioresour Technol. 2017;224:166–73. https://doi.org/10.1016/j.biortech.2016.11.033
29 Zhao C, Dong L, Zhang F, Luo Y, Yang Z, Zhang X, et al. Screening and characterization of a salt-tolerant aflatoxin B1-degrading strain isolated from Doubanjiang, a Chinese typical red pepper paste. Food Sci Tech. 2022;42:e122621. https://doi.org/10.1590/fst.122621

Downloaded from http://karger.com/mmp/article-pdf/34/1/182/4276784/000540803.pdf by guest on 31 December 2025

doi:10.6342/NTU202600056